Submitted in accordance with the requirements for the degree of
Doctor of Philosophy

UNIVERSITY OF LEEDS

SCHOOL OF PHYSICS & ASTRONOMY

A Quantum Approach to Cavity Mediated Laser Cooling

Tony Blake

September 2011

The candidate confirms that the work submitted is his own, except where work which has formed part of jointly-authored publications has been included. The contribution of the candidate and the other authors to this work has been explicitly indicated below. The candidate confirms that appropriate credit has been given within the thesis where reference has been made to the work of others.

Chapters 2, 3 and 4 are based on jointly-authored publications .

Chapters 2 is based on work carried out with my supervisor Almut Beige and a postdoctoral researcher Andreas Kurcz. It has been published as *J. Mod. Opt* **58**, 1317 (2011).

Chapter 3 is based on work carried out with my supervisor Almut Beige, a postdoctoral researcher Andreas Kurcz and a master's student Norah S. Saleem. It has been published as *Phys. Rev. A* **84**, 053416 (2011) Chapter 4 is based on work carried out with my supervisor Almut Beige, and a postdoctoral researcher Andreas Kurcz. It is currently a work in progress.

In all of the above work, the main research was undertaken by myself with guidance and assistance provided by the other authors. In of some of the numerical work Andreas Kurcz wrote programmes in Fortran to numerically integrate 14 coupled differential equations in Chapter 2, 23 coupled differential equations for Chapter 3 and the 25 coupled differential equations for Chapter 4 and made the corresponding time graphs in GNUplot. Both Andreas Kurcz and myself made contour plots and phase portraits for the figures in Chapters 2, 3 and 4. We decided to use the GNUplot figures that Andreas Kurcz made instead of the figures I made in Mathematica as the presentation was clearer in GNUplot.

Acknowledgements

Firstly, I would like to give a massive thank you to my family. Both my parents Arthur and Mary have always given me support and encouragement over the last 8 years of which I have the deepest appreciation and gratitude. I would like thank both my sisters Maria and Anne who have always been there for me and who themselves are extremely creative and gifted in their own way.

Secondly I would like thank my supervisor Dr. Almut Beige. There were many times over the last 4 years where it seemed as if all was lost. Yet through all these moments of discouragement Almut would always find a way to get back on track. I would like to express my appreciation for her continuous support and the confidence she gave me to keep going.

Thirdly I would like to thank Dr. Thomas Busch for starting me on this path and always believing that I had the ability to succeed. I would also like to give a special mention to all my former class mates from UCC who made those 4 years some of the best years I've ever had. Dan Hurley, Padraig Mccarron, David Mulcahy, Dave O' Regan, and Dave O Farrell and Shane Mansfield, Ger McCarthy, Fergal Harrington, Reggie, Alice Daly, Marlene Spans and Clare Shelley, Diarmuid Early, Danny Gleeson, John Cuffe, Chris Daunt, Kyle Flavin and anybody else I've forgotten. Without you guys I probably would not be where I am right now.

Fourthly I would like to thank all the people I've met and shared the office and become friends with over the last 4 years. Rob Wagner, Jess Cooper, Neil Lovett, Katherine Brown, Giovanni Vacanti, Adam Stokes, Veiko Palge, Katie Barr, Michal Hajdusek, Ville Latinen, James Wooten, Martin Aulbach, Mark Williamson, Jenny Hide, Shane Dooley, Suva De, Luis, and all the experimental people, my flatmates Behrouz Ghoranhi, Miguel Fornes, CK, Stergios Markus, and of course Andreas Kurcz. I want to give some extra thanks to Andreas who I have had some great times with and who has helped me out a lot over the last few years.

I would also like to thank Dr. Peter Horak and Dr. Jacob Dunningham for agreeing to take time out of their schedules to be my examiners.

I also want to thank Dr. Jacob Dunningham, Dr. Viv Kendon, Dr. Jiannis Pachos, Prof. Ben Varcoe, Prof. Vlatko Vedral and Prof. Tim Spliller. Anytime I wanted to discuss

physics, maths, science or stuff in general I would always be able to rely on you guys to answer my questions.

Lastly I would like to give a big shout out to all my closest and oldest friends. Will Devine, Oran Mordaunt, Patrick Haughey, Lee and Lisa Statham, Seb Orr, Taffy Huges, Gregg Santry, and Scott Wade. Through good times and bad over the last 20 years of my life you guys have always listened to my constant talk about physics and mathematics and deep house music so thanks again lads. The last decade of my life has been quite intense and you lot were always there. Nice one!

Abstract

Tony Blake, "Quantum Approach to Cavity Mediated Laser Cooling", Ph.D. thesis, University of Leeds, September 2011

Cavity-mediated cooling has the potential to become one of the most efficient techniques to cool molecular species down to very low temperatures. This thesis studies the use of rate equations to analyse the cooling process in such systems. In particular the master equation is used to find rate equations that can determine the rate of change of phonons in the system. The general idea behind cavity cooling is the continuous conversion of phonons into cavity photons. While there is no spontaneous emission and decay rate associated with the concept of phonons, photons are created after a change in the phonon number has occurred and can then leak out through the cavity mirrors easily. Hence the conversion of phonons into photons can result in the constant removal of phonon energy from the system.

In this thesis we compare cavity mediated cooling with single particle laser cooling. It is shown that cavity cooling is essentially the same as ordinary laser cooling. This is done by calculating the stationary state phonon number m^{ss} and the cooling rate γ as a function of the system parameters. For example, when the trap phonon frequency ν is either much larger or much smaller than the cavity decay rate κ, the minimum stationary state phonon number scales as $\kappa^2/16\nu^2$ (strong confinement regime) and as $\kappa/4\nu$ (weak confinement regime), respectively. Replacing κ with Γ yields the steady states associated with ordinary laser cooling.

The main result of this thesis is the development of a method which allows for a relatively straightforward analysis of the cooling process without having to apply the so called Lamb-Dicke approximation or semiclassical theories.

Contents

List of Figures

Thesis publications

1. 'Laser cooling of a confined particle beyond standard approximations' Tony Blake, Andreas Kurzc, Norah S. Saleem, Almut Beige, Physical Review A **84** 053416 (2011).

2. 'Comparing cavity and ordinary laser cooling within the Lamb-Dicke regime' Tony Blake, Andreas Kurzc, Almut Beige, J. Mod. Opt. **58** 1317 (2011).

3. 'Cavity cooling beyond the Lamb-Dicke approximation' Tony Blake, Andreas Kurzc, Almut Beige, (in preparation).

Chapter 1

Introduction

"A good problem proves its worth by fighting back". This was said by some guy whose name I don't know but by his definition the problem of this thesis was definitely a good one because to say it fought back would be an understatement! The problem in question concerns developing a quantum approach to cavity mediated laser cooling. First attempts at a description of laser cooling can be attributed to Hänsch and Schalow [1] and independently for trapped ions by Wineland and Dehmelt [2]. It was noticed that the scattering of light from single particles affected the particles external motion. Such effects resulted in significant changes of the vibrational energy of massive particles. Several other laser cooling techniques have been developed that allow atoms and ions to be cooled to the micro and nanokelvin temperatures needed for quantum coherence and degeneracy [3–5]. Examples of these are Sisyphus cooling [6] and evaporative cooling [7].

In this thesis we focus our attention on the cooling of trapped particles confined to a harmonic potential [8]. It is in this environment that a full quantum description of the cooling process can be realised as here the cooling process has the potential to move the initial state of the particle to the motional ground state. An example of another cooling scheme where the particle is *not* confined to a harmonic potential but can also have a quantum mechanical description would be velocity selective coherent population trapping or VSCPT. Here, a so called darkstate is formed when the atomic state cannot be excited by light at a certain frequency of polarisation. A superposition state of the particle will have its excited state vanish for a particular momentum associated to the particles external motion. The quantum description of the particle's motion must be accounted for by a kinetic energy operator which will have associated eigenstates [9]. However for the purposes of this thesis we shall concentrate on models that characterise the centre of mass motion of the particle with a confining harmonic potential.The idea of laser sideband cooling of a single trapped particle can be understood with respect to the particles external motion. If the trapping potential of the particle is strong enough

for its centre of mass motion to become quantised then the energy of this motion can be described as vibrational quanta or *phonons*. The laser drives the electronic transition of the particle. Quantum mechanical effects can manifest as vibrational quanta when the particle is confined to a fraction of the wavelength of the driving laser. The electronic transition of the particle coupled to the dynamics of its centre of mass motion will have a corresponding absorption spectrum which can be measured by varying the detuning between the laser frequency and atomic resonance and observing the photon scattering rate. If the phonon frequency is much larger than the spontaneous decay rate of the excited electronic state, it becomes possible to resolve the resonances with the cooling laser and selectively drive transitions between vibrational states. One such resonance is the so called red sideband transition where the excitation of the excited electronic state of the trapped particle on this resonance is most likely accompanied by the annihilation of a phonon. When followed by the spontaneous emission of a photon, the particle returns into its electronic ground state without regaining a phonon which implies cooling. The cooling cycle only stops when the particle reaches a state with almost no phonons. The final population of excited vibrational states is in general very small and only due to highly off-resonant excitations of the ground state of the atom-phonon system.

Even though the idea of laser cooling and also cavity mediated laser cooling are not new ones, the aim of the thesis is to develop a new formalism that can provide more insights into the complicated dynamics present at the interaction of a particle and a cavity field. In fact the formalism developed here is mathematically equivalent to the standard formulations [10–19]. So there are no new fundamental results. That being said, there is a novelty to be observed from solving old problems with alternative methods. As is often the case, certain advantages can become apparent when approaching some problems from a new point of view. For example, in the case of a particle interacting with a free radiation field, by using a new formalism that shall be introduced in chapter 3, it will become apparent that adiabatically eliminating the particle's excited state is unnecessary. Often such a step is critical in the analysis of a system's cooling dynamics. Indeed, the first theoretical analysis of laser cooling with red-detuned light based on a combination of simple classical and quantum ideas can be found in Ref. [8] by Wineland and Itano. Lindberg and Stenholm later introduced the tool for a full quantum treatment of laser cooling by deriving a master equation for spontaneously emitting atoms with atomic recoil included [20] (cf. also Refs. [12, 21–24]). An alternative but consistent analysis of the laser cooling of trapped ions in a running and in a standing wave configuration has been presented by Cirac *et al.* in Ref. [11]. The main result of these papers is a cooling equation of the form

$$\dot{m} \;=\; -(A_- - A_+)\, m + A_+ \,, \tag{1.1}$$

where m denotes the mean phonon number. The $A_{\pm}$ can be interpreted as transition rates between states with different phonon numbers and hence relate to the actual cooling and heating rates. The stationary state phonon rate m_{ss} is consequently given by [10, 11, 13, 20]

$$m_{ss} = \frac{A_+}{A_- - A_+}. \tag{1.2}$$

Experimental results confirm the general dependence of this stationary state phonon number on the emission rate of the excited electronic state of the trapped particle Γ and on its phonon frequency ν [25]. For reviews on this topic see for example Refs. [10, 13, 26, 27].

The theory of the single trapped particle and associated cooling methods have been quite successful. Having said that, there are inherent limitations within each cooling scheme and with regard to sideband laser cooling this would be characterised by the atomic line width and the number of times the closed atomic transition needs to be repeated. Extending the sideband cooling method to clouds of cold atoms or molecules presents significant difficulties in so far as repeating the transition cycle will generally end up with the excited state population being distributed between the molecular rotational and vibrational states. With a cloud of atoms, repetition of the transition cycle will increase the probability of heating effects arising from multiple absorption and recoil events thereby limiting the density of the cloud. When it comes to the cooling of a large number of particles, evaporative and sympathetic cooling is a much more efficient approach [28–31]. As we shall see, the final steady state phonon number is a function of the atomic line width thereby establishing this property of the particle as a fundamental limit on the sideband cooling mechanism. Overcoming this limit has been the goal of many approaches in the last few years. Foremost among these among these approaches has been the use of the optical resonator or cavity.

Purcell first pointed out that the rate of spontaneous emission can be enhanced by the cavity field in an optical resonator [32]. A natural extension to the above ideas would be to use the cavity enhancement to alter the cooling rate and steady state of the single particle. Such coherent scattering inside an optical resonator has the advantage that the lowest temperature reachable is not limited by the atomic line width Γ but by the cavity line width κ which can be significantly lower. First indications that cavity-based laser cooling might allow us to cool particles, like trapped atoms, ions and molecules, to much lower temperatures than other laser cooling techniques had been observed already in Paris in 1995 [33, 34]. Systematic experimental studies of cavity cooling have subsequently been reported by the group of Rempe [35–38], Vuletić [39–42], and others [43, 44]. Recent atom-cavity experiments access an even wider range of experimental parameters by using optical ring cavities [45, 46] and by combining op-

tical cavities with atom chip technology [47, 48], atomic conveyer belts [49, 50], and ion traps [51]. Recent experiments even reported the occurrence of collective strong coupling effects in lossy optical cavities [52].

There is still much to be understood from cavity mediated cooling experiments. Cavity mediated cooling is a subject in its infancy and it is therefore important to increase our understanding of the complex physical processes which can occur in atom-cavity systems. The road to understanding the complex interplay of the cavity dynamics between particle and field began when cavity cooling of free particles was first discussed in Refs. [53, 54]. Later, Ritsch and collaborators [55–59], Vuletić *et al.* [19, 60], Murr *et al.* [61–63], and others [64] developed semiclassical theories to model cavity cooling processes, including the cooling of polarisable particles [65–67]. Moreover, Xuereb *et al.* [68] introduced a simple input-output formalism which can in principle be applied to a variety of cooling scenarios. The analysis of cavity cooling based on a master equation approach has been pioneered by Cirac *et al.* in 1993 [15]. Refs. [15, 16] calculate the cooling rate and the final temperature of a single two-level particle trapped inside an optical resonator with the help of a Lamb-Dicke approximation. The same master equation approach has been used later by other authors [14, 17, 18, 69]. With the exception of Ref. [14] which applies only to relatively large phonon frequencies ν, these papers suggest that cavity and ordinary laser cooling are essentially the same. Also cavity sideband cooling has been analysed for the case of certain molecules [70] and recently cavity cooling methods using EIT have been explored [71].

In addition, it is worth mentioning the recent progress made in the development of cooling methods for molecules and ultra cold chemistry. The different approaches taken serve to highlight how the use of a cavity can aid in achieving the low temperature required for ultra cold chemistry. To date the most successful cooling methods for molecules apply to polar species. Methods used consist of slowing down gases of polar molecules using Stark deceleration [72], or buffer gas cooling whereby a warm gas of polar molecules interacts with a buffer gas of cryogenically cooled helium. A magnetic potential with a magnetic field minimum can then attract molecules in the low field seeking state and repel molecules that are strong field seeking [73]. However such methods require high density samples of cold molecules in specific states. A combination of both these methods into a single experiment that produces a high density slow beam of cold polar molecules has been developed by the Rempe group [74]. This method allows a much wider class of molecules with an electric dipole moment to be addressed. Temperatures of between approximately $1 - 100$ mK can be achieved with these methods. Lower temperatures can be achieved from the formation of heteronuclear molecules using Feshbach resonance techniques [75] and photoassociation of precooled atoms [76]. Such techniques have the drawback of sometimes leaving the molecule in highly excited vibrational levels. Although it is possible to reach the

vibronic ground state as was shown by the Demille group whose photoassocation technique has brought the RbCs polar molecule to its ground vibronic state with a translational temperature of $\sim 100\ \mu$K [77]. In fact in a recent experiment the Demille group have developed a technique that successfully laser cooled the diatomic molecule SrF to a temperature of 300 μK [78]. The Demille technique is however limited to those molecules that have closed electronic transitions with diagonal Frank-Condon factors. In a recent paper Zeppenfeld *et al* have proposed to use electric-field interaction energy in lieu of photon recoil to remove energy from a molecular ensemble [79].

The above molecular cooling schemes all needed to find some means through which to use a closed electronic transition for optical cooling cycles. In general molecules have a large number of states into which an excited state can decay all of which would need to be repumped using additional lasers to obtain closed electronic transitions. The complexity of such a task is the major practical limitation of molecular cooling schemes. However the strong coupling of a molecule to the cavity field of an optical cavity provides an alternative approach to molecular cooling that can avoid the closed electronic transitions needed for cooling cycles [80]. Proposals to use cavity-enhanced Raman scattering to cool both the internal and the external degrees of freedom of molecules have been demonstrated using simulations based on ab- initio calculations for OH and NO radicals [81, 82]. In a recent proposal, Kowalewski *et al* have shown theoretically that cavity-enhanced sideband cooling of molecules and molecular ions in a strongly confining external potential is possible for experimentally feasible set ups [70].

The structure of the thesis is as follows. In chapter 2 we present our model that describes the interaction of a harmonically confined particle with the single mode of a cavity field. Here we derive the relevant Hamiltonian and show how to apply the powerful approximation technique of adiabatically eliminating the excited state. We next introduce the Lamb-Dicke approximation and use it with the quantum optical master equation for atom-cavity systems [15, 16] to derive a closed set of rate equations. These equations are linear differential equations which describe the time evolution of expectation values. Only two of the variables in these cooling equations are populations: the mean phonon number m and the mean number of photons in the cavity n. All other variables are coherences. More concretely, we assume that the mean phonon number m evolves on a much slower time scale than all the other expectation values which are included in the cooling equations, as it applies for a very wide range of experimental parameters. This allows us to simply reduce the above mentioned cooling equations to a single effective cooling equation via an adiabatic elimination of all expectation values other than m. As a result, we obtain the cooling rate and the stationary state phonon number as a function of the system parameters.

In chapter 3 we revisit the case of the trapped particle interacting with the free radiation field. It is in this chapter that we introduce a new formalism that makes use

of 2 different unitary transformations, one of which changes the atomic lowering operator σ^- to a new operator x and the other transformation which takes the phonon annihilation operator b and changes it to a new operator y. These correspond to particles that are neither atoms nor phonons and also commute with each other. Most importantly, they provide a representation of the Hamiltonian which no longer contains atomic displacement operators. Instead it depends on terms like $x^\dagger x(y - y^\dagger)$ which take non-linear effects in the atom-phonon interaction into account [83]. We use this Hamiltonian to obtain a manageable set of cooling equations which are differential equations for the time derivatives of expectation values. Our calculations are more straightforward than previous calculations. As in Refs. [10–13, 20], we are interested in the dynamics of the cooling process on the very slow time scale given by the cooling rate γ_c which scales as η^2 with $\eta \ll 1$. The only approximation involved in the following calculations of stationary state phonon numbers and effective cooling rates is to neglect higher order terms in the Lamb-Dicke parameter η.

The technique of ordinary laser cooling is already well established. Thus the main motivation in introducing a new formalism is to establish and test a framework for the modelling of laser cooling which can be extended relatively easily to more complex cooling scenarios like cavity-mediated laser cooling [14, 69, 84] and the study of possible quantum optical heating mechanisms in sonoluminescence experiments [85]. In fact this will be the subject of chapter 4; the application of our method to cavity-mediated laser cooling.

Chapter 2

Cavity Mediated Cooling within the Lamb-Dicke Approximation

To establish the setting for our quantum approach to cavity mediated laser cooling this chapter shall describe the model we employ to derive our results. The model considered is shown in Figure 2.1 . It consists of a single two-level particle with ground state $|0\rangle$ and excited state $|1\rangle$ trapped inside an optical cavity. In this model, we assume confinement of the motion of the particle in the direction of the cooling laser which enters the setup orthogonal to the cavity axis. Population in the cavity mode can leak into the environment via spontaneous emission at a decay rate κ. The energy levels considered in this model are shown in Figure 2.3. In what follows we shall denote the detuning of the cavity and of the laser with respect to the 0–1 transition of the particle by Δ and $\Delta + \delta$, respectively.

2.1 Theoretical Model

The experimental set up of a single two-level particle inside an optical cavity is depicted in Fig. 2.1. The geometry of the system is such that an incident laser field interacts with the particle in a direction perpendicular to the cavity axis. The particle is in a harmonic trapping potential so that its motion is restricted to one dimension. Here we assume that this motion is aligned with the direction of the incident laser light. Here we take the x axis to be along the direction of the cavity axis, the z axis to be along the direction of the incident laser and the y axis to be perpendicular to the plane made by x-z axes. The field of the incident laser light is linearly polarised so that its transverse oscillation is in the x direction. This induces a transverse oscillation in the particle in the x direction. We next assume that the particle emits a photon into the cavity mode which is in the x direction along the cavity axis. In this way the possible polarisation directions of the emitted photon are in the z and y directions. Since the particle is

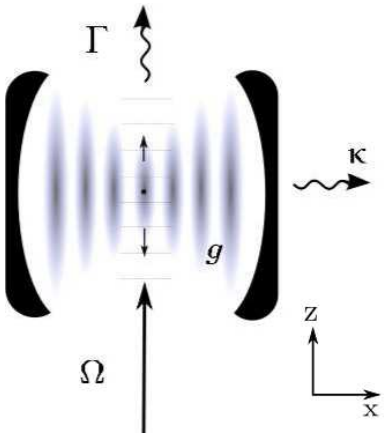

Figure 2.1: Experimental setup of a single two-level particle inside an optical cavity with coupling constant g and spontaneous decay rates κ and Γ. The motion of the particle orthogonal to the cavity axis is strongly confined by an externally applied harmonic trapping potential with phonon frequency ν. The cooling of this vibrational mode can be done with the help of the cooling laser with Rabi frequency Ω.

oscillating in the x direction the component of its dipole moment will be perpendicular to the possible polarisation directions of the emitted photon. Fig. 2.2 illustrates the different polarisation cases. So using the above assumptions for the polarisation of the incident laser light and emitted photon it is possible to see how the induced dipole moment of the particle does not affect the emitted photon. On the other hand if the incident laser light was linearly polarised so that its transverse oscillation was in the y direction then the induced oscillation of the particle in the y direction *will* interact with the emitted photon with linear polarisation in the y direction. This coupling of the dipole oscillation in the y direction and the polarisation of the emitted photon in the y direction is what allows for the cooling of the trapped particle in the cavity. Therefore, we have to assume in the set up in Fig. 2.1 that the incident laser is linearly polarised in the y direction.

The system described in this model has a Hamiltonian that can be written as

$$H = H_{\text{par}} + H_{\text{phn}} + H_{\text{cav}} + H_{\text{L}} + H_{\text{par-cav}}\,. \tag{2.1}$$

The energy of the electronic states of the trapped particle, its quantised vibrational mode, and the quantised cavity field mode are described by the first three terms. This model describes the particle as a two-level system with ground state $|0\rangle$ and excited state $|1\rangle$ such that the energies $\hbar\omega_0$, $\hbar\nu$, and $\hbar\omega_{\text{c}}$ are the energy of a single atomic excitation, a single phonon, and a single cavity photon, respectively. The first three terms in Eq. (2.1) can hence be written as

$$H_{\text{par}} = \hbar\omega_0\,\sigma^+\sigma^-, H_{\text{phn}} = \hbar\nu\; b^\dagger b, H_{\text{cav}} = \hbar\omega_{\text{c}}\,c^\dagger c\,, \tag{2.2}$$

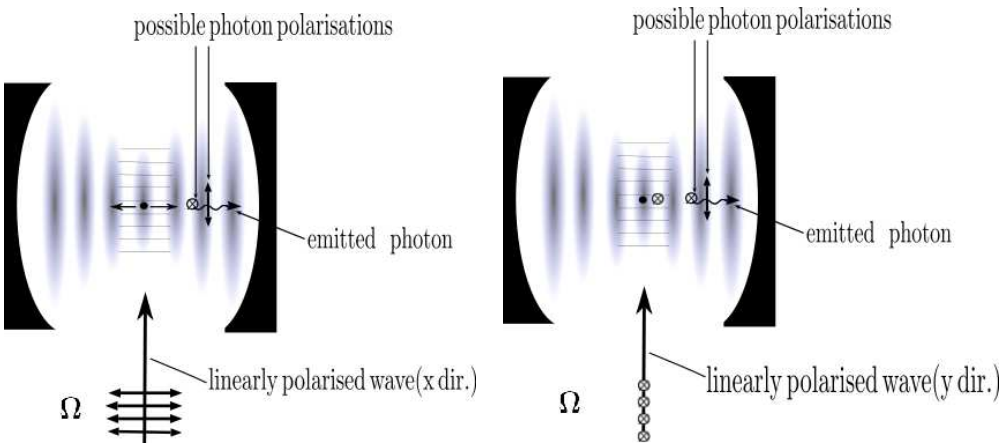

Figure 2.2: The first figure shows how a plane wave linearly polarised in the x direction induces a dipole oscillation in the x direction which does not interact with both possible emitted photon polarisations which are orthogonal to the dipole motion. The second picture shows a plane wave polarised in the y direction which induces a dipole oscillation in the y direction and would in fact interact with the y polarisation of the emitted photon. The set up in Fig. 2.1 assumes polarisation of the incident laser in the y direction.

where the operators $\sigma^- \equiv |0\rangle\langle 1|$ and $\sigma^+ \equiv |1\rangle\langle 0|$ are the atomic lowering and raising operators, and b and c are the phonon and the photon annihilation operators with the commutator relations

$$[b, b^\dagger] = [c, c^\dagger] = 1\,. \tag{2.3}$$

The two remaining terms in Eq. (2.1), i.e. H_{L} and $H_{\mathrm{par-cav}}$, are the Hamiltonian describing the interaction between the particle and the laser and the Hamiltonian describing the interaction between the trapped particle and the cavity mode. The single laser is used to establish a coupling between the electronic states $|0\rangle$ and $|1\rangle$ of the trapped particle and its quantised motion. In the dipole approximation, it can be written as

$$H_{\mathrm{L}} \;=\; e\mathbf{D}\cdot\mathbf{E}_{\mathrm{L}}(\mathbf{R},t)\,, \tag{2.4}$$

where e is the charge of an electron, $\mathbf{D}$ is the atomic dipole moment, and $\mathbf{E}_{\mathrm{L}}(\mathbf{R},t)$ is the electric field of the laser at the position $\mathbf{R}$ of the particle relative to its equilibrium position at $\mathbf{R}=0$ at time t. More concretely, the dipole moment $\mathbf{D}$ can be written as

$$\mathbf{D} \;=\; \mathbf{D}_{01}\,\sigma^- + \mathrm{H.c.}\,, \tag{2.5}$$

where $\mathbf{D}_{01}$ is a 3-dimensional complex vector, while

$$\mathbf{E}_{\mathrm{L}}(\mathbf{R},t) = \mathbf{E}_0\,\mathrm{e}^{\mathrm{i}(\mathbf{k}_{\mathrm{L}}\cdot\mathbf{R}-\omega_{\mathrm{L}}t)} + \mathrm{c.c.} \tag{2.6}$$

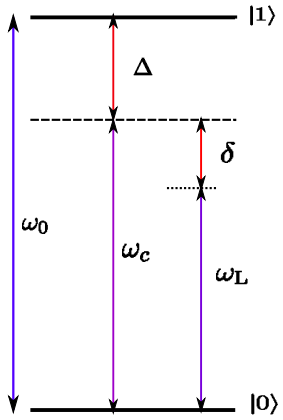

Figure 2.3: Level configuration showing a single particle with ground $|0\rangle$ and excited state $|1\rangle$. Here ω_c and ω_L are the frequency of the cavity and of the cooling laser. The corresponding detunings with respect to frequency of the 0–1 transition, ω_0, are Δ and $\Delta + \delta$.

where $\mathbf{E}_0$, $\mathbf{k}_L$, and ω_L are the amplitude, the wave vector, and the frequency of the cooling laser. Here the cooled motion of the trapped particle is the centre of mass motion in the laser direction. To see more clearly the underlying quantum dynamics we must take a closer look at the harmonic trap. When the trapped particle emits a photon it gains energy in the form of recoil which can be expressed as $E_{rec} = \hbar^2 k_L^2/2M$ and where M is the mass of the particle. In the trap the particles external motion is quantified in units of vibrational energy so that as it moves up and down a level in the trap it gains or loses a quanta of vibrational energy respectively in the form of $\hbar\nu$. Therefore if the recoil energy is greater than $\hbar\nu$ it is possible for the particle to make transitions that are greater than 1 vibrational quantum state. Conversely if $E_{rec} \ll \hbar\nu$ then the transitions which change the vibrational quantum number by more than 1 are suppressed. Thus we can define an interaction parameter η between the internal states of the ion and its external motional states.

$$\eta = \sqrt{\frac{\hbar k_L^2}{2M\nu}} = \sqrt{\frac{E_R}{\hbar\nu}}, \tag{2.7}$$

This parameter is the so called *Lamb-Dicke parameter*. The Lamb-Dicke regime or Lamb-Dicke limit can next be derived by considering the root mean square of the particles position expectation value.

$$\langle z\rangle_{rms} = \sqrt{\langle m|(z)^2|m\rangle} = \sqrt{\langle m|\left(\frac{\hbar}{2M\nu}\right)\left(b+b^\dagger\right)^2|m\rangle} = \sqrt{\left(\frac{\hbar}{2M\nu}\right)(2m+1)}. \tag{2.8}$$

When the root mean square of the position expectation value is much less than the wavelength of the laser then the vibrational motion of the particle will be such that the transitions which change the vibrational quantum number by more than 1 are suppressed. This then is the *Lamb - Dicke regime*. More specifically we find the following conditions are necessary to enter the quantum regime characterised by the Lamb-Dicke limit.

$$\begin{aligned} \langle z\rangle_{\mathrm{rms}} &\ll 1/k_{\mathrm{L}} \\ k_{\mathrm{L}}\langle z\rangle_{\mathrm{rms}} &\ll 1 \\ \sqrt{k_{\mathrm{L}}^2}\sqrt{\langle m|(z)^2|m\rangle} &\ll 1 \\ \sqrt{\langle m|k_{\mathrm{L}}^2(z)^2|m\rangle} &\ll 1 \\ \sqrt{\eta^2(2m+1)} &\ll 1 \end{aligned} \tag{2.9}$$

In the ground state $|0\rangle$, $m = 0$, so from the conditions in Eq. (2.9) it is easy to see that $\eta \ll 1$ is a direct consequence of the size of the trap ground state, a_0, in relation to the wavelength of the laser or more precisely

$$a_0 \equiv \sqrt{\langle 0|(z)^2|0\rangle} \;\ll\; \frac{1}{k_{\mathrm{L}}} \;\rightarrow\; \eta \ll 1\,. \tag{2.10}$$

This of course means that $E_{\mathrm{rec}} \ll \hbar\nu$ which thereby guarantees that the transitions of the particle in the trap whose vibrational quantum number is greater than 1 will be suppressed. For a tightly confined ion trap the Lamb-Dicke parameter will be small (0.01 to 0.1 in most experiments).

So by considering the Lamb - Dicke regime we can no longer treat the quantity $\mathbf{k}_{\mathrm{L}}\cdot\mathbf{R}$ as a number. Instead the important relationship between the laser wavelength and position of the ion must be expressed by using the definition of the position operator $\mathbf{R}$ in terms of the annihilation and creation operators b and $b^\dagger$. This yields

$$\mathbf{k}_{\mathrm{L}}\cdot\mathbf{R} \;=\; \eta(b + b^\dagger), \tag{2.11}$$

where the Lamb-Dicke parameter η is as described above [10]. Introducing the particle displacement operator D as

$$D(\mathrm{i}\eta) \;\equiv\; \mathrm{e}^{-\mathrm{i}\eta(b+b^\dagger)}, \tag{2.12}$$

and substituting Eqs. (2.5), (2.6), (2.11) into Eq. (2.4), it is easy to see that the laser

Hamiltonian can be written as

$$H_{\mathrm{L}} \quad = \quad e\left[\mathbf{D}_{01}\,\sigma^{-} + \mathrm{H.c.}\right]\cdot\mathbf{E}_{0}^{*}\,D(\mathrm{i}\eta)\,\mathrm{e}^{\mathrm{i}\omega_{\mathrm{L}}t} + \mathrm{H.c.} \tag{2.13}$$

This equation shows that the laser couples the vibrational and electronic states of the particle.

Next there is the interaction Hamiltonian describing the coupling between the electronic states of the trapped particle and the cavity. In the dipole approximation this interaction equals

$$H_{\mathrm{par-cav}} \quad = \quad e\mathbf{D}\cdot\mathbf{E}_{\mathrm{cav}}(\mathbf{R}), \tag{2.14}$$

where $\mathbf{E}_{\mathrm{cav}}(\mathbf{R})$ is the observable for the quantised electric field inside the resonator. Denoting the coupling constant between the particle and the cavity field as g, this Hamiltonian can be written as

$$H_{\mathrm{par-cav}} \quad = \quad \hbar g(\sigma^{-}+\sigma^{+})\,c + \mathrm{H.c.} \tag{2.15}$$

which describes the possible exchange of energy between atomic states and the cavity mode. Here we also note that the interaction strength g between the particle and the cavity is constant. This because we have taken the direction of the cavity field to be in the x direction along the cavity axis and assumed the field to be constant in this direction. Next we move into an interaction picture from which we can take advantage of the fact that the experimental parameters δ, ν, g, and Δ are in general much smaller than the optical frequencies, i.e.

$$\delta\,,\,\nu\,,\,g\,,\,\Delta \quad \ll \quad \omega_{\mathrm{L}},\ \omega_{\mathrm{c}}\,. \tag{2.16}$$

Choosing

$$H_{0} \quad = \quad \hbar\omega_{\mathrm{L}}\,\sigma^{+}\sigma^{-} + \hbar\omega_{\mathrm{L}}\,c^{\dagger}c\,, \tag{2.17}$$

and defining $U_0(t,0) \equiv \mathrm{e}^{-\mathrm{i}H_0 t/\hbar}$ we find that the interaction Hamiltonian H_{I},

$$H_{\mathrm{I}} = U_{0}^{\dagger}(t,0)\,(H-H_{0})\,U_{0}(t,0), \tag{2.18}$$

contains terms which oscillate with frequencies close to $2\omega_{\mathrm{L}}$. Neglecting these relatively fast oscillating terms as part of the rotating wave approximation, H_{I} becomes

$$\begin{aligned} H_{\mathrm{I}} \quad = \quad & \left(\frac{1}{2}\hbar\Omega\,D(\mathrm{i}\eta)\sigma^{-} + \hbar g\,\sigma^{-}c^{+}\right) + \mathrm{H.c.} \\ & +\hbar(\Delta+\delta)\,\sigma^{+}\sigma^{-} + \hbar\nu\,b^{\dagger}b + \hbar\delta\,c^{\dagger}c\,, \end{aligned} \tag{2.19}$$

where

$$\Omega \equiv \frac{2e}{\hbar}\mathbf{D}_{01}\cdot\mathbf{E}_0^* \tag{2.20}$$

denotes as usual the laser Rabi frequency which is also much smaller than the optical frequencies in Eq. (2.16). Eq. (2.19) is now time independent but using this equation to analyse the cooling process can lead to many complicated equations. This is due to the Hamiltonian in Eq. (2.19) describing both the interaction between the particle and laser and the interaction between the cavity and the particle. The analysis becomes less complicated when the Hamiltonian reduces to describing a single interaction. As such the following section shall describe an approximation technique whereby the effective Hamiltonian will consist of a single interaction.

On a final note a potential real life realisation of this simplified one dimensional model would consist of confining a single $^{88}Sr^{+}$ ion in a linear R.F Paul trap with motional frequencies $\omega_{x,y,z} = 2\pi \times (1.45, 1.2, 0.87)$ MHz. This trap could then be placed inside a 5cm long cavity with a finesse $F = 2.56 \times 10^4$ giving a cavity linewidth of $\kappa = 2\pi \times 117$ kHz. The cavity would have a detuning from the $S_{1/2} \longleftrightarrow P_{1/2}$ transition by a few tens of MHz. The transition itself would have a wavelength of $\lambda = 422$ nm and a population decay rate of $\Gamma = 2\pi \times 20.2$ nm. The ion trap axis would then be oriented so that it is aligned with the cavity axis. A 422nm cooling laser oriented perpendicular to the ion trap axis could then be used to attempt a cooling mechanism. A more detailed version of this experimental set up has been performed by the Vuletic group [41].

2.2 Adiabatic elimination

The magnitude of Δ with respect to the other system parameters allows us to make use of a powerful approximation technique that is commonly applied for quantum optics systems. Such systems can be described by equations that tell us how populations and coherences in a system change over time. These equations have a time development determined by the system parameters. One can then split the equations into 2 groups. One group of equations will have a time development determined by large parameters and the other by the smaller parameters. The assumption then made is that the equations whose time development is determined by the smaller parameters rapidly approach quasi - stationary values. These values can be obtained by setting the left hand side of these equations to equal zero. By substituting the expressions obtained for the quasi - stationary values into the remaining equations, the large parameter group of equations have been removed or "eliminated".

Example.
Suppose we have N equations describing a systems dynamics and 1 group of equations has time development parameters α_i whereas the remaining group of equations has time development parameters β_i for $(i = 1, \ldots N)$, where $\alpha_i = \alpha$, $\beta_i = \beta$ and ξ is a coupling constant.

$$\begin{aligned} \dot{C}_1 &= \xi C_2 - \alpha C_1 \\ &\vdots \\ \dot{C}_l &= \xi C_{l+1} - \alpha C_l \\ \dot{C}_{l+1} &= \xi C_{l+2} - \beta C_1 \\ &\vdots \\ \dot{C}_N &= \xi C_1 - \beta C_N \end{aligned} \tag{2.21}$$

If $\alpha \ll \beta$ we can use the adiabatic approximation by setting the time derivatives of $C_{l+1}, \ldots, C_N$ equal to zero. This will result in the expression $C_{l+1} = f(C_{l+2}, \ldots C_N)$. Substituting this expression into the remaining equations effectively eliminates the large parameter group of equations.

The long relaxation time or the long lifetime of the small parameter group of equations allows it to slave the subsystem defined by the large parameter group [86]. In our model, as we shall see, the rate of change of population in the excited state is governed by an equation whose time development is determined by Δ. Whereas the rate of change of population in the ground state is governed by an equation whose time development is determined by a parameter that is much smaller than Δ.
To reduce Eq. (2.19) from describing 2 interactions to describing a single interaction it necessary to replace both interactions (cavity - particle and particle - laser) with a new single interaction. The best way to do this is to have our new interaction describing a cavity- laser interaction. This can be achieved by eliminating the equation that describes the rate of change of population in the excited state. Doing so will mean that the population of the excited state, on the timescale defined by the evolution the ground state population, will have become negligible. A negligible excited state population can be established by the presence of a relatively large detuning. It enables us to eliminate the excited state from the system. We make this approximation by assuming the following size relations between parameters.

$$\Delta \gg \Omega, \delta, \nu, g, \Gamma, \kappa. \tag{2.22}$$

The state of the system can be defined using a basis that is the tensor product of the atomic, phonon number and photon number states, j, m, and n respectively so that

$$|\psi\rangle = \sum_{j=0}^{1} \sum_{m,n=0}^{\infty} c_{jmn} |jmn\rangle , \tag{2.23}$$

Then, from this representation of the state of the system we can determine 2 coupled differential equations, one for each state of the 2 level system, using

$$\dot{c}_{j'm'n'} = -\frac{\mathrm{i}}{\hbar} \sum_{j=0}^{1} \sum_{m,n=0}^{\infty} c_{jmn} \langle j'm'n'|H_{\mathrm{cond}}|jmn\rangle . \tag{2.24}$$

and where

$$H_{\mathrm{cond}} = H_{\mathrm{I}} - \frac{\mathrm{i}\Gamma}{2}\sigma^{+}\sigma^{-} . \tag{2.25}$$

A full derivation of the conditional Hamiltonian H_{cond} and how it can be found using the quantum jump approach is the subject of appendix A.1. We now determine the differential equation corresponding to the excited state ($j = 1$) by using (2.19) with (2.24). These are

$$\begin{aligned} \mathrm{i}\dot{c}_{1m'n'} = & \sum_{mn} c_{0mn} \left\langle 1m'n' \left| \frac{\Omega}{2} \left(D(\mathrm{i}\eta)\sigma^{-} + g\,\sigma^{-}c^{+} + \mathrm{H.c} \right) \right| 0mn \right\rangle \\ & + \sum_{mn} c_{0mn} \left\langle 1m'n' \left| \nu b^{\dagger}b + \left(\Delta + \delta - \frac{\mathrm{i}\Gamma}{2} \right) \sigma^{+}\sigma^{-} + \delta c^{\dagger}c \right| 0mn \right\rangle \\ & + \sum_{mn} c_{1mn} \left\langle 1m'n' \left| \frac{\Omega}{2} \left(D(\mathrm{i}\eta)\sigma^{-} + g\,\sigma^{-}c^{+} + \mathrm{H.c} \right) \right| 1mn \right\rangle \\ & + \sum_{mn} c_{1mn} \left\langle 1m'n' \left| \nu b^{\dagger}b + \left(\Delta + \delta - \frac{\mathrm{i}\Gamma}{2} \right) \sigma^{+}\sigma^{-} + \delta c^{\dagger}c \right| 1mn \right\rangle \end{aligned} \tag{2.26}$$

Letting the atomic raising and lowering operators act on the electronic states of the particle in Eq. (2.24) results in unit eigenvalues for some atomic terms and cancels the remaining ones. The action of the phonon and photon number operators results in their respective eigenvalues. Overall we find the equation

$$\begin{aligned} \mathrm{i}\dot{c}_{1m'n'} = & \sum_{mn} c_{0mn} \left\langle m'n' \left| \frac{\Omega}{2} \left(D(\mathrm{i}\eta)^{\dagger} + gc \right) \right| mn \right\rangle \\ & + c_{1m'n'} \left(m\nu + \delta n + \Delta + \delta - \frac{\mathrm{i}\Gamma}{2} \right) . \end{aligned} \tag{2.27}$$

The remaining differential equation corresponding to the ground state ($j = 0$) can be determined by working through the same steps again.

$$\begin{aligned}
\mathrm{i}\dot{c}_{0m'n'} &= \sum_{mn} c_{0mn} \left\langle 0m'n' \left| \frac{\Omega}{2} \left(D(\mathrm{i}\eta)\sigma^- + \mathrm{H.c} \right) \right| 0mn \right\rangle \\
&+ \sum_{mn} c_{0mn} \left\langle 0m'n' \left| \nu b^\dagger b + \left(\Delta + \delta - \frac{\mathrm{i}\Gamma}{2} \right) \sigma^+\sigma^- + \delta c^\dagger c \right| 0mn \right\rangle \\
&+ \sum_{mn} c_{1mn} \left\langle 0m'n' \left| \frac{\Omega}{2} \left(D(\mathrm{i}\eta)\sigma^- + \mathrm{H.c} \right) \right| 1mn \right\rangle \\
&+ \sum_{mn} c_{1mn} \left\langle 0m'n' \left| \nu b^\dagger b + \left(\Delta + \delta - \frac{\mathrm{i}\Gamma}{2} \right) \sigma^+\sigma^- + \delta c^\dagger c \right| 1mn \right\rangle \quad (2.28)
\end{aligned}$$

Once more the expression reduces to a simpler form which is only dependent on phonon and photon eigenvalues,

$$\mathrm{i}\dot{c}_{0m'n'} = \sum_{mm} c_{1mn} \left\langle m'n' \left| \frac{\Omega}{2} \left(D(\mathrm{i}\eta) + gc^\dagger \right) \right| mn \right\rangle + c_{0m'n'}(m\nu + \delta n)\,. \quad (2.29)$$

The complex parameters $\mathrm{i}(m\nu + \delta n + \Delta + \delta) + \frac{\Gamma}{2}$ and $\mathrm{i}(m\nu + \delta)$ affect the time evolution of Eq. (2.27) and Eq. (2.29) respectively.

$$\begin{aligned}
\dot{c}_{1m'n'} &= -\mathrm{i}\sum_{m} c_{0mn} \left\langle m'n' \left| \frac{\Omega}{2} \left(D(\mathrm{i}\eta)^\dagger + gc \right) \right| mn \right\rangle \\
&+ \left(-\frac{\Gamma}{2} - \mathrm{i}(m\nu + \delta n + \Delta + \delta) \right) c_{1m'n'} \\
\dot{c}_{0m'n'} &= -\mathrm{i}\sum_{mn} c_{1mn} \left\langle m'n' \left| \frac{\Omega}{2} \left(D(\mathrm{i}\eta) + gc^\dagger \right) \right| mn \right\rangle - \mathrm{i}(\nu m + \delta n) c_{0m'n'}\,. \quad (2.30)
\end{aligned}$$

The rate of change of population in the excited state is described by the function $c_{1mn}(t)$ which evolves in time according to the large parameter $\mathrm{i}(m\nu + \delta n + \Delta + \delta) + \frac{\Gamma}{2}$. The rate of change of population in the ground state is described by the function $c_{0mn}(t)$ which evolves according to $(\nu\, m + \delta\, n)$. This means

$$c_{1nm}(t) \;\propto\; \mathrm{e}^{-\frac{\Gamma}{2}t} e^{-\mathrm{i}(m\nu+\delta n+\Delta+\delta)t} \quad \text{and} \quad c_{0nm} \;\propto\; \mathrm{e}^{\mathrm{i}(\nu m+\delta n)t}\,. \quad (2.31)$$

The complex parameter that defines the evolution of the excited state population clearly indicates that it will eventually to decay to a stationary state with a decay envelope of $\Gamma/2$. On the other hand the complex parameter that defines the evolution of the ground state has no decay envelope and so would indicate that it oscillates continuously. In addition due to condition (2.22) $c_{1mn}(t)$ evolves much more quickly than $c_{0mn}(t)$ and

so reaches a quasi - stationary state on the time scale that $c_{0mn}(t)$ evolves on. Since the period of time that $c_{1mn}(t)$ takes to reach the quasi - stationary state is so short on the timescale defined by the time evolution of $c_{0mn}(t)$ then $c_{1mn}(t)$ remains effectively constant over the duration of $c_{0mn}(t)$ evolution. We can therefore say that

$$\mathrm{i}\dot{c}_{1m'n'} = 0 \tag{2.32}$$

from which it is possible to derive

$$c_{1m'n'} = -\frac{1}{2\Delta - \mathrm{i}\Gamma}\sum_{m,n=0}^{\infty} c_{0mn}\langle m'n'|\left[2g\,c + \Omega\,D^{\dagger}(\mathrm{i}\eta)\right]|mn\rangle \tag{2.33}$$

which holds up to first order in $1/\Delta$. We can now just change the primes on the indices

$$c_{1mn} = -\frac{1}{2\Delta - \mathrm{i}\Gamma}\sum_{m',n'=0}^{\infty} c_{0m'n'}\langle mn|\left[2g\,c + \Omega\,D^{\dagger}(\mathrm{i}\eta)\right]|m'n'\rangle \tag{2.34}$$

Substituting this result into the differential equations for $c_{0m'n'}$, we obtain the following equation,

$$\begin{aligned}\mathrm{i}\dot{c}_{0m'n'} = {} & (m\nu + \delta n)\,c_{0m'n'} - \frac{1}{2\Delta - \mathrm{i}\Gamma}\sum_{mn}\sum_{m'n'} c_{0m'n'}\left\langle m'n'\middle|\Omega\left(D(\mathrm{i}\eta) + 2gc^{\dagger}\right)\middle|mn\right\rangle \\ & \times\langle mn|\left[2g\,c + \Omega\,D^{\dagger}(\mathrm{i}\eta)\right]|m'n'\rangle\,.\end{aligned} \tag{2.35}$$

Making use of the closure relation $1 = \sum_{mn}|mn\rangle\langle mn|$, and expanding out the terms in the circular brackets Eq. (2.34) can now be written as,

$$\mathrm{i}\dot{c}_{0m'n'} = \frac{1}{\hbar}\sum_{m'n'} c_{0m'n'}\langle m'n'|H_I - \frac{\mathrm{i}\Gamma}{2}\tilde{\sigma}^{+}\tilde{\sigma}^{-}|m'n'\rangle\,, \tag{2.36}$$

where $\tilde{\sigma}^{+}\tilde{\sigma}^{-} = \frac{1}{4\Delta^2+\Gamma^2}\left(D(\mathrm{i}\eta) + 2gc^{\dagger}\right)\left(2g\,c + \Omega\,D^{\dagger}(\mathrm{i}\eta)\right)$ are operators that represent the atomic pauli operators after adiabatically eliminating the excited state. Detailed expressions for these operators shall be derived in the following section. H_I is the effective interaction Hamilitonian

$$H_{\mathrm{I}} = \hbar g_{\mathrm{eff}}\,D(\mathrm{i}\eta)c + \mathrm{H.c.} + \hbar\nu\,b^{\dagger}b + \hbar\delta_{\mathrm{eff}}\,c^{\dagger}c \tag{2.37}$$

with the (real) cavity coupling constant g_{eff} given by

$$g_{\mathrm{eff}} \equiv -\frac{2g\Delta\Omega}{4\Delta^2 + \Gamma^2} \tag{2.38}$$

and the effective detuning δ_{eff} as defined as

$$\delta_{\text{eff}} \equiv \delta - \frac{4\Delta g^2}{4\Delta^2 + \Gamma^2}. \tag{2.39}$$

The interaction Hamiltonian H_{I} in Eq. (2.37) holds up to first order in $1/\Delta$. It no longer contains any atomic operators. Instead, Eq. (2.37) describes a direct interplay between phonons and cavity photons. Eq. (2.37) is the canonical Hamiltonian for the cavity model from which all subsequent derivation, analysis and numerical simulation shall be based upon. In the following sections it will be used to investigate dynamical quantities in the form of populations and coherences of phonons and photons.

2.3 Master equation

We are now in a position to launch the first attack on the problem that this thesis is concerned with, finding a quantum approach to cavity mediated laser cooling. Having just determined an effective Hamiltonian for the cavity - phonon system (q.v Eq. (2.37)) we shall now use the quantum optical master equation for atom-cavity systems [15, 16] to derive a closed set of rate equations. For many of the systems considered in quantum optics it is not in general possible to find a closed set of rate equations that describe the dynamics of the systems variables [87]. Many different forms of approximation techniques have been put to use in the quest to find the elusive closed set. They can range from small parameter perturbative techniques [88, 89] to small scale versus large scale energy comparison approximations [90–92]. In our case we use the idea of the small parameter and the focus of this chapter shall be to understand how the equations that describe the system's dynamics behave according to this approximation. In fact this approximation has a name. It is called *The Lamb - Dicke approximation* as the small parameter in question is the same parameter that we already met in Eq. (2.7).

What we wish to obtain is a function that can describe the rate of change of the phonon number in the system described by the cavity model. A closed set of rate equations can allow us to do this. Unfortunately one encounters an infinite hierarchy in attempting to derive a set of rate equations with respect to $m \equiv \langle b^\dagger b \rangle$. The source of this problem is the commutator relation between the displacement operator defined in Eq. (2.12) and m. Using the Lamb-Dicke approximation is one way of stopping an infinite hierarchy of equations from arising. It has become one of the staples of ion trap theory and quantum information implementations [87]. In what follows we shall show how expanding to first order in η allows us to derive a closed set of rate equations.

The rate equations include the variables m, the mean number of phonons in the system, and n, the mean number of photons in the cavity. All other variables described by the equations are coherences. The desired function that describes the rate of change

of phonon number can then be obtained by solving the closed set of rate equations. Expanding to first order in η as we shall see will result in a set of 14 coupled first order differential equations. Such a set of coupled equations must be solved numerically as finding a solution involves determining the roots of a 14 degree polynomial otherwise known as the characteristic polynomial of a 14×14 matrix. An analytic solution is also possible with the aid of further approximation. Assuming that the mean phonon number m evolves on a much slower time scale than all other expectation values, we can use the approximation of adiabatic elimination to set equal to zero all rate equations that evolve on the faster time scale as explained in section (2.2). This leaves us with a single effective cooling equation in the variable m. As a result we obtain the cooling rate and stationary state phonon number as a function of the system parameters. The assumption of the mean phonon number moving slower than the other expectation values will be checked in later sections (q.v sec. 4.2, app. B.2 and app.B.3).

A necessary condition for the use of the Lamb - Dicke approximation as described in subsection (2.1) is that the displacement $\mathbf{x}$ of the particle is confined to within one wavelength of the laser. To justify this condition we suppose the particle has already been cooled enough to ensure that it remains in the vicinity of its equilibrium position $\mathbf{R} = 0$. More concretely, we assume in the following that the displacement $\mathbf{x}$ of the particle is confined to within one wavelength of the cooling laser. Then $\mathbf{k}_{\mathrm{L}} \cdot \mathbf{x}$ in Eq. (2.11) is much smaller than one, and the Lamb-Dicke approximation with

$$\eta \ll 1 \tag{2.40}$$

can be applied. This means, Eq. (2.12) simplifies to

$$D(\mathrm{i}\eta) = 1 - \mathrm{i}\eta(b + b^\dagger). \tag{2.41}$$

Substituting this into Eq. (2.37), we finally obtain the interaction Hamiltonian

$$H_{\mathrm{I}} = \hbar g_{\mathrm{eff}}\, c - \mathrm{i}\hbar\, \eta g_{\mathrm{eff}} (b + b^\dagger) c + \mathrm{H.c.} + \hbar\nu\, b^\dagger b + \hbar\delta_{\mathrm{eff}}\, c^\dagger c \tag{2.42}$$

which contains cavity interactions, the phonon-photon interaction, the phonon energy term, and a level shift. Next we must consider the rest of the story as up to now we have only described a system whose energy is conserved. In other words there has been no attempt to use the atomic and photon operators to describe how the system loses energy through the cavity mirrors or by spontaneous emission from the excited state. This we shall now do.

As discussed previously in Section 2.2 the effective Hamiltonian in Eq. (2.37) no longer contains any atomic operators. To account for the effect of spontaneous emission we will use the so called Liouvillian terms of the master equation which do contain

atomic operators. The master equation also accounts for dissipation from the cavity through the loss of photons from the cavity mirrors. It is the equation that describes the evolution of the state of the system accounted for by the density operator $\rho \equiv |\psi\rangle\langle\psi|$ and has the the form

$$\dot{\rho} = -\frac{\mathrm{i}}{\hbar}\left[H,\rho\right] + \mathcal{L}_{\mathrm{par}}(\rho) + \mathcal{L}_{\mathrm{cav}}(\rho), \tag{2.43}$$

where $\mathcal{L}_{\mathrm{cav}}(\rho)$ is the Liouvillian that describes the loss of cavity photons from the cavity system. Defining κ to be the cavity decay rate or the rate at which photons are lost from the cavity then has the following form $\mathcal{L}_{\mathrm{cav}}(\rho)$.

$$\mathcal{L}_{\mathrm{cav}}(\rho) = \frac{1}{2}\kappa\left(2c\rho c^{\dagger} - c^{\dagger}c\rho - \rho c^{\dagger}c\right). \tag{2.44}$$

The Liouvillian for the particle must also account for the angular distribution of spontaneous emission which quantifies the degree of randomness in the direction of the emited photon. This is achieved when the Liouvillian is written in the following form where $N(\zeta) \equiv 1 + |d_3|^2 + \left(1 - 3|d_3|^2\right)\zeta^2$ is the factor that represents the angular distribution of spontaneous emission and d_3 is the normalised component of the dipole in the z direction.

$$\mathcal{L}_{\mathrm{par}}(\rho) = \frac{3\Gamma}{8}\int_{-1}^{1} d\zeta N(\zeta)\sigma^{-}D(\mathrm{i}\eta\zeta)\rho D(\mathrm{i}\eta\zeta)^{\dagger}\sigma^{+} - \frac{\Gamma}{2}(\sigma^{+}\sigma^{-}\rho + \rho\sigma^{+}\sigma^{-}) \tag{2.45}$$

A detailed derivation of $\mathcal{L}_{\mathrm{par}}(\rho)$ can be found in apps. A.1 and A.2. Having already imposed the conditions of Eq. (2.22) to justify the adiabatic elimination of the electronic states of the particle which then resulted in the effective Hamiltonian Eq. (2.37) we must also consider the Liouvillian part of the master equation as this will also be affected due to the presence of the atomic operators. We must use the relationship obtained in Eq. (2.34) to determine the relationship that expresses the atomic operators in terms of the displacement operators and the photon operators. This can be achieved by firstly writing Eq. (2.34) in the following way and 'cleverly' adding zero.

$$\begin{aligned}\langle 1m'n'|\psi\rangle = &-\frac{1}{2\Delta - \mathrm{i}\Gamma}\sum_{m,n=0}^{\infty} c_{0mn}\langle 0m'n'|\left[2g\,c + \Omega D^{\dagger}(\mathrm{i}\eta)\right]|0mn\rangle \\ &-\frac{1}{2\Delta - \mathrm{i}\Gamma}\sum_{m,n=0}^{\infty} c_{1mn}\langle 0m'n'|\left[2g\,c + \Omega D^{\dagger}(\mathrm{i}\eta)\right]|1mn\rangle\end{aligned} \tag{2.46}$$

Next we left-multiply both sides of Eq. (2.46) by $|0m'n'\rangle$ and sum over all $m'n'$ on both

sides.

$$\sum_{m,n=0}^{\infty} |0m'n'\rangle\langle 1m'n'|\psi\rangle = -\frac{1}{2\Delta - \mathrm{i}\Gamma} \sum_{m,n=0}^{\infty} \sum_{m,n=0}^{\infty} |0m'n'\rangle\langle 0m'n'| \left[2g\,c + \Omega D^{\dagger}(\mathrm{i}\eta)\right] \times \left(c_{0mn}|0mn\rangle + c_{1mn}|1mn\rangle\right) \tag{2.47}$$

Then using the completeness relationship $1 = \sum_{mn} |mn\rangle\langle mn|$ and the definition of $|\psi\rangle$ from Eq. (2.23) we find that Eq. (2.47) simplifies to the following neat relationship.

$$\sigma^{-}|\psi\rangle = -\frac{1}{2\Delta - \mathrm{i}\Gamma} \left[2g\,c + \Omega D^{\dagger}(\mathrm{i}\eta)\right] |\psi\rangle. \tag{2.48}$$

Using the relationship of Eq. (2.48) it is easy to see that the first term in the Liouvillian of Eq. (2.45) is proportional to $1/\Delta^2$.

$$\sigma^{-}\tilde{\rho}\sigma^{+} = \frac{1}{4\Delta^2 + \Gamma^2} \left[2g\,c + \Omega D^{\dagger}(\mathrm{i}\eta)\right] \tilde{\rho} \left[2g\,c^{\dagger} + \Omega D(\mathrm{i}\eta)\right] \tag{2.49}$$

and here $\tilde{\rho} = 3\Gamma/8 \int_{-1}^{1} d\zeta N(\zeta) D(\mathrm{i}\eta\zeta) \rho D(\mathrm{i}\eta\zeta)^{\dagger}$. In a similar manner the second term in Eq. (2.45) is proportional to $1/\Delta^2$. The conditions of Eq. (2.22) ensures that the prefactor of $1/\Delta^2$ makes the expectation values that can be derived from the Liouvillian of Eq. (2.45) so small as to be negligible in comparison to all the expectation values in the rate equations. In this way it is justifiable to neglect the $\mathcal{L}_{\mathrm{par}}$ Liouvillian term in Eq. (3.21). So after the adiabatic elimination of the electronic states of the particle, the only relevant decay channel in the system is the leakage of photons through the cavity mirrors. We then find that Eq. (3.21) simplifies to the following form.

$$\dot{\rho} = -\frac{\mathrm{i}}{\hbar} \left[H_{\mathrm{I}}, \rho\right] + \frac{1}{2}\kappa \left(2\,c\rho c^{\dagger} - c^{\dagger}c\rho - \rho c^{\dagger}c\right) \tag{2.50}$$

with H_{I} as in Eq. (2.37). Finally we have the master equation to describe the dynamics of our cavity system.

2.4 Analysis of the cooling process

We now have everything we need to extract the information we seek to describe the cavity systems cooling dynamics. This is exactly why the master equation $\dot{\rho}$ is so powerful as it contains all the information about the systems dynamics. In section 2.3 we talked about finding a function to describe the rate of change of the phonon number. We can now do so by using Eq. (2.50) to derive the aforementioned set of 14 rate equa-

tions with respect to the phonon number m. From these equations, we can calculate the stationary state phonon number m^{ss} and the effective cooling rate γ as a function of the experimental parameters η, g_{eff}, κ, ν, and δ_{eff}. The objective of this section is to obtain an analytic solution for the special case where the cavity decay rate κ and the phonon frequency ν are both relatively large but still both much smaller than Δ. In this situation then

$$\kappa, \nu \quad \gg \quad \eta g_{\text{eff}} \,. \tag{2.51}$$

In section 2.2 we demonstrated how a set of coupled equations can be split into 2 groups according to the relative size of their time development parameters. The group whose time development depended on the value of large parameters could then be adiabatically eliminated. In the situation just described by the conditions in Eq. (2.51) we can apply the adiabatic elimination approximation with respect to the timescales defined by these conditions. As we shall see the mean phonon number m evolves in this case on a much slower time scale than all other expectation values which are included in the cooling equations. The latter can hence be eliminated adiabatically from the time evolution of the system. We shall now determine the set of coupled equations.

2.4.1 Cooling equations

The next equation that we will introduce is without a doubt the most useful tool that has been brought to bear in the development of the quantum approach that we have taken to investigate the mechanism of cavity based laser cooling. Indeed it is so useful that we will apply it in all three parts of this thesis. In fact it is quite simple to write down. The definition of the expectation value of an operator is $\langle A \rangle = \text{Tr}(A\rho)$ so the time derivative of the expectation value of an operator A equals

$$\langle \dot{A} \rangle \quad = \quad \text{Tr}(A\dot{\rho}) \,. \tag{2.52}$$

Then using the master equation in Eq. (2.50) and the cyclic property of the trace we find the generalised rate equation

$$\langle \dot{A} \rangle \quad = \quad -\frac{\mathrm{i}}{\hbar} \left\langle \left[A, H_{\text{I}}\right] \right\rangle + \frac{1}{2}\kappa \left\langle 2\, c^{\dagger} A c - A c^{\dagger} c - c^{\dagger} c A \right\rangle \tag{2.53}$$

from which we can generate our closed set of rate equations. Using the commutator relations in Eq. (2.3) and the interaction Hamiltonian in Eq. (2.42) and applying Eq. (2.53) to the mean phonon number $m = \langle b^{\dagger} b \rangle$ we find that we need to only con-

sider the mean photon number $n = \langle c^\dagger c \rangle$, and the following coherences

$$\begin{aligned}
&k_x = \mathrm{i}\langle b - b^\dagger \rangle\,, \quad k_y = \mathrm{i}\langle c - c^\dagger \rangle\,,\\
&k_u = \langle b + b^\dagger \rangle\,, \quad k_w = \langle c + c^\dagger \rangle\,,\\
&k_1 = \langle (b + b^\dagger)(c + c^\dagger) \rangle\,, \quad k_2 = \mathrm{i}\langle (b + b^\dagger)(c - c^\dagger) \rangle\,,\\
&k_3 = \mathrm{i}\langle (b - b^\dagger)(c + c^\dagger) \rangle\,, \quad k_4 = \langle (b - b^\dagger)(c - c^\dagger) \rangle\,,\\
&k_5 = \langle c^2 + c^{\dagger 2} \rangle\,, \quad k_6 = \mathrm{i}\langle c^2 - c^{\dagger 2} \rangle\,,\\
&k_7 = \langle b^2 + b^{\dagger 2} \rangle\,, \quad k_8 = \mathrm{i}\langle b^2 - b^{\dagger 2} \rangle
\end{aligned} \tag{2.54}$$

to obtain a closed set of differential equations. So on substituting all 14 expectation values into Eq. (2.53) we find the rate equations

$$\begin{aligned}
\dot{k}_x &= -2\eta g_{\mathrm{eff}} k_y + \nu\, k_u\,,\\
\dot{k}_y &= 2g_{\mathrm{eff}} + \delta_{\mathrm{eff}} k_w - \frac{1}{2}\kappa\, k_y\,,\\
\dot{k}_u &= -\nu\, k_x\,,\\
\dot{k}_w &= 2\eta g_{\mathrm{eff}} k_u - \delta_{\mathrm{eff}} k_y - \frac{1}{2}\kappa\, k_w
\end{aligned} \tag{2.55}$$

and

$$\begin{aligned}
\dot{n} &= g_{\mathrm{eff}} k_y + \eta g_{\mathrm{eff}} k_1 - \kappa\, n\,,\\
\dot{k}_1 &= 2\eta g_{\mathrm{eff}} \left(k_7 + 2m + 1\right) - \nu\, k_3 - \delta_{\mathrm{eff}} k_2 - \frac{1}{2}\kappa\, k_1\,,\\
\dot{k}_2 &= 2g_{\mathrm{eff}} k_u + \nu\, k_4 + \delta_{\mathrm{eff}} k_1 - \frac{1}{2}\kappa\, k_2\,,\\
\dot{k}_3 &= -2\eta g_{\mathrm{eff}} (k_6 - k_8) + \nu\, k_1 + \delta_{\mathrm{eff}} k_4 - \frac{1}{2}\kappa\, k_3\,,\\
\dot{k}_4 &= -2g_{\mathrm{eff}} k_x - 2\eta g_{\mathrm{eff}} (k_5 - 2n - 1) - \nu\, k_2 - \delta_{\mathrm{eff}} k_3 - \frac{1}{2}\kappa\, k_4\,,\\
\dot{k}_5 &= -2g_{\mathrm{eff}} k_y + 2\eta g_{\mathrm{eff}} k_1 - 2\delta_{\mathrm{eff}} k_6 - \kappa\, k_5\,,\\
\dot{k}_6 &= 2g_{\mathrm{eff}} k_w + 2\eta g_{\mathrm{eff}} k_2 + 2\delta_{\mathrm{eff}} k_5 - \kappa\, k_6\,,\\
\dot{k}_7 &= -2\eta g_{\mathrm{eff}} k_4 - 2\nu\, k_8\,,\\
\dot{k}_8 &= -2\eta g_{\mathrm{eff}} k_2 + 2\nu\, k_7\,,
\end{aligned} \tag{2.56}$$

while

$$\dot{m} = \eta g_{\mathrm{eff}} k_4\,. \tag{2.57}$$

Notice that these differential equations, the cooling equations, have been derived without further approximations.

2.4.2 Stationary state phonon number

Having found 14 rate equations we can now calculate an expression for the stationary state by assuming the existence of such a state and setting the right hand side of the above cooling equations equal to zero. Doing so, we find that Eq. (2.55) yields

$$\begin{aligned} k_{\mathrm{x}}^{\mathrm{ss}} &= 0\,, \quad k_{\mathrm{y}}^{\mathrm{ss}} = \frac{4g_{\mathrm{eff}}\kappa\nu}{\mu^3}\,, \quad k_{\mathrm{u}}^{\mathrm{ss}} = \frac{8\eta g_{\mathrm{eff}}^2\kappa}{\mu^3}\,, \\ k_{\mathrm{w}}^{\mathrm{ss}} &= \frac{8g_{\mathrm{eff}}(4\eta^2 g_{\mathrm{eff}}^2 - \delta_{\mathrm{eff}}\nu)}{\mu^3} \end{aligned} \tag{2.58}$$

with the cubic frequency μ^3 defined as

$$\mu^3 \equiv \nu(\kappa^2 + 4\delta_{\mathrm{eff}}^2) - 16\eta^2 g_{\mathrm{eff}}^2\delta_{\mathrm{eff}}\,. \tag{2.59}$$

Moreover, we obtain the stationary state values

$$\begin{aligned} n^{\mathrm{ss}} &= \frac{\eta^2 g_{\mathrm{eff}}^2(\kappa^2+4\nu^2)}{2\delta_{\mathrm{eff}}\mu^3} + \frac{4g_{\mathrm{eff}}^2\nu^2(\kappa^2+4\delta_{\mathrm{eff}}^2)}{\mu^6} \\ &\quad - \frac{128\eta^2 g_{\mathrm{eff}}^4\nu\delta_{\mathrm{eff}}}{\mu^6} + \frac{256\eta^4 g_{\mathrm{eff}}^6}{\mu^6}\,, \\ k_1^{\mathrm{ss}} &= \frac{\eta g_{\mathrm{eff}}\kappa(\kappa^2+4\delta_{\mathrm{eff}}^2)}{2\delta_{\mathrm{eff}}\mu^3} - \frac{64\eta g_{\mathrm{eff}}^3\kappa\nu\delta_{\mathrm{eff}}}{\mu^6} \\ &\quad + \frac{256\eta^3 g_{\mathrm{eff}}^5\kappa}{\mu^6}\,, \\ k_2^{\mathrm{ss}} &= \frac{\eta g_{\mathrm{eff}}(\kappa^2+4\delta_{\mathrm{eff}}^2)}{\mu^3} + \frac{32\eta g_{\mathrm{eff}}^3\kappa^2\nu}{\mu^6}\,, \\ k_3^{\mathrm{ss}} &= \frac{\eta g_{\mathrm{eff}}}{\delta_{\mathrm{eff}}}\,, \quad k_4^{\mathrm{ss}} = k_8^{\mathrm{ss}} = 0\,, \\ k_5^{\mathrm{ss}} &= -\frac{8g_{\mathrm{eff}}^2\nu^2(\kappa^2-4\delta_{\mathrm{eff}}^2)}{\mu^6} + \frac{\eta^2 g_{\mathrm{eff}}^2(\kappa^2-4\delta_{\mathrm{eff}}^2)}{\delta_{\mathrm{eff}}\mu^3} \\ &\quad - \frac{256\eta^2 g_{\mathrm{eff}}^4\nu\delta_{\mathrm{eff}}}{\mu^6} + \frac{512\eta^4 g_{\mathrm{eff}}^6}{\mu^6}\,, \\ k_6^{\mathrm{ss}} &= -\frac{32g_{\mathrm{eff}}^2\kappa\nu^2\delta_{\mathrm{eff}}}{\mu^6} + \frac{4\eta^2 g_{\mathrm{eff}}^2\kappa}{\mu^3} + \frac{128\eta^2 g_{\mathrm{eff}}^4\kappa\nu}{\mu^6}\,, \\ k_7^{\mathrm{ss}} &= \frac{\eta^2 g_{\mathrm{eff}}^2(\kappa^2+4\delta_{\mathrm{eff}}^2)}{\nu\mu^3} + \frac{32\eta^2 g_{\mathrm{eff}}^4\kappa^2}{\mu^6}\,, \end{aligned} \tag{2.60}$$

and most importantly the expression for the steady state phonon number

$$\begin{aligned} m^{\mathrm{ss}} &= \frac{\kappa^2+4\delta_{\mathrm{eff}}^2}{16\nu\delta_{\mathrm{eff}}}+\frac{\eta^2 g_{\mathrm{eff}}^2(\kappa^2-8\nu^2+16\nu\delta_{\mathrm{eff}}+4\delta_{\mathrm{eff}}^2)}{2\nu\mu^3} \\ &\quad +\frac{\nu(\kappa^2+4\delta_{\mathrm{eff}}^2)(\nu-2\delta_{\mathrm{eff}})}{4\delta_{\mathrm{eff}}\mu^3}+\frac{16\eta^2 g_{\mathrm{eff}}^4\kappa^2}{\mu^6}. \end{aligned} \tag{2.61}$$

These equations can be checked easily by substituting them back into Eqs. (2.55)–(2.57).

In this particular cavity model we are considering the parameter regime of a tightly confined particle inside a relatively leaky optical cavity described by Eq. (2.51). This parameter regime is consistent with the Lamb-Dicke approximation in Eq. (2.40). Calculating m^{ss} up to second order in η^2 correctly would require us to go beyond the current first order Lamb-Dicke approximation and to take terms proportional to η^2 in the system Hamiltonian into account. The above expression for the stationary state phonon number hence applies only up to first order in η. Taking this into account, Eq. (2.61) simplifies to

$$m^{\mathrm{ss}} = \frac{\kappa^2+4(\nu-\delta_{\mathrm{eff}})^2}{16\nu\delta_{\mathrm{eff}}}. \tag{2.62}$$

Here we must also note that we are considering δ_{eff} to be positive. Eq. (2.22) tells us that the detuning Δ is large in relation to g and δ. Since $\delta_{\mathrm{eff}} \equiv \delta - \frac{4\Delta g^2}{4\Delta^2+\Gamma^2}$ then δ_{eff} will be positive if δ is positive. Fig. 2.3 shows that $\delta = \omega_{\mathrm{c}} - \omega_{\mathrm{L}}$. So if $\delta < 0$ then $\omega_{\mathrm{L}} > \omega_{\mathrm{c}}$. In this case the particle will favour transitions to higher vibrational trap states which corresponds to heating. On the excitation spectrum of the particle in the strong confinement regime these transitions correspond to the so called blue detuned frequencies located to the right of the carrier resonance. In our analysis we will be considering the situation when $\omega_{\mathrm{L}} < \omega_{\mathrm{c}}$ so that $\delta > 0$ and δ_{eff} is positive. In this case the particle will favour transitions to lower vibrational trap states and hence cooling.

Since Eq. (2.51) does not pose a condition on the size of the effective detuning δ_{eff}, we can find a value for this parameter that will minimise the stationary state phonon number m^{ss} in Eq. (2.62). This value will be in the form of an expression found by the usual means of minimising a function by differentiating the function defined by m_{ss} with respect to δ_{eff}, setting the resulting expression equal to zero and solving for δ_{eff}.

Calculating the derivative then of m^{ss} with respect to δ_{eff} we find that the optimal choice for δ_{eff} is

$$\delta_{\mathrm{eff}} = \frac{1}{2}\sqrt{\kappa^2+4\nu^2}. \tag{2.63}$$

In the parameter regime which is the most interesting from an experimental point of

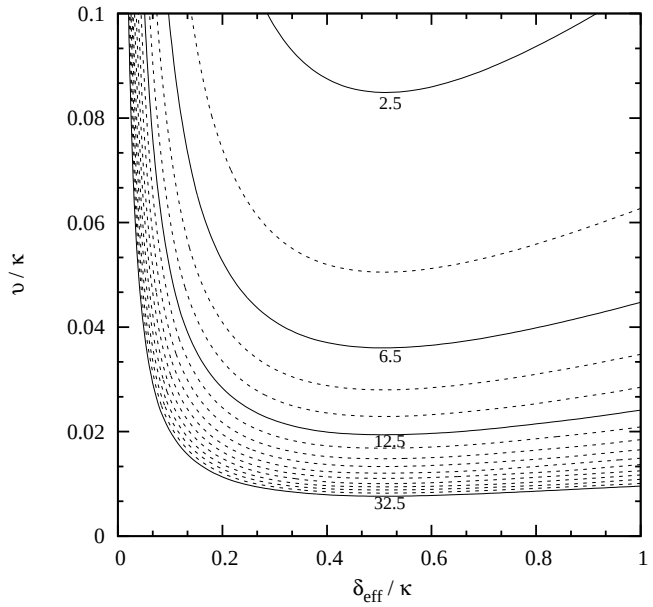

Figure 2.4: Logarithmic contour plot of the stationary state phonon number m^{ss} in Eq. (2.61) as a function of δ_{eff} and ν for $\eta = 0.1$ and $g_{\text{eff}} = 0.0001\,\kappa$. The result is in very good agreement with the simpler expression in Eq. (2.62).

view, i.e. in the case of relatively small phonon frequencies ν (weak confinement regime $\kappa \gg \nu$), the effective detuning in Eq. (2.63) becomes

$$\delta_{\text{eff}} = \frac{1}{2}\,\kappa\,. \tag{2.64}$$

Substituting this detuning into Eq. (2.62), we obtain the stationary state phonon number

$$m^{ss}_{\delta_{\text{eff}}=\frac{1}{2}\kappa} \quad = \quad \frac{\kappa}{4\nu} \tag{2.65}$$

which is in good agreement with Figure 2.4. To see this more clearly we calculate some values for m_{ss} using Eq. (2.65) in the following example.

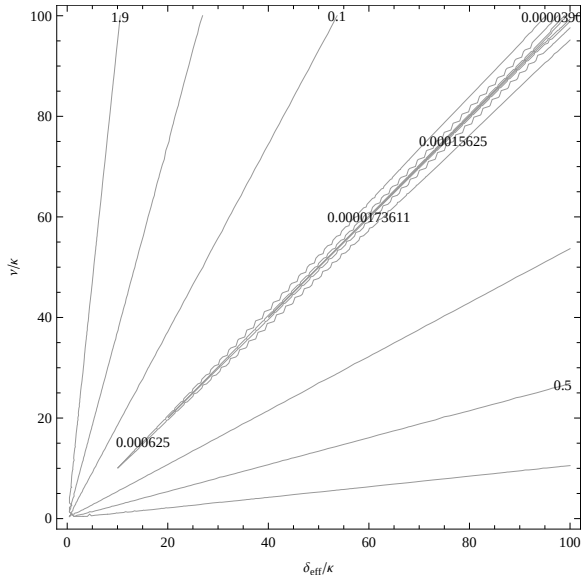

Figure 2.5: Contour plot of the stationary state phonon number m^{ss} in Eq. (2.61) as a function of δ_{eff} and ν for the same η and g_{eff} as in Figure 2.4 but for much larger phonon frequencies ν. The result is again in very good agreement with Eq. (2.62).

Example. We can use Eq. (2.65) to find values for m_{ss} when $\delta_{\text{eff}} = 1/2\kappa$. Suppose we consider the following values for ν ,

$$\nu \quad = \quad 0.02\,\kappa,\, 0.04\,\kappa,\, 0.06\,\kappa,\, 0.09\,\kappa. \tag{2.66}$$

Then using Eq. (2.65) we find that the values for m_{ss} are respectively

$$m_{\text{ss}} \quad = \quad 12.5,\, 6.25,\, 4.17,\, 2.78\,. \tag{2.67}$$

Refering to Fig. 2.4 we see that these values of m_{ss} correspond quite well to the relevant values for ν on the vertical line for δ_{eff} .

In the other extreme case, i.e. when the phonon frequency ν is much larger than the cavity decay rate κ (strong confinement regime), the effective detuning in Eq. (2.63) simplifies to

$$\delta_{\text{eff}} = \nu \tag{2.68}$$

which corresponds to

$$m^{\text{ss}}_{\delta_{\text{eff}}=\nu} \quad = \quad \frac{\kappa^2}{16\nu^2}\,. \tag{2.69}$$

This result is confirmed by Figure 2.5 which considers much larger phonon frequencies

ν than Fig. (2.4). Again to illustrate the more simpler version of Eq. (2.69) we use it to calculate some values for m_{ss} in the following example.

Example. Taking $\delta_{\text{eff}} = \nu$ we can use Eq. (2.69) to find values for m_{ss}. We consider the following values for ν.

$$\nu \quad = \quad 10\kappa,\, 20\kappa,\, 40\kappa,\, 60\kappa. \tag{2.70}$$

These result in very small and very close in value results for the steady state which are respectively given by

$$m_{ss} \quad = \quad 0.000625,\, 0.00015625,\, 0.0000390625,\, 0.0000173611\,. \tag{2.71}$$

Looking at Fig. (2.5) we can see that all these values of m_{ss} line up almost exactly on the diagnonal $\nu = \delta_{\text{eff}}$ which is of course what we would expect for the values of the steady in the strong confinement regime defined by Eq. (2.69).

Cooling to very low temperatures means minimising the stationary state phonon number. As we have just seen this is limited by the relative size of the phonon frequency ν with respect to the cavity decay rate κ. Comparing the two choices of effective detunings δ_{eff} in Eqs. (2.64) and (2.68), we find that on the one hand we must have the cavity decay rate κ much smaller than the phonon frequency ν to minimise the final number of phonons in the system (strong confinement regime). In this case the corresponding stationary state phonon number $m^{ss}_{\delta_{\text{eff}}=\nu}$ will be found to be approximately given by $\kappa^2/16\nu^2$. On the other hand however, if κ is much larger than ν (weak confinement regime), one should choose $\delta_{\text{eff}} = \frac{1}{2}\kappa$ to minimise the final phonon number since in this case $m^{ss}_{\delta_{\text{eff}}=\frac{1}{2}\kappa}$ equals $\kappa/4\nu$ to a very good approximation. Comparing the explicit analytical expressions for $m^{ss}_{\delta_{\text{eff}}=\frac{1}{2}\kappa}$ and $m^{ss}_{\delta_{\text{eff}}=\nu}$, we find that

$$m^{ss}_{\delta_{\text{eff}}=\frac{1}{2}\kappa} \quad = \quad \sqrt{m^{ss}_{\delta_{\text{eff}}=\nu}} \tag{2.72}$$

for a wide range of experimental parameters. It is easy to see from this comparison and the above examples that in strong confinement regime when $\kappa \ll \nu$ the final phonon number $m^{ss}_{\delta_{\text{eff}}=\nu}$ will always be less than one and in the weak confinement regime when $\kappa \gg \nu$ the final phonon number will be greater than one. Clearly when the cavity system is operated in the strong confinement regime a lower steady state will be reached than in the weak confinement regime. However when the trapped particle cannot be so strongly confined that it is *not* possible to cool to phonon numbers below one, it is better to choose $\delta_{\text{eff}} = \frac{1}{2}\kappa$ than choosing $\delta_{\text{eff}} = \nu$ since in this case

$$m^{ss}_{\delta_{\text{eff}}=\frac{1}{2}\kappa} \quad = \quad \sqrt{m^{ss}_{\delta_{\text{eff}}=\nu}} \;<\; m^{ss}_{\delta_{\text{eff}}=\nu}\,. \tag{2.73}$$

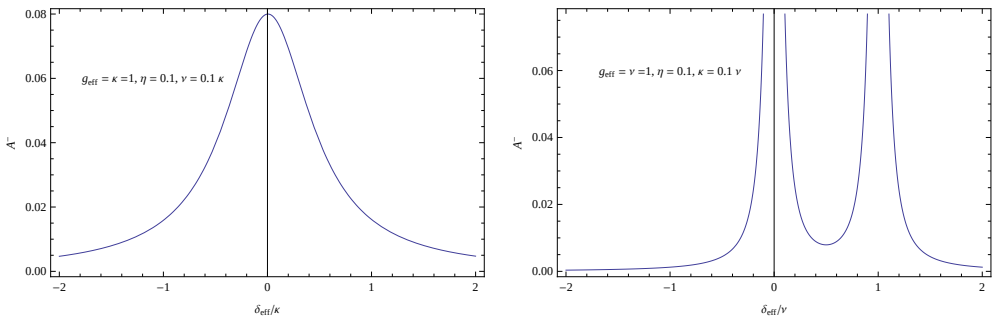

Figure 2.6: The above figures show the excitation spectrum of particle for making the red sideband transition which is quanrified by the transition rate A^-. The first figure shows the case of weak confinement whereby $\kappa \gg \nu$ and the resonance width is κ.In this instance optimal cooling occurs at $\delta_{\text{eff}} = \kappa/2$ is exactly at the half width of the resonace. The second figure shows the case of strong confinement where $\kappa \ll \nu$. Here we can clearly see the resolved sidebands at $\delta_{\text{eff}} = 0, \nu$.

So whenever the endpoint of the cooling process is such that the final phonon number is not less than one, choosing the detuning δ_{eff} different from the phonon frequency ν, as it has been suggested in Refs. [16–19], yields a significant enhancement of the cavity cooling process.

Discussion

To gain a clearer picture of the cooling dynamics it shall be instructive to look at the excitation spectrum of the particle in the cavity. This spectrum can be quantified by the transition rate A^- that tells us about the process of the particle losing a phonon as it makes the transition $|0,m\rangle \rightarrow |1,m-1\rangle$. As pointed out in the introduction (q.v. Eq. (1.1)) the cooling can be expressed in the form of transition rate notation. As we shall see in the following sections the cooling rate can be expressed as $\gamma = \frac{4\eta^2\kappa g_{\text{eff}}^2}{\kappa^2+4(\delta_{\text{eff}}-\nu)^2} - \frac{4\eta^2\kappa g_{\text{eff}}^2}{\kappa^2+4(\delta_{\text{eff}}+\nu)^2}$. If we follow the lead of previous authors [10, 11, 13, 20] we can determine the form of the lowering transition rate from the cooling rate in the transition rate notation.

$$A^- = \frac{4\eta^2\kappa g_{\text{eff}}^2}{\kappa^2 + 4(\delta_{\text{eff}} - \nu)^2} + \frac{4\eta^2\kappa g_{\text{eff}}^2}{\kappa^2 + 4(\delta_{\text{eff}})^2} \tag{2.74}$$

Fig. 2.6 illustrates the different behaviour of the lowering transition rate for both the weak and strong confinment regimes respectively. However, the hierarchy of motional states means that the particle can couple to several excited states. Thus a series of resonances can be excited by the detuning δ_{eff} at intervals of the trap frequency ν. The spectral resolution of the resonances depends on the relationship between ν and κ. The first picture in Fig. 2.6 shows the resonance curve for the weak confinement regime which has a resonance width of κ. All states are excited whose transition frequencies

fall inside this curve. The halfwidth at $\delta_{\text{eff}} = \kappa/2$ is the point on the curve that will optimise the probability of the red sideband transition occuring. This behaviour is clearly illustrated in Fig. 2.4. Take the vertical line at $\delta_{\text{eff}} = 0.1\kappa$. Then between $\nu = 0.02\kappa$ and $\nu = 0.1\kappa$ m_{ss} changes steeply from 32.5 to 12.5. But if we take the vertical line at $\delta_{\text{eff}} = 0.5\kappa$ then between $\nu = 0.04\kappa$ and $\nu = 0.1\kappa$ m_{ss} only varies slightly from 6.5 to 2.5 thus indicating the optimality of the $\kappa/2$ detuning. The situation changes when we look at the strong confinement case. In Fig. 2.6 we see in the second picture two resonance peaks. These peaks correspond to the carrier transition ($|0,m\rangle \rightarrow |1,m\rangle$) and the red sideband transition ($|0,m\rangle \rightarrow |1,m-1\rangle$). The red sideband here is resolved and so the detuning can be tuned to this frequency thus selectively driving the transitions between the vibrational states $|0,m\rangle \rightarrow |1,m-1\rangle$. Again this behaviour can be clearly seen in Fig. 2.5. The line for which $\delta_{\text{eff}} = \nu$ is actually the diagonal in the diagram and every point that lies along this line is lower than the points on lines that are not diagonal from the bottom left hand corner thus indicating that $\delta_{\text{eff}} = \nu$ is the optimal choice for minimising m_{ss}. In addition as the value of ν increases, the contours have a wider spread and the change in m_{ss} becomes less gradual whilst at the same time remaining below 1. This shows that in the strong confinement regime when $\nu \gg \kappa$ the steady state reaches the ground state and remains there for a large range of parameter values.

2.4.3 Initial state

The next part of the cooling analysis will require us to determine the initial state of the cavity model in Figure 2.1. To do so we assume that the cooling laser is turned on at $t = 0$. We also assume that the particle does not experience any other cooling processes and $\Omega = 0$. So our initial state corresponds to the situation when the laser is not on. In this case g_{eff} also becomes zero due to Eq. (2.38). Then our effective Hamilitonian of Eq. (2.37) reduces to just the $\hbar\nu\, b^\dagger b$ and $\hbar\delta_{\text{eff}} c^\dagger c$ terms. Taking this into account we find that the right hand side of the cooling equations (2.55) and (2.56) become zero, which corresponds to a state with all coherences and the cavity photon number being equal to zero, i.e.

$$n(0) = k_{\text{a}}(0) = k_i(0) = 0 \tag{2.75}$$

for $\text{a} = \text{x}, \text{y}, \text{u}, \text{w}$ and $i = 1, ..., 8$, while there can be any mean initial number of phonons m in the vibrational mode of the particle. This initial condition is consistent with the particle being trapped which means that it is located around the centre of a trap and that it has no initial momentum away from its equilibrium position. The first of these two statements implies $k_{\text{u}}(0) = 0$ and the second one implies $k_{\text{x}}(0) = 0$.

2.4.4 Cooling dynamics

As we discussed at the beginning of this section only one of the variables in the above cooling equations, namely the mean phonon number m, evolves on a relatively slow time scale. This then allows us to calculate the effective cooling rate γ, as all other variables, i.e. the mean photon number n and the coherences, evolve on the fast time scale given by ν and κ. In the parameter regime of Eq. (2.51), these can then be eliminated adiabatically from the time evolution of the system, leaving us only with a single effective cooling equation. Doing so and setting the time derivatives in Eqs. (2.55) and (2.56) equal to zero and assuming that we are at the beginning of the cooling process where $m \gg 1$, we find

$$k_4 = -\frac{64\eta g_{\text{eff}} \nu \kappa \delta_{\text{eff}}}{(\kappa^2 + 4\nu^2)^2 + 8\delta_{\text{eff}}^2(\kappa^2 - 4\nu^2) + 16\delta_{\text{eff}}^4} m\,. \tag{2.76}$$

This equation holds up to first order in ηg_{eff} and is consistent with the Lamb-Dicke approximation introduced in Section 2.3. Eq. (3.39) shows that the photon-phonon coherence k_4 is essentially the cooling rate of the trapped particle. Substituting Eq. (2.76) into Eq. (2.57), we obtain the final cooling equation

$$\dot{m} = -\gamma m \tag{2.77}$$

with the cooling rate γ given by

$$\gamma = \frac{64\eta^2 g_{\text{eff}}^2 \nu \delta_{\text{eff}} \kappa}{(\kappa^2 + 4\nu^2)^2 + 8\delta_{\text{eff}}^2(\kappa^2 - 4\nu^2) + 16\delta_{\text{eff}}^4}\,. \tag{2.78}$$

The standard solution to this differential equation is of course

$$m(t) = \mathrm{e}^{-\gamma t} m(0)\,. \tag{2.79}$$

Remark

We must point out that the cooling rate is of order η^2 while our calculations only consider expressions up to order η in the Lamb-Dicke limit. In this way it is then possible that our expression for γ may not be complete as there may be other terms that could contribute to the cooling rate when calculating expressions up to order η^2 in the Lamb-Dicke limit. In fact we will explore this deficiency further in the following chapters and show that it necessary to consider terms to second order in η. However our steady state and cooling rate expressions agree with the results of previous authors and we will show that going to second order in η does in fact yield the same expressions for m_{ss} and γ as those found here in second order. This apparent paradox will be explained later by showing how the time averaged values for certain coherences are equivalent to their stationary state values even though in first order no such stationary state values exist.

We now have an approximate analytic solution of the cooling equations. It is quite simple as it is literally a decreasing exponential function which in our case describes the reduction in the number of phonons i.e. cooling. We can also numerically integrate Eqs. (2.55)–(2.57) to find the behaviour of the function for $m(t)$. Figures 2.7 and 2.8 show exacly this. In fact both figures compare the full set of cooling equations (solid lines) to the exponential cooling process with the rate γ in Eq. (2.78) (dashed lines) and both show that γ is a very good approximation for the cooling rate as long as the actual phonon number m is much larger than one. We see that it is only as m approaches its stationary state value that the exponential reduction of m slows down. The figures also show that as the value of ν/κ increases the speed of the cooling process increases.
Again we can examine our choice of δ_{eff} where the phonon frequency ν is either much smaller or much larger than the cavity decay rate κ as this will also determine the rate at which the system reaches its stationary state. As we have already seen in Subsection 2.4.2 when ν is much smaller than the cavity decay rate κ we need to choose $\delta_{\text{eff}} = \frac{1}{2}\kappa$ (q.v Eq. (2.64)) so as to minimise the stationary state phonon number. When we do this we also change the rate at which the system cools which is reflected in Eq. (2.78) simplifing to

$$\gamma_{\delta_{\text{eff}}=\frac{1}{2}\kappa} = \frac{8\eta^2 g_{\text{eff}}^2 \nu \kappa^2}{\kappa^4 + 4\nu^4}. \tag{2.80}$$

Going to the other extreme when ν is much larger than the cavity decay rate κ we need to choose $\delta_{\text{eff}} = \nu$ (q.v Eq. (2.68)) to minimise the stationary state phonon number. Again this choice of δ_{eff} changes the rate at which the system cools. It equals

$$\gamma_{\delta_{\text{eff}}=\nu} = \frac{64\eta^2 g_{\text{eff}}^2 \nu^2}{\kappa(\kappa^2 + 16\nu^2)}. \tag{2.81}$$

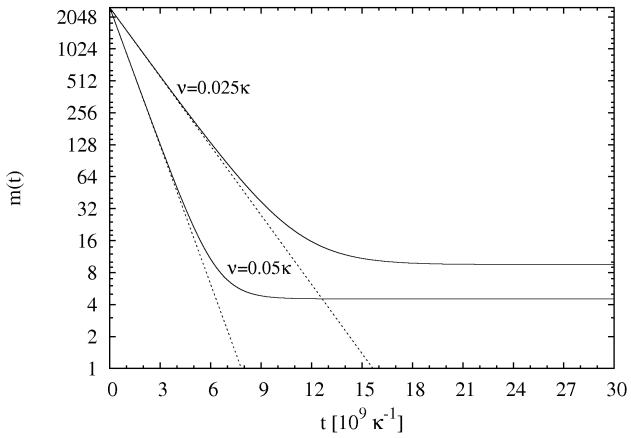

Figure 2.7: Logarithmic plot of the time evolution of the mean phonon number m for $\eta = 0.1$, $g_{\text{eff}} = 0.0005\,\kappa$, and $\delta_{\text{eff}} = \frac{1}{2}\kappa$ for two different phonon frequencies ν. The solid lines have been obtained from a numerical solution of the cooling equations (2.55)–(2.57) for the initial conditions in Eq. (2.75) and $m(0) = 2500$. The dashed lines assume an exponential cooling process with the rate γ in Eq. (2.78). Both solutions coincide very well when m is far away from its stationary state value.

When we compare the explicit analytic expressions for the cooling rates $\gamma_{\delta_{\text{eff}}=\nu}$ and $\gamma_{\delta_{\text{eff}}=\frac{1}{2}\kappa}$ of Eq. (2.80) and (2.81) respectively we find that

$$\frac{\gamma_{\delta_{\text{eff}}=\frac{1}{2}\kappa}}{\gamma_{\delta_{\text{eff}}=\nu}} \quad = \quad \frac{\kappa}{8\nu}. \tag{2.82}$$

Looking at this in another way, choosing $\delta_{\text{eff}} = \frac{1}{2}\kappa$ instead of $\delta_{\text{eff}} = \nu$ yields a speed up of the cooling process as $\gamma_{\delta_{\text{eff}}=\frac{1}{2}\kappa}$ is about $\kappa/8\nu$ times larger than $\gamma_{\delta_{\text{eff}}=\nu}$ when $\kappa > 8\nu$. This is confirmed by Figures 2.7 and 2.8 which show that choosing $\delta_{\text{eff}} = \frac{1}{2}\kappa$ in the weak confinement regime not only leads to a lower stationary state phonon number but also to a significant speed up of the cooling process. This detuning is also the better choice in order to minimise the stationary state phonon number in the weak confinement regime. Large cooling rates are important when the purpose of using a cavity is to avoid spontaneous emission from the particle. In the next section we discuss the importance of speeding up the cooling process so that spontaneous emission from the excited state $|1\rangle$ remains negligible for a much wider range of single particle-cavity cooperativity parameters $g^2/\kappa\Gamma$ [93].

Further Discussion

Looking once more at Figs. 2.7 and 2.8 we can see that both feature plots where the parameters used for ν are less than κ. Thus *both these figures* reflect the cooling be-

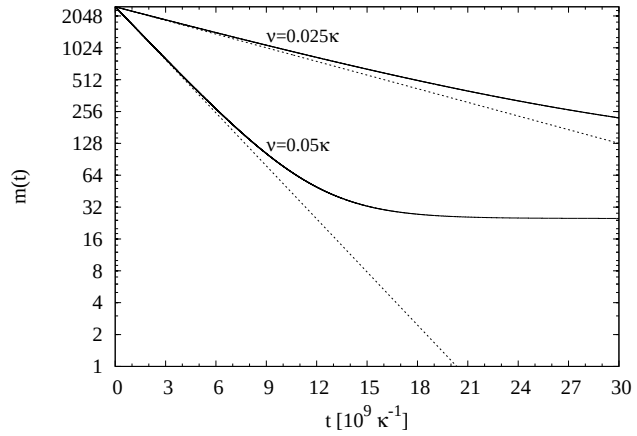

Figure 2.8: Logarithmic plot of the time evolution of the mean phonon number m for the same experimental parameters as in Figure 2.7 but with $\delta_{\text{eff}} = \nu$. Again, the solid lines have been obtained from a numerical solution of the cooling equations (2.55)–(2.57) for the initial conditions in Eq. (2.75) and $m(0) = 2500$. The dashed lines assume an exponential cooling process with the cooling rate γ in Eq. (2.78). Although κ and ν remain the same, we now observe slower cooling processes with higher stationary state phonon numbers m^{ss}.

haviour of the particle when it operates in the *weak confinement regime*. As we have already pointed out using Fig. 2.6, all motional states that are at ν intervals that fall under the resonance will become excited. Then, when the detuning is set to half the resonance width the probability of the red sideband transition occuring is optimised. This can be clearly seen when both Fig. 2.7 and Fig. 2.8 are compared. In Fig. 2.8 the cooling rate is gradual and more slow than in Fig. 2.7 where the cooling rate is actually quite fast and results in much smaller values of m_{ss} than in Fig. 2.8. This is consistent with the weak confinement regime and the choice of parameter values for δ_{eff} as indicated in Fig. 2.6. The optimal value of $\delta_{\text{eff}} = \kappa/2$ was used in Fig. 2.7 and this gave enhanced cooling rates and lower values of m_{ss} than in Fig. 2.8 where $\delta_{\text{eff}} = \nu$ was used.

2.4.5 Avoiding spontaneous emission from the particle

Avoiding spontaneous emission from the excited electronic state $|1\rangle$ *into free space* is especially important when it comes to the cooling of molecules, where it could result in the population of states, where the particle no longer experiences the cooling laser. As briefly mentioned in the introduction, the interaction between a molecule and a cavity can play an important role in the cooling dynamics of such a system. In this section we shall elaborate a bit more on the mechanics of this role and use some of our earlier results to shed some light on understanding what lies behind this mechanism. Then, as

a final point we shall show how previous work by other authors ties in with our own deductions.

To begin it will be useful to define the so called cooperativity parameter of the cavity system $\eta_c = g^2/\kappa\Gamma$ where the interaction strength between the cavity field and the atom g is defined as

$$g \equiv \frac{2d}{\hbar}\sqrt{\frac{\hbar\omega_c}{2\epsilon_0\mathcal{V}}}. \tag{2.83}$$

Here $d = |\mathbf{D}_{01}|$ is the dipole matrix element of the atomic transition and $\mathcal{V}$ is the volume of the cavity mode [94] . As we shall see η_c is also the ratio of the spontaneous emission rate into the cavity to the spontaneous emission rate into free space. One can write η_c purely as a function of the cavity parameters

$$\eta_c \;=\; \frac{3Q\lambda_c^3}{4\pi^2\mathcal{V}} \tag{2.84}$$

and where Q is the quality factor of the cavity which in our case is $Q = \omega_c/\kappa$, and $\lambda_c = 2\pi c/\omega_c$ is the wavelength of the cavity field resonant with the atomic transition [94]. Using the definition of the cavity atom interaction strength we find the aforementioned ratio through the calculation

$$\eta_c \;=\; \frac{g^2}{\kappa\Gamma} \;=\; \frac{2d^2\omega_c}{\hbar\epsilon_0 L^3\kappa\Gamma} \;=\; \frac{2d^2Q}{\hbar\epsilon_0\mathcal{V}\Gamma} \;=\; \frac{\Gamma_c}{\Gamma}, \tag{2.85}$$

where Γ_c is the spontaneous emission rate into the cavity

$$\Gamma_c \;=\; \frac{2d^2Q}{\hbar\epsilon_0\mathcal{V}}. \tag{2.86}$$

Clearly then when $\eta_c < 1$ the probability for the light to be scattered into free space is the dominant effect making it more likely that in the case of molecular cooling the states where the molecule does not see the cooling laser will become populated. Thus for the case of molecular cooling it will be useful to estimate the parameter regime where spontaneous emission from the particle into free space remains highly unlikely. In the Lamb-Dicke limit and the parameter regime given by Eq. (2.22), Eq. (2.34) shows that the population in $|1\rangle$ scales essentially as Ω^2/Δ^2. We therefore assume in the following that

$$\gamma \;\gg\; \frac{\Gamma\Omega^2}{4\Delta^2}, \tag{2.87}$$

i.e. that the cooling rate is much larger than the probability density for the spontaneous

emission of a photon from the particle. For $\delta_{\text{eff}} = \frac{1}{2}\kappa$ and γ as in Eq. (2.80) and when taking the definition of g_{eff} in Eq. (2.38) into account, we see that this condition applies when

$$\frac{g^2}{\kappa\Gamma} \gg \frac{\kappa^4 + 4\nu^4}{8\eta^2\nu\kappa^3}. \tag{2.88}$$

Since $\eta \ll 1$, the right hand side of this equation is in general much larger than one. This means, spontaneous emission from the particle is only negligible, when the cavity is operated in the so-called strong coupling regime. If the cavity decay rate κ is much smaller than 4ν, one should choose $\delta_{\text{eff}} = \nu$ and the cooling rate simplifies to the expression in Eq. (2.81). In this case, condition (2.87) simplifies to

$$\frac{g^2}{\kappa\Gamma} \gg \frac{\kappa^2 + 16\nu^2}{64\eta^2\nu^2}. \tag{2.89}$$

Since $\eta \ll 1$, we find again that the cavity needs to be operated within the strong coupling regime.

The Vuletic group and Morigi and co workers have all found that the cooperativity parameter plays a role in determining the size of the final phonon number [18, 39]. In fact the experiments carried out by the Vuletic group measure scatter rates into the cavity against scatter rates into free space for an experimental determination of the cooperativity parameter η_c [41]. Both groups have found an analytic expression of a similar form for m_{ss} which looks like

$$m_{\text{ss}} = \frac{\kappa^2}{16\nu^2} + \frac{C}{4\eta_c}\left(1 + \frac{\kappa^2}{16\nu^2}\right) \tag{2.90}$$

where C is a dimensionless parameter that depends on the cooling geometry. Using the Vuletic-Morigi form of m_{ss} it is easy to see how the cooperativity parameter affects cooling to the ground state. If $\Gamma_c \gg \Gamma$ then η_c becomes much larger than 1 and the Vuletic-Morigi steady state in Eq. (2.90) reduces to the same result we found for m_{ss} in the strong confinement regime (q.v Eq. (2.69)). Also to get this result Vuletic-Morigi need $\eta_c \gg 1$ which corresponds to the strong coupling regime. This then is consistent with the deduction we have just made regarding the parameter regime for suppression of spontaneous emission being the strong coupling regime. On the other hand there is the situation of moderate coupling when $\eta_c \lesssim 1$. In this case $\Gamma_c \lesssim \Gamma$ and we find that the Vulteic-Morigi final phonon number is proportional to $1/\eta_c$. It is limited by the value of the cooperativity parameter or $m_{\text{ss}} \propto \eta_c^{-1}$. In other words for $\eta_c \sim 1$ the cooling process becomes a mixture of cavity and ordinary laser cooling.

On a final note we shall briefly explain why the Vuletic-Morigi steady state feature η_c yet it seems to play no role in our expression for m_{ss} in Eq. (2.69). When one relaxes the

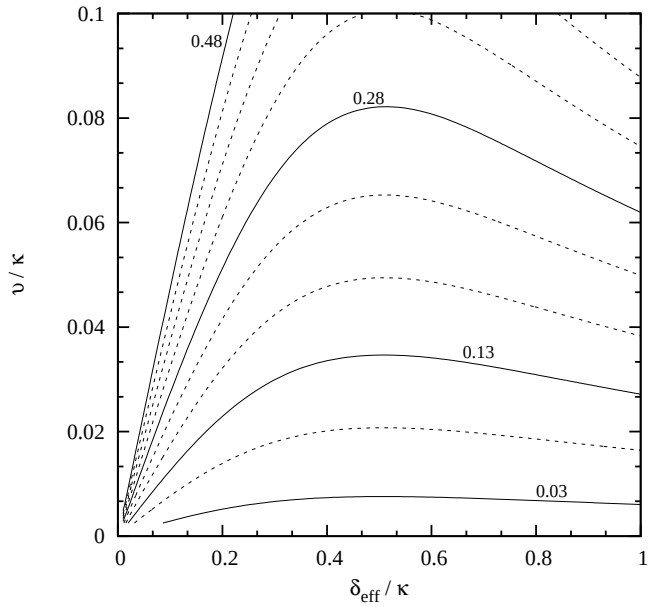

Figure 2.9: Contour plot of $m^{ss}/m^{ss}_{\delta_{eff}=\nu}$ as a function of δ_{eff} and ν. This plot has been obtained using Eq. (2.61) for $\eta = 0.1$ and $g_{eff} = 0.0001\,\kappa$ and shows that choosing the detuning δ_{eff} comparable to κ leads to much lower stationary state phonon numbers when $\nu \ll \kappa$.

condition of eliminating the excited state adiabatically in the conditions of Eq. (2.22) we find Γ dependent corrections to Eqs. (2.55), (2.56), and (2.57). These come from the previously neglected Liouvillian $\mathcal{L}_{par}(\rho)$ of Eq. (2.45) calculated to leading order in Δ that corresponded to the spontaneous emission of the particle.

In conclusion then, using the various definitions of the cooperativity parameter one can see that the final phonon number and corresponding steady state temperature is determined by the opposing mechanisms of cooling from photons scattered into the cavity and heating from the recoil energy created by the photons scattered into free space.

2.4.6 Comparing $\delta_{eff} = \nu$ with $\delta_{eff} = \frac{1}{2}\kappa$ in cavity cooling

Previous papers (see e.g. Refs. [16–19]) mainly focus their analysis on cavity cooling in the strong confinement regime, where one should choose $\delta_{eff} = \nu$ and where it is in principle possible to cool the trapped particle to phonon numbers well below one. Our purpose here is to point out that there are three distinct advantages in choosing δ_{eff} differently, i.e. close to $\frac{1}{2}\kappa$ (q.v Eq. (2.63)), when it is experimentally not possible to enter the strong confinement regime:

1. A reduction of the stationary state phonon number. As already pointed out in Eq. (4.4.2), $m^{ss}_{\delta_{eff}=\frac{1}{2}\kappa}$ equals the square root of the stationary state phonon number $m^{ss}_{\delta_{eff}=\nu}$ and is hence significantly smaller than $m^{ss}_{\delta_{eff}=\nu}$ for a wide range of

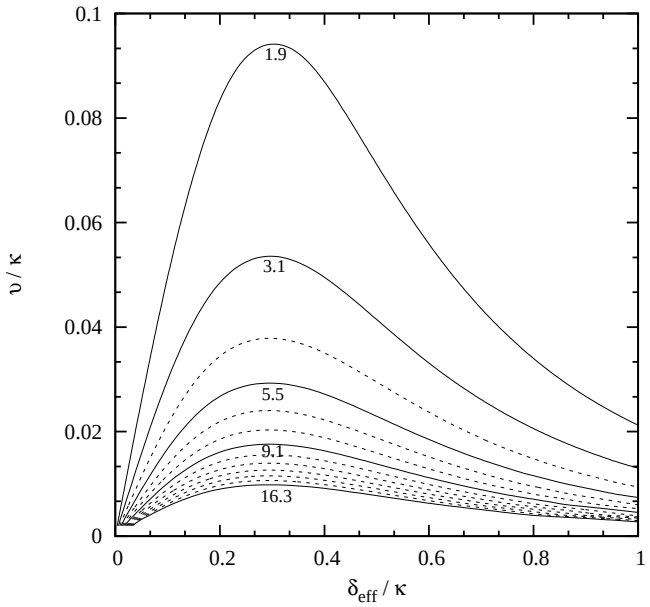

Figure 2.10: Contour plot of $\gamma/\gamma_{\delta_{\rm eff}=\nu}$ as a function of $\delta_{\rm eff}$ and ν for the same parameters as in Figure 2.9. This plot has been obtained using Eq. (2.78) and shows that that choosing the detuning $\delta_{\rm eff}$ comparable to κ leads to a significant speed up the cooling process when $\nu \ll \kappa$.

experimental parameters. This result is confirmed by Figure 2.9 which shows $m^{\rm ss}/m^{\rm ss}_{\delta_{\rm eff}=\nu}$ for relatively small phonon frequencies ν and a wide range of effective detunings $\delta_{\rm eff}$. In order to minimise the stationary state phonon number, one should choose $\delta_{\rm eff}$ as in Eq. (2.63).

2. An increase of the cooling rate. Calculating the ratio $\gamma_{\delta_{\rm eff}=\frac{1}{2}\kappa}/\gamma_{\delta_{\rm eff}=\nu}$ using Eqs. (2.80) and (2.80) for fixed values of η, $g_{\rm eff}$, κ, and ν, we find

$$\frac{\gamma_{\delta_{\rm eff}=\frac{1}{2}\kappa}}{\gamma_{\delta_{\rm eff}=\nu}} \;=\; \frac{\kappa}{2\nu}\cdot\frac{\kappa^2(\kappa^2+16\nu^2)}{4\kappa^4+16\nu^4} \tag{2.91}$$

which scales approximately as $\kappa/8\nu$, as already pointed out in Eq. (2.82). This means, choosing $\delta_{\rm eff}$ close to $\frac{1}{2}\kappa$ results in a significant speedup of the cooling process. This result is confirmed by Figure 2.10 which shows $\gamma/\gamma_{\delta_{\rm eff}=\nu}$ for the same parameters as in Figure 2.9.

3. Minimising spontaneous emission from the excited electronic state $|1\rangle$ of the trapped particle. This is important, when it comes for example to the cooling of molecules, where such an emission might populate states, where the particle no longer experiences the cooling laser. As pointed out in the previous paragraph, the cooling rate γ is much higher when $\delta_{\rm eff}$ is close to $\frac{1}{2}\kappa$. As a consequence, the restrictions which need to be imposed on the minimum size of the single particle cooperativity parameter $g^2/\kappa\Gamma$ are therefore much weaker in this case. The re-

duction of the cooling time might moreover help to balance unconsidered heating processes which are, for example, due to stray fields.

2.5 Problem with above analysis

It must be pointed out that in all of our previous analyses we made considerable use of the difference in timescales associated with the evolution of the system's dynamic variables. In particular we were able to use the conditions of Eq. (2.51) to find expressions for the quasi-stationary states. This is all well and good as long as such quasi - stationary states are actually reached by the system. On closer inspection of Eqs. (2.55) and (2.56) we find that there are 4 equations that evolve on a timescale defined by ν. In fact if we replace the variables that move on the timescale defined by κ by their quasi stationary values in these 4 equations we can write them in the form of a single matrix equation in η

$$\begin{pmatrix} \dot{k}_x \\ \dot{k}_u \\ \dot{k}_7 \\ \dot{k}_8 \end{pmatrix} = \begin{pmatrix} 0 & -\nu & 0 & 0 \\ \nu & 0 & 0 & 0 \\ 0 & 0 & 0 & -2\nu \\ 0 & 0 & 2\nu & 0 \end{pmatrix} \begin{pmatrix} k_x \\ k_u \\ k_7 \\ k_8 \end{pmatrix} + \begin{pmatrix} -2\eta g_{\text{eff}} k_y^{ss} \\ 0 \\ -2\eta g_{\text{eff}} k_4^{ss} \\ -2\eta g_{\text{eff}} k_2^{ss} \end{pmatrix}. \tag{2.92}$$

The matrix equation in this equation has the eigenvalues

$$\{\lambda_1, \lambda_2, \lambda_3, \lambda_4\} \quad = \quad \{i\nu, -i\nu, i2\nu, -i2\nu\}. \tag{2.93}$$

Clearly the the eigenvalues do not have negative real parts meaning of course that our 4 rate equations in Eq. (2.92) do not evolve to a steady state solution. They fail the eigenvalue negative real part criteria for stability. Thus there are no quasistationary states for these equations in zeroth or first order. It is therefore necessary to go to an order higher in the η parameter to determine whether stationary state solutions do actually exist.

Taking into account terms in the rate equations that go one order higher in the small parameter η one would obviously make the Lamb-Dicke expansion to second order in Eq. (2.41). Doing so then introduces the second order terms into the Hamiltonian for the system and subsequently all rate equations will change and new coherences will be formed. This approach has the disadvantage of being unable to choose what new coherences will emerge as the result of the second order contribution in the Hamiltonian. However, there exists another approach to going to second order in the small parameter which is different to performing a Lamb-Dicke expansion. We shall explore this approach in the next chapter. We shall see that its advantage lies in its technique

for using groups of rate equations to determine expressions for coherenece to a certain order. Such coherences can then be substituted back into other groups of rate equations thereby determining another coherence to a required order. Before attempting to use this approach on the model of the trapped particle in a cavity we firstly test this new approach within the scenario of the trapped particle interacting with the free radiation field.

Chapter 3

Laser Cooling of Single Trapped Particle beyond the Lamb - Dicke Approximation

The chapter shall highlight one of the most important distinctions in quantum mechanics, namely the difference between a fermionic system and a bosonic one. The previous chapter explored the system of a weakly driven two level system interacting with a cavity which experiences photon loss. In the weak saturation limit of the laser it was possible to make the approximation of eliminating the excited state of the 2 level system. In this chapter we shall explore the system of the so called free particle. The term "free particle" is a bit of a misnomer as the system which we wish to investigate is actually that of a particle confined to a potential which experiences photon loss from spontaneous emission through interaction with the environment. The description of free refers to the "free radiation field" in space as opposed to the field within the cavity. Indeed, from the choice of formalism that describes the confined particle, it is possible to define commutator relationships that allow us to continue with the rate equation approach whilst at the same time including the action of a fermionic algebra. To paint the picture in a different way, using the cavity model of the previous chapter and having eliminated the excited state found us working with the bosonic algebra defined by $[b, b^\dagger] = 1$. In the "free particle" model however we shall find ourselves working not only with the familiar bosonic algebra but also with an additional fermionic algebra defined by the operators that describe the 2 level system of the particle.

3.1 Theoretical Model

The free particle model is similar to the cavity model from the previous chapter. The main difference being obviously no cavity and a description of the effect of the interac-

tion with the environment. Both of these differences combine to make the spontaneous emission of the particle significant as opposed to this effect being negligible in the strong coupling regime of the cavity environment. So then, we can begin by describing the theoretical model and the experimental set up. As already mentioned we have a confined particle where the particle is driven by a laser field. If the trapping potential is approximately harmonic [95] we can describe the motional states of the particle by a harmonic oscillator Hamiltonian. Again we describe the external motion of the particle as quantised with the annihilation operator b. We now also introduce the model which allows us to predict the time evolution of the mean phonon number.

3.1.1 The Hamiltonian

Our model of a single particle trapped in a one dimensional potential inside a free radiation field whose electronic transition is driven by an external laser field can be written as

$$H = H_{\text{electron}} + H_{\text{nucleus}} + H_{\text{field}} + H_{\text{dip}}\,. \tag{3.1}$$

The first two terms of the Hamiltonian describe the free energy of the electronic states and the quantised vibrational modes of the trapped particle. The energy of the free radiation field surrounding the trapped particle is described by the third term. The dipole interaction of the electronic states of the particle with both electromagnetic fields present in the system, which in our case are the laser and the free radiation fields, are taken into account by the last term. In the following we consider the particle to be effectively a two level system with ground state $|0\rangle$ and excited state $|1\rangle$ and the energies $\hbar\omega_0$, $\hbar\nu$, and $\hbar\omega_k$ denote the energy of a single atomic excitation, of a single phonon excitation of the quantised vibrational mode of the trapped particle, and of the modes of the free radiation field, respectively. Here we take into account the free radiation field. It is the interaction between this field and the particle that causes the excited state of the particle to spontaneously decay. In the cavity model we adiabatically eliminated the excited state thereby relinquishing the need to consider spontaneous decay (c.f. Section 2.3). The first three terms of Eq. (3.1) can then be written as

$$\begin{aligned} H_{\text{electron}} &= \hbar\omega_0\,\sigma^+\sigma^-\,, \\ H_{\text{nuclei}} &= \hbar\nu\; b^\dagger b\,, \\ H_{\text{field}} &= \sum_{\mathbf{k}\lambda} \hbar\omega_k\, a^\dagger_{\mathbf{k}\lambda} a_{\mathbf{k}\lambda}\,, \end{aligned} \tag{3.2}$$

where the operators $a_{\mathbf{k}\lambda}$ are the annihilation operator of a photon with wavevector $\mathbf{k}$ and polarisation λ. These operators obey the commutator relation

$$\left[a_{\mathbf{k}\lambda}, a^{\dagger}_{\mathbf{k}\lambda}\right] = 1 \tag{3.3}$$

which is the usual commutator relation for bosonic annihilation operators. All other photon commutators are equal to zero. Next we have a closer look at H_{dip}, the dipole Hamiltonian. As previously mentioned, this Hamiltonian describes the dipole interaction of the electronic states $|0\rangle$ and $|1\rangle$ of the trapped particle with the free radiation field and the applied laser field. Within the usual dipole approximation[1], it can be written as

$$H_{\mathrm{dip}}(t) = e\mathbf{D}\cdot\left[\mathbf{E}_{\mathrm{field}}(\mathbf{R}) + \mathbf{E}_{\mathrm{L}}(\mathbf{R},t)\right]. \tag{3.4}$$

As in the previous chapter we denote the electronic charge of the electron as e and the dipole moment of the particle as $\mathbf{D}$. In fact in this case $\mathbf{D}$ is the position operator of the outer most electron of the particle with respect to its atomic nuclei at position $\mathbf{R}$ while $\mathbf{E}_{\mathrm{field}}(\mathbf{R})$ and $\mathbf{E}_{\mathrm{L}}(\mathbf{R},t)$ denote the electric field of the free radiation and of the laser field at time t, respectively. Using Eq. (2.5) we find he electric field operators are given by

$$\begin{aligned}\mathbf{E}_{\mathrm{field}}(\mathbf{R}) &= \mathrm{i}\sum_{\mathbf{k}\lambda}\sqrt{\frac{\hbar\omega_k}{2\epsilon_0 L^3}}\,\epsilon_{\mathbf{k}\lambda}\,a_{\mathbf{k}\lambda}\,\mathrm{e}^{\mathrm{i}\mathbf{k}\cdot\mathbf{R}} + \mathrm{H.c.}\,,\\ \mathbf{E}_{\mathrm{L}}(\mathbf{R},t) &= \mathbf{E}_0\,\mathrm{e}^{\mathrm{i}(\mathbf{k}_{\mathrm{L}}\cdot\mathbf{R}-\omega_{\mathrm{L}}t)} + \mathrm{c.c.}\end{aligned} \tag{3.5}$$

with L^3 being the quantisation volume of the free radiation field and $\epsilon_{\mathbf{k}\lambda}$ being a unit length polarisation vector orthogonal to $\mathbf{k}$. Here $\mathbf{E}_0$, $\mathbf{k}_{\mathrm{L}}$, and ω_{L} are the amplitude, the wave vector of length k_{L}, and the frequency of the applied laser field.

3.1.2 The displacement operator

Having become familiar with our Hamiltonian friends we are now in a position to understand the central role played by the dipole Hamiltonian that facilitates the energy changing process which ultimately results in a cooling mechanism. As pointed out in the previous chapter, when the recoil energy of the particle is much smaller than the energy difference $\hbar\nu$ between subsequent trap levels then transitions that change the vibrational quantum number m by more than 1 are suppressed. This situation occurs if the extension of the traps ground state wave function is much smaller than the wavelength of the laser

[1] This means, we assume that the size of the atom is small compared to the relevant optical wavelength.

$$\begin{aligned} \sqrt{\langle 0|\mathbf{R}^2|0\rangle} &\ll \lambda_{\mathrm{L}} \\ \sqrt{\langle 0|(\mathbf{k}\cdot\mathbf{R})^2|0\rangle} &\ll 1\,. \end{aligned} \tag{3.6}$$

H_{dip} features the interaction of both the free radiation field and the laser field with the particle. However both fields are distinct from each other and as such correspond to distinct wave vectors. To highlight this distinction in direction between both field it will prudent to assume different directions for each field. This difference in direction also contributes to changing the displacement of the particles position. We shall assume that the incoming laser has the same direction as the quantised motion of the trapped particle so as to maximise the effect of the cooling laser. Doing so we can establish the relationship between the wavevector of the laser field and the phonon operators which we are already familiar with from the previous chapter (c.f. Eq. (2.11))[2]. Taking Eq. (2.11) into account, it is easy to see how the laser interaction affects the position of the particles since the Hamiltonian itself is a function of the particle displacement operator [97]

$$D(\mathrm{i}\eta) \equiv \mathrm{e}^{-\mathrm{i}\eta(b+b^\dagger)} \tag{3.7}$$

which is a unitary operator with the pairwise consistent relations

$$\begin{aligned} D(\mathrm{i}\eta)\, b\, D(\mathrm{i}\eta)^\dagger &= b + \mathrm{i}\eta\,, \\ D(\mathrm{i}\eta)^\dagger\, b\, D(\mathrm{i}\eta) &= b - \mathrm{i}\eta\,. \end{aligned} \tag{3.8}$$

The direction of the free radiation field can now be distinguished from $\mathbf{k}_{\mathrm{L}}$ by defining its direction in terms of the general wave vector $\mathbf{k}$ of length k with the polar coordinates ϑ and φ such that

$$\mathbf{k} = k \begin{pmatrix} \sin\vartheta\cos\varphi \\ \sin\vartheta\sin\varphi \\ \cos\vartheta \end{pmatrix}. \tag{3.9}$$

Then, if we choose the z-axis in the direction of the cooling laser we find that

$$\mathbf{k}\cdot\mathbf{R} = k\sin\vartheta\left[R_x\cos\varphi + R_y\sin\varphi\right] + \frac{\eta k\cos\vartheta}{k_{\mathrm{L}}}\left(b + b^\dagger\right), \tag{3.10}$$

[2]Notice that Eq. (2.11) applies as long as the trapping potential seen by the atom does not depend on its respective electronic state. This means, the following calculations apply to a trapped ion, to a single atom confined in a magneto optical trap, and to single atoms with a so-called magical wavelength [96].

where R_x and R_y are the x and the y component of the vector $\mathbf{R}$. It should also be noted that here $\mathbf{R}$ is a vector whose z component is an operator and *not* a number. As such the R_z component actually represents the position operator of the particle with respect to the z - direction. R_x and R_y are numbers multiplied by the identity and as such can commute with any operator. From the commutativity property we find that

$$\mathrm{e}^{-\mathrm{i}\mathbf{k}\cdot\mathbf{R}}\,\rho\,\mathrm{e}^{\mathrm{i}\mathbf{k}\cdot\mathbf{R}} = \mathrm{e}^{-\mathrm{i}\frac{\eta k\cos\vartheta}{k_\mathrm{L}}\left(b+b^\dagger\right)}\,\rho\,\mathrm{e}^{\mathrm{i}\frac{\eta k\cos\vartheta}{k_\mathrm{L}}\left(b+b^\dagger\right)}. \tag{3.11}$$

So quantising the motion in the z direction allows us to cancel the displacement operators defined by the R_x and R_y components.

Remark. It is worth mentioning the importance of Eq. (3.10) with respect to the displacements to the particle from the interaction between it and both electromagnetic fields. Indeed, by choosing the laser direction along the z-axis, Eq. (3.10) reflects the combined effect of the displacements caused by both the laser and free radiation fields. The combination of both effects is introduced through the z - component dependence in the following manner.

$$k\cos\vartheta R_z \;=\; k\cos\vartheta\sqrt{\frac{\hbar}{2m\nu}}\left(b+b^\dagger\right) \;=\; \frac{\eta k\cos\vartheta}{k_\mathrm{L}}\left(b+b^\dagger\right). \tag{3.12}$$

Here also we have made use of the relation $\eta/k_\mathrm{L} = \sqrt{\hbar/2m\nu}$. Thus the laser interaction forms part of the recoil contribution due to the free radiation field!

We can now write the Hamiltonian H_dip in Eq. (3.4) as a function of displacement operators, so that it becomes

$$\begin{aligned} H_\mathrm{dip}(t) \;=\; & e\left[\mathbf{D}_{01}\,\sigma^- + \mathrm{H.c.}\right]\cdot\Bigg[\mathbf{E}_0^*\,D(\mathrm{i}\eta)\,\mathrm{e}^{\mathrm{i}\omega_\mathrm{L}t} \\ & -\mathrm{i}\sum_{\mathbf{k}\lambda}\sqrt{\frac{\hbar\omega_k}{2\epsilon_0 L^3}}\,\epsilon_{\mathbf{k}\lambda}\,a_{\mathbf{k}\lambda}^\dagger\,D\left(\frac{\mathrm{i}\eta k\cos\vartheta}{k_\mathrm{L}}\right)\mathrm{e}^{-\mathrm{i}k\sin\vartheta\left[R_x\cos\varphi+R_y\sin\varphi\right]}\Bigg] \\ & +\mathrm{H.c.} \end{aligned} \tag{3.13}$$

This equation reflects the coupling that is established by the cooling laser between the electronic states $|0\rangle$ and $|1\rangle$ of the trapped particle and its quantised motion. In addition the coupling to the free radiation field is the origin of spontaneous emission and recoil effects which limit the final phonon number of the cooling process as we shall see shortly.

3.1.3 Interaction picture

Next, we wish to move to an interaction picture that will be more convenient for the derivation of the master equation. Choosing

$$H_0 \;=\; \hbar\omega_{\mathrm{L}}\,\sigma^{+}\sigma^{-} + H_{\mathrm{field}} \tag{3.14}$$

with H_{field} as in Eq. (3.2) and neglecting relatively fast oscillating terms as part of the usual rotating wave approximation, the interaction Hamiltonian H_{I},

$$H_{\mathrm{I}} = U_0^{\dagger}(t,0)\,(H - H_0)\,U_0(t,0)\,, \tag{3.15}$$

becomes

$$\begin{aligned} H_{\mathrm{I}} \;=\; & \sum_{\mathbf{k}\lambda} \hbar g_{\mathbf{k}\lambda}\,\sigma^{-} a_{\mathbf{k}\lambda}^{\dagger}\, D\left(\frac{\mathrm{i}\eta k\cos\vartheta}{k_{\mathrm{L}}}\right) \mathrm{e}^{-\mathrm{i}k\sin\vartheta\left[R_x\cos\varphi + R_y\sin\varphi\right]}\, \mathrm{e}^{\mathrm{i}(\omega_k-\omega_{\mathrm{L}})t} \\ & + \frac{1}{2}\hbar\Omega\, D(\mathrm{i}\eta)\sigma^{-} + \mathrm{H.c.} + \hbar\Delta\sigma^{+}\sigma^{-} + \hbar\nu\; b^{\dagger}b\,. \end{aligned} \tag{3.16}$$

Here Δ denotes the detuning between the laser and the relevant atomic transition and Ω and $g_{\mathbf{k}\lambda}$,

$$\begin{aligned} \Omega \;&=\; \frac{2e\,\mathbf{D}_{01}\cdot\mathbf{E}_0^{*}}{\hbar}\,, \\ g_{\mathbf{k}\lambda} \;&=\; -\mathrm{i}e\sqrt{\frac{\omega_k}{2\hbar\epsilon_0 L^3}}\,\mathbf{D}_{01}\cdot\epsilon_{\mathbf{k}\lambda} \end{aligned} \tag{3.17}$$

are the usual laser Rabi frequency and the atom-field coupling constant.

3.1.4 Spontaneous emission and recoil

Our free particle model is an example of a system - reservoir interaction which can also be called an open quantum system [98, 99]. Analysis of the energy change in such systems is governed by the dynamics of the master equation. The state of such systems can be represented by a density matrix whose evolution is determined by von Neumann - Liouville equation . Solving the equation requires use of second order perturbation theory through iterative integration. However validity of the solution is based on the assumption that the density matrix represents an ensemble of states. Before single particle systems were experimentally feasible the use of the density matrix approach to deriving a master equation could be applied to most quantum systems that comprised many particles. However a density matrix that describes an ensemble of states led to difficulties when used to describe a system of a single particle. In experiments that observe photon emission from a large atomic ensemble a density matrix is sufficient to

describe the observed fluorescence signal as the average over many individual trajectories. The ensemble description applied to a single particle system meant that probability densities were being calculated for the emission of *any* photon at times $t_1, \cdots, t_n$ in a time interval $[0, t]$. So the big problem with applying the density matrix formalism to single particle systems was that many more photons could have been emitted between times t_i. Thus was motivated the need for an approach to describe sequential photon emissions as otherwise many emission events would be hidden when using a density matrix approach. Several new methods were developed to account for the situation of the single particle. [98, 100–102]. The method favoured in our analysis is that used by Hegerfeld. The method is based upon repeated gedanken measurements of the system considered. This is achieved by considering the concept of environment-induced measurements in rapid succession at times Δt apart [101]. Here Δt should be much smaller than the level lifetimes but should also be larger than the inverse optical frequencies. So

$$1/\omega_0 \ll \Delta t \ll 1/\Gamma\,. \tag{3.18}$$

The environment induced measurements on a single two level system can be interpreted as an ensemble of many 2 level systems each of which has its own quantised radiation field whereby our 2 level system is a member of the ensemble. Thus the ensemble represents a collection of different states all of whom can be collectively described by the appropriate density operator $\rho(\Delta t)$.

There are 2 distinct parts to this approach. In the periods of time between photon detections the time development of the state of the atom will now be described by a so-called *Conditional Hamiltonian* or H_{cond}, the condition being that no photons are detected. The first part of this approach involves determining this non-Hermitian operator. Once a photon is detected the atom "resets" back to its ground state. The second part of the approach is determining the *Reset Operator* or $\mathcal{R}(\rho)$ which is defined in terms of the density operator $\rho(\Delta t)$.

In our system we suppose the state of the laser-driven trapped particle is at $t = 0$ given by the density matrix ρ, while the free radiation field is in its vacuum state $|0\rangle$. Taking this into account, the density matrix $\rho(\Delta t)$ of the particle at time Δt can be written as [101]

$$\rho(\Delta t) \;=\; U_{\rm cond}(\Delta t, 0)\,\rho\, U^{\dagger}_{\rm cond}(\Delta t, 0) + \mathcal{R}(\rho)\Delta t\,, \tag{3.19}$$

where Δt denotes the typical response time of the environment, i.e. the typical time it

takes the environment to absorb a photon from the free radiation field, and where

$$\begin{aligned} U_{\text{cond}}(\Delta t,0) &= \langle 0|\, U_{\text{I}}(\Delta t,0)\,|0\rangle\,, \\ \mathcal{R}(\rho) &= \lim_{\Delta t\to 0}\frac{1}{\Delta t}\sum_{\mathbf{k}\lambda}\langle 1_{\mathbf{k}\lambda}|\, U_{\text{I}}(\Delta t,0)\,|0\rangle\,\rho\,\langle 0|\, U_{\text{I}}^{\dagger}(\Delta t,0)\,|1_{\mathbf{k}\lambda}\rangle\,. \end{aligned} \tag{3.20}$$

The first term in Eq. (3.19) describes the subensemble with no photon emission in Δt. The second term in this equation is the unnormalised state of the subensemble after emission and then absorption by the environment of the respective photon in Δt [103]. Taking the time derivation of $\rho(\Delta t)$ on the coarse grained time scale Δt into account, we obtain the usual master equation

$$\dot{\rho} = -\frac{\mathrm{i}}{\hbar}\left[H_{\text{cond}}\,\rho - \rho\,H_{\text{cond}}^{\dagger}\right] + \mathcal{R}(\rho) \tag{3.21}$$

in Lindblad form. As we have already stated a second order perturbation is used to solve the von Neumann - Liouville equation and indeed a similar approach is used to calculate H_{cond} and $\mathcal{R}(\rho)$. Since the displacement operator $D(\mathrm{i}\eta)$ is a unitary operator, i.e.

$$D(\mathrm{i}\eta)D(\mathrm{i}\eta)^{\dagger} = D(\mathrm{i}\eta)^{\dagger}D(\mathrm{i}\eta) = 1\,, \tag{3.22}$$

the derivation of the conditional Hamiltonian H_{cond} remains exactly the same as in the case, where the motion of the particle is not quantised. This means, we find that

$$H_{\text{cond}} = \frac{1}{2}\hbar\Omega\,D(\mathrm{i}\eta)\sigma^{-} + \text{H.c.} + \hbar\Delta\,\sigma^{+}\sigma^{-} + \hbar\nu\,b^{\dagger}b - \frac{\mathrm{i}}{2}\hbar\Gamma\,\sigma^{+}\sigma^{-}\,, \tag{3.23}$$

where the spontaneous decay rate Γ of the excited electronic state $|1\rangle$ is given by

$$\Gamma = \frac{e^2\omega_0^3}{3\pi\epsilon_0\hbar c^3}\,|\mathbf{D}_{01}|^2\,. \tag{3.24}$$

The displacement operator $D\left(\frac{\mathrm{i}\eta k\cos\vartheta}{k_{\text{L}}}\right)$ is, however, featured in the reset operator and represents the effect of recoil from spontaneous emission. The appearance of the displacement operator in the Liouvillian part of the master equation is a direct consequence of Eq. (3.16) that represents quantising the external motion of the particle. A detailed derivation of this expression based on quantum optical standard approximations can be found in App. A.2. Proceeding as described there and using first order perturbation theory to evaluate $U_{\text{I}}(\Delta t,0)$ in Eq. (3.20), we find that

$$\mathcal{R}(\rho) = \frac{3\Gamma}{8}\int_{-1}^{1}\mathrm{d}\zeta\,\sigma^{-}D(\mathrm{i}\eta\zeta)\,\rho\,D(\mathrm{i}\eta\zeta)^{\dagger}\sigma^{+}\left[\,1+|d_3|^2+\left(1-3|d_3|^2\right)\zeta^2\,\right] \tag{3.25}$$

where d_3 denotes the z-component of the normalised dipole vector $\mathbf{D}_{01}/|\mathbf{D}_{01}|$. The above reset operator is different from the one often used in the literature [10–12]. The reason for this is that the authors of these references consider only the case where $d_3 = 0$ which is well justified for certain atomic level schemes and laser configurations.

Remark. In our calculation of the conditional Hamilitonian H_{cond} no specific direction was chosen for the dipole vector. It is quite remarkable that in defining a general vector for $\mathbf{D}_{01}/|\mathbf{D}_{01}|$ it is possible to express the d_1 and d_2 degrees of freedom in terms of just the single d_3 degree of freedom which then vanishes in the calculation Γ (c.f. Eq. (A.32)).

Actually it's not that remarkable when one considers the polarisations of the driving laser. Suppose that the components of the normalised dipole (d_1, d_2, d_3) are aligned with the cartesian axes (x, y, z) respectively. Then, using a similar argument to that shown previously for the cavity in section 2.1 and Fig. 2.2, if the polarisation of the incident laser is in the x direction, then the induced dipole will oscillate in the x-direction. Since the dipole does not oscillate in the z direction then $d_3 = 0$.

The above reset operator $\mathcal{R}(\rho)$ is consistent with the reset operator of a free particle whose motion of the particle is not quantised. In this case, the displacement operator $D(\mathrm{i}\eta\cos\vartheta)$ becomes a number and it becomes straightforward to perform the integration over ζ. The result is indeed $\mathcal{R}(\rho) = \Gamma\,\sigma^-\,\rho\,\sigma^+$ which is independent of d_3, as it should.

3.2 Cooling equations

So now we come to our favourite part of the analysis of the free particle model from which we can find the differential equations of the expectation values like those that we encountered in Section 2.4.1. However in the free particle model as was already pointed out the effect of spontaneous emission is no longer negligible as the trapped particle experiences the interaction with the free radiation field. As such our generalised rate equation will have a different form which accounts for the presence of the displacement operator D in Eqs. (3.23) and (A.55). The task of deriving our rate equations which include the effects of the displacement operator is not as straightforward as the work involved in section (2.4.1).To overcome this problem, we now introduce two new operators x and y which replace the particle and the phonon operators σ^- and b, respectively. Both operators describe neither electronic excitations nor phonons. In the following we use these operators to derive a closed set of rate equations which predict the time evolution of the mean phonon number m. These are then used in Sections 4.3 and 4.4 to analyse the cooling process analytically as well as numerically.

3.2.1 Transformation of the Hamilitonian

We define the new operator x which we write, using the displacement operator, as

$$x \equiv D(\mathrm{i}\eta)\,\sigma^{-}\,. \tag{3.26}$$

The operator x differs from σ^{-} only by the fact that its application not only transforms $|1\rangle$ into $|0\rangle$ but also induces a kick, i.e. it simultaneously displaces the motion of the particle. The commutator relation between x and its adjoint highlights the fundamental difference between this model (free particle) and the other model (cavity) presented in this thesis. The difference being the fermionic algebra used to relate the atomic operators. Using the commutator relation Eq. (3.3), one can easily show that x obeys the commutator relation

$$\left[x, x^{\dagger}\right] = 1 - 2\,x^{\dagger}x\,. \tag{3.27}$$

The x operator is thus defined by the fermionic relationship of Eq. (3.27). The outcome of this will become apparent in the cooling equation derivations. Using Eqs. (3.3), (3.8), and (3.26) we find that the x operator and its adjoint $x^{\dagger}$ has the following commutator relation

$$\begin{aligned} [x, b] = -\left[x, b^{\dagger}\right] &= \mathrm{i}\eta\, x\,, \\ \left[x^{\dagger}, b\right] = -\left[x^{\dagger}, b^{\dagger}\right] &= -\mathrm{i}\eta\, x^{\dagger}\,. \end{aligned} \tag{3.28}$$

with respect to the phonon operators b and $b^{\dagger}$. Using these relations we can further show that

$$\begin{aligned} &\left[x, b^{\dagger}b\right] = -\mathrm{i}\eta\, x(b - b^{\dagger}) - \eta^2\, x\,, \\ &\left[x^{\dagger}, b^{\dagger}b\right] = \mathrm{i}\eta(b - b^{\dagger})x^{\dagger} + \eta^2\, x^{\dagger}\,, \\ &\left[x^{\dagger}x, b\right] = \left[x^{\dagger}x, b^{\dagger}\right] = \left[x^{\dagger}x, b^{\dagger}b\right] = 0\,. \end{aligned} \tag{3.29}$$

As the operators x and b and functions of them do not commute in general we find it more straightforward to transform b via a unitary transformation that will enable the x and y operators to commute. Defining y to be

$$y \equiv b - \mathrm{i}\eta\, x^{\dagger}x \tag{3.30}$$

and using the commutator relations in Eq. (3.29), we can easily show that y is a bosonic operator which obeys the commutator relation

$$\left[y, y^{\dagger}\right] = 1\,. \tag{3.31}$$

Then taking the commutators of x and y operators we find that they all commute.

$$\left[x, y\right] = \left[x^\dagger, y\right] = \left[x, y^\dagger\right] = \left[x^\dagger, y^\dagger\right] \quad = \quad 0\,. \tag{3.32}$$

All of these can be checked using the commutator relations in Eqs. (3.28) and (3.31).

Using the notation introduced in this section, the conditional Hamiltonian $H_{\rm cond}$ in Eq. (3.23) and the reset operator $\mathcal{R}(\rho)$ in Eq. (A.55) become

$$\begin{aligned} H_{\rm cond} &= \frac{1}{2}\hbar\Omega\left(x + x^\dagger\right) - \mathrm{i}\hbar\eta\nu\, x^\dagger x(y - y^\dagger) + \hbar\left(\Delta + \eta^2\nu\right) x^\dagger x + \hbar\nu\, y^\dagger y - \frac{\mathrm{i}}{2}\hbar\Gamma\, x^\dagger x\,, \\ \mathcal{R}(\rho) &= \frac{3\Gamma}{8}\int_{-1}^{1} \mathrm{d}\zeta\, x D(\mathrm{i}\eta(1-\zeta))^\dagger\, \rho\, D(\mathrm{i}\eta(1-\zeta))x^\dagger \\ &\quad \times\left[\,1 + |d_3|^2 + \left(1 - 3|d_3|^2\right)\zeta^2\,\right]. \end{aligned} \tag{3.33}$$

3.2.2 Time evolution of expectation values

We are now ready to begin deriving our cooling equations. Once again we shall be using the extremely useful generalised rate equation for the time derivative of the expectation value of an arbitrary operator A (c.f. Eq. (2.52)) which we previously encountered in Section 2.4.1. The difference this time being the last term $\mathcal{R}(\rho)$ which takes into account the recoil due to the combined effects of the free radiation and laser fields. Combining the master equation in Eq. (3.21) with Eq. (3.33), we get

$$\begin{aligned} \langle\dot{A}\rangle &= -\frac{\mathrm{i}}{\hbar}\left\langle AH_{\rm cond} - H_{\rm cond}^\dagger A\right\rangle + \frac{3\Gamma}{8}\int_{-1}^{1}\mathrm{d}\zeta\,\left\langle x^\dagger D(\mathrm{i}\eta(1-\zeta))AD(\mathrm{i}\eta(1-\zeta))^\dagger x\right\rangle \\ &\quad\times\left[\,1 + |d_3|^2 + \left(1 - 3|d_3|^2\right)\zeta^2\,\right]. \end{aligned} \tag{3.34}$$

So if the conditional Hamiltonian $H_{\rm cond}$ is the same as in Eq. (3.33), then this equation describes the time evolution of the expectation value $\langle A\rangle$ within the interaction picture which we introduced in Section 3.1.3.

As in the previous chapter we wish to determine the time evolution of the mean phonon number m,

$$m \quad \equiv \quad \langle b^\dagger b\rangle\,. \tag{3.35}$$

In this chapter, since we have made use of a unitary transformation to turn b into y, we need to account for this transformation by establishing a relationship between the mean phonon number m and the expectation values that are a result of the transformation. Using Eqs. (3.26) and (3.30), we find that this relationship is

$$m \quad \equiv \quad n_2 - \eta\, k_{12} + \eta^2\, n_1 \tag{3.36}$$

with n_1, n_2, and k_{12} defined as

$$n_1 \equiv \langle x^\dagger x \rangle\,, \;\; n_2 \equiv \langle y^\dagger y \rangle\,, \;\; k_{12} \equiv \mathrm{i}\,\langle x^\dagger x (y - y^\dagger) \rangle\,. \tag{3.37}$$

So to find out the behaviour of m as it evolves in time we need to calculate the time evolution of these three expectation values. In fact, to obtain a closed set of cooling equations we also need to consider the expectation values

$$\begin{aligned} &k_7 \equiv \langle y + y^\dagger \rangle\,, \;\; k_8 \equiv \mathrm{i}\,\langle y - y^\dagger \rangle\,, \;\; k_9 \equiv \langle y^2 + y^{\dagger 2} \rangle\,, \\ &k_{10} \equiv \mathrm{i}\,\langle y^2 - y^{\dagger 2} \rangle\,, \;\; k_{11} \equiv \langle x^\dagger x (y + y^\dagger) \rangle \end{aligned} \tag{3.38}$$

and the expectation values defined in App. A.3. Since all of these variables are expectation values of Hermitian operators, they are real and their time evolution is given by real differential equations.

The operator expectation values defined by n_2 and k_7 to k_{10} are all based on the y operators. If we use the generalised rate equation of Eq. (3.34) to calculate the time derivatives of these five variables, we find that

$$\begin{aligned} \dot{n}_2 &= \eta\nu\, k_{11} - \eta\Gamma\, k_{12} + \eta^2\theta\Gamma\, n_1\,, \\ \dot{k}_7 &= 2\eta\nu\, n_1 - \nu\, k_8\,, \\ \dot{k}_8 &= \nu\, k_7 - 2\eta\Gamma\, n_1\,, \\ \dot{k}_9 &= -2\nu\, k_{10} + 2\eta\nu\, k_{11} + 2\eta\Gamma\, k_{12} - 2\eta^2\theta\Gamma\, n_1\,, \\ \dot{k}_{10} &= 2\nu\, k_9 + 2\eta\nu\, k_{12} - 2\eta\Gamma\, k_{11}\,. \end{aligned} \tag{3.39}$$

The factor θ in this equation,

$$\theta \equiv \frac{1}{5}(7 - |d_3|^2)\,, \tag{3.40}$$

depends explicitly on the direction of the emitting dipole moment. It relates to the parameter α used in previous papers [10–13] via the equation

$$\theta \;\; = \;\; 1 + \alpha - \frac{1}{5}\,|d_3|^2\,. \tag{3.41}$$

Here also we should add that for the orientation of the laser interacting with the trapped particle in our particular configuration $\alpha = 2/5$. This corresponds to the case where the components of the normalised dipole (d_1, d_2, d_3) are aligned with the cartesian axes (x, y, z) respectively and the incident laser field is propagating in the z direction with a linear polarisation in the x direction. Of course if the laser was oriented in a different direction the value of alpha would be different. For example if the laser was propagating in the y direction then it turns out $\alpha = 3/10$. Javanainen and Stenholm have written a

good paper that discusses how different orientations of the laser driven trapped particle produce different values for α [104]. The time derivatives of the k_{11}, k_{12}, other mixed operator expectation values, n_1 and the remaining x expectation values can be found in App. A.4.

3.2.3 Weak confinement regime

Further analysis of the cooling process can be made easier by considering different frequency regimes. One such regime is defined by the situation where the trapped particle experiences a relatively weak trapping potential and where the Lamb-Dicke parameter η is much smaller than one. More specifically we assume that

$$\nu \ll \Gamma \quad \text{and} \quad \eta \ll 1\,. \tag{3.42}$$

In addition we assume that the Rabi frequency Ω and the detuning Δ are at most comparable to Γ and definitely not much larger. However we must point out that we have made no restriction on the driving parameter. In this way we do *not* demand that Ω is much smaller than Γ. The conditions of Eq. (3.42) mean that this choice of parameters causes the y operator expectation values n_2 and k_7 to k_{10} to a evolve on a much slower time scale than all other relevant expectation values. This can be seen when comparing the cooling equations of App. A.4 with Eq. (3.39) which clearly shows that the variables defined by all x or mixed operator expectation values decay with the spontaneous atomic decay rate Γ whereas n_2 and k_7 to k_{10} all evolve at a much slower rate defined by the conditions of Eq. (3.42).

The time scale separation between the y operator expectation values and all other expectation values allow us to eliminate n_1, k_1, k_2, and k_{13} to k_{24} adiabatically from the system dynamics. Doing so, we obtain a closed set of five effective cooling equations which applies after a relatively short transition time and which can be written as

$$\left(\dot{n}_2, \dot{k}_7, \dot{k}_8, \dot{k}_9, \dot{k}_{10}\right)^{\mathrm{T}} \;=\; M\left(n_2, k_7, k_8, k_9, k_{10}\right)^{\mathrm{T}} + \left(\beta_1, \beta_2, \beta_3, \beta_4, \beta_5\right)^{\mathrm{T}}\,. \tag{3.43}$$

Going back to Eq. (3.39) we see that the time derivatives of the y operator expectation values n_2, and k_7 to k_{10} depend only on n_1, k_{11}, and k_{12}. The calculation of the 5×5 matrix M therefore only requires the calculation of n_1, k_{11}, and k_{12} which can be found in App. A.4.

Before proceeding further we shall pause and describe the general method of solution. We would like to find a set of 5 differential equations in 5 unknowns from Eq. (3.39) so that we can form the matrix equation that is Eq. (3.43). What we require to do so are expressions for n_1, k_{11}, and k_{12} in zeroth and first order. For example, let

us look at the rate equation for n_2. Ultimately we want an equation of the form

$$\dot{n}_2 \quad = \quad \eta^2(\text{some number})\, n_2 + \eta^2(\text{some other number}) \tag{3.44}$$

Now to bring the order of η^2 into the equation we need to consider the orders of η that are already in the equation. So looking again at Eq. (3.39) we can see that the prefactors before k_{11}, k_{12} and n_1 are η, η and η^2 respectively. So, to get the n_2 rate equation into the form

$$\dot{n}_2 \quad = \quad \alpha_{11}\, n_2 + \alpha_{12}\, k_7 + \alpha_{13}\, k_8 + \alpha_{14}\, k_9 + \alpha_{15}\, k_{10} + \beta_1 \tag{3.45}$$

so that it can turn into Eq. (3.44) we need to calculate expressions for k_{11} and k_{12} up to zeroth and first order, while we only need to calculate n_1 up to zeroth order. To calculate k_{11} to zeroth order we take the group of 6 rate equations

$$\{\dot{k}_{11}, \dot{k}_{12}, \dot{k}_{15}, \dot{k}_{16}, \dot{k}_{17}, \dot{k}_{18}\} \tag{3.46}$$

up to zeroth which can be found in app. A.4 in Eq. (A.62). As we noted earlier the time scale separation between the y-operator expectation values and all other expectation values allows us to adiabatically eliminate the x and mixed operator expectation values from the systems dynamics. Therefore we can set $\{\dot{k}_{11}, \dot{k}_{12}, \dot{k}_{15}, \dot{k}_{16}, \dot{k}_{17}, \dot{k}_{18}\}$ equal to zero and get the following zeroth order expression for k_{11}.

$$k_{11}^{(0)} \quad = \quad \frac{\Omega^2}{\mu^4 \Gamma}\left[\mu^2 \Gamma\, k_7 - (3\Gamma^2 - 4\Delta^2)\nu\, k_8\right] \tag{3.47}$$

Notice how the zeroth order expression for k_{11} is only dependent on k_7 and k_8. Similarly the zeroth order expression for k_{12} is only dependent on k_7 and k_8. Then, since the prefactor of k_{11} is $\eta\nu$ and k_{12} is $\eta\kappa$ we will find that the coefficients α_{12} and α_{13} are first order in η. $n_1^{(0)}, k_1^{(0)}, k_2^{(0)}$ are found in a similar manner. Next we must consider $\{\dot{k}_{11}, \dot{k}_{12}, \dot{k}_{15}, \dot{k}_{16}, \dot{k}_{17}, \dot{k}_{18}\}$ to first order in η which is Eq. (A.66) in app. A.4. The first order in eta terms in these equations include the coherences $\{k_{13}^{(0)}, k_{14}^{(0)}, k_{19}^{(0)}, k_{20}^{(0)}, k_{21}^{(0)}, k_{22}^{(0)}\}$.

So, to solve $\{\dot{k}_{11}, \dot{k}_{12}, \dot{k}_{15}, \dot{k}_{16}, \dot{k}_{17}, \dot{k}_{18}\}$ to first order in η we must firstly solve

$$\{\dot{k}_{13}, \dot{k}_{14}, \dot{k}_{19}, \dot{k}_{20}, \dot{k}_{21}, \dot{k}_{22}\} \tag{3.48}$$

in zeroth order which is Eq. (A.68) in app. A.4. Then having found zeroth order expressions for n_1, k_1, k_2, k_{13}, k_{14}, k_{19}, k_{20}, k_{21}, k_{22} we can finally set $\{\dot{k}_{11}, \dot{k}_{12}, \dot{k}_{15}, \dot{k}_{16}, \dot{k}_{17}, \dot{k}_{18}\}$

in first order in η equal to zero and get first order in η expressions for k_{11} and k_{12}.

$$\begin{aligned} k_{11}^{(1)} &= \frac{4\eta\nu\Omega^2}{\mu^4}\left[2\Delta k_{10}+\Gamma\right], \\ k_{12}^{(1)} &= \frac{8\eta\nu\Delta\Omega^2}{\mu^4}\left[2n_2-k_9+1\right] \end{aligned} \tag{3.49}$$

Notice that the first order expressions for k_{11} and k_{12} only depend on n_2, k_9 and k_{10}. Like before, since the prefactor of k_{11} is $\eta\nu$ and k_{12} is $\eta\kappa$ we will find that the coefficients α_{11} ,α_{14} and α_{15} are second order in η. In a similar way we determine the α_{ij}'s for $\{\dot{k}_7,\dot{k}_8,\dot{k}_9,\dot{k}_{10}\}$ Substituting Eqs. (A.60), (A.63), (A.65), and (A.69) into Eq. (3.39), we find that M can be written as

$$M = \begin{pmatrix} \alpha_{11}^{(2)} & \alpha_{12}^{(1)} & \alpha_{13}^{(1)} & \alpha_{14}^{(2)} & 0 \\ 0 & 0 & -\nu & 0 & 0 \\ 0 & \nu & \alpha_{33}^{(2)} & 0 & 0 \\ \alpha_{41}^{(2)} & \alpha_{42}^{(1)} & \alpha_{43}^{(1)} & \alpha_{44}^{(2)} & -2\nu \\ 0 & \alpha_{52}^{(1)} & \alpha_{53}^{(1)} & 2\nu & \alpha_{55}^{(2)} \end{pmatrix}. \tag{3.50}$$

The first order matrix elements $\alpha_{ij}^{(1)}$ in this equations are given by

$$\begin{aligned} &\alpha_{12}^{(1)} = -\frac{2\eta\nu\Omega^2}{\mu^4}(\Gamma^2-4\Delta^2-\Omega^2),\ \ \alpha_{13}^{(1)} = -\frac{\eta\Gamma\Omega^2}{\mu^2}, \\ &\alpha_{42}^{(1)} = \frac{4\eta\nu\Omega^2}{\mu^4}(\Omega^2+2\Gamma^2),\ \ \alpha_{43}^{(1)} = \frac{2\eta\Gamma\Omega^2}{\mu^2}, \\ &\alpha_{52}^{(1)} = -\alpha_{43}^{(1)},\ \ \alpha_{53}^{(1)} = \alpha_{42}^{(1)} \end{aligned} \tag{3.51}$$

with μ^2 defined as in Eq. (A.61). The non-zero matrix elements $\alpha_{ij}^{(2)}$ of M in second order in η and first order in ν are given by

$$\begin{aligned} &\alpha_{11}^{(2)} = \alpha_{33}^{(2)} = \alpha_{44}^{(2)} = \alpha_{55}^{(2)} = -\frac{16\eta^2\nu\Delta\Gamma\Omega^2}{\mu^4}, \\ &\alpha_{14}^{(2)} = \frac{8\eta^2\nu\Delta\Gamma\Omega^2}{\mu^4},\ \ \alpha_{41}^{(2)} = \frac{32\eta^2\nu\Delta\Gamma\Omega^2}{\mu^4}. \end{aligned} \tag{3.52}$$

We determine β_1 by firstly finding the expression for $\dot{n}_2$ that is a function of n_2 and k_7 to k_{10}. We do this by substituting in the zeroth and first order expressions for, k_{11} and k_{12} from Eqs. (A.63), and (A.69) and zeroth and first order expressions for, n_1 from Eqs. (A.60), and (A.65), into the differential equation for $\dot{n}_2$ in Eq. (3.39) which are as

follows

$$\begin{aligned} k_{11} &= \frac{\Omega^2}{\mu^4\Gamma}\left[\mu^2\Gamma\, k_7 - (3\Gamma^2 - 4\Delta^2)\nu\, k_8\right] + \frac{4\eta\nu\Omega^2}{\mu^4}\left[2\Delta\, k_{10} + \Gamma\right], \\ k_{12} &= \frac{\Omega^2}{\mu^4\Gamma}\left[(3\Gamma^2 - 4\Delta^2)\nu\, k_7 + \mu^2\Gamma\, k_8\right] + \frac{8\eta\nu\Delta\Omega^2}{\mu^4}\left[2n_2 - k_9 + 1\right], \\ n_1 &= \frac{\Omega^2}{\mu^2} + \frac{8\eta\nu\Delta\Omega^2}{\mu^4}\, k_8 \end{aligned} \tag{3.53}$$

We then use the expressions for the relevant α_{ij}'s and define

$$\beta_1 = \dot{n}_2\,(n_2, k_7, k_8, k_9, k_{10}) - \alpha_{11}\, n_2 - \alpha_{12}\, k_7 - \alpha_{13}\, k_8 - \alpha_{14}\, k_9 - \alpha_{15}\, k_{10}\,. \tag{3.54}$$

Doing so, we find that β_1 up to second order in η is given to a very good approximation by $\beta_1 = \beta_1^{(2)}$ with

$$\beta_1^{(2)} = \frac{\eta^2\Gamma\Omega^2}{\mu^2}\,\theta\,. \tag{3.55}$$

In a similiar manner we find that the coefficients β_2 to β_5 in Eq. (3.43) are in first order in η given by

$$\beta_2^{(1)} = \frac{2\eta\nu\Omega^2}{\mu^2},\;\; \beta_3^{(1)} = -\frac{2\eta\Gamma\Omega^2}{\mu^2},\, \beta_4^{(1)} = \beta_5^{(1)} = 0\,. \tag{3.56}$$

On a final note it will be prudent to explain why we only need to consider $\beta_2, \ldots, \beta_5$ to first order. Consider once again the rate equation for n_2. For the terms $\alpha_{12}^{(1)} k_7$ and $\alpha_{13}^{(1)} k_8$ to be second order in η the expressions for k_7 and k_8 need to be first order in η. To determine the first order expressions for k_7 and k_8 it is only necessary to consider β_2 and β_3 to first order. A similar argument holds for β_4 and β_5.

We now have a closed set of five differential equations which can be used to analyse the time evolution of the y operator expectation values analytically and numerically. It is now also easy to see that the weak confinement regime which we introduced in Eq. (3.42) does not allow for the adiabatic elimination of the y operator coherences k_7 to k_{10}. The conditions of Eq. (3.42) ensure that the following condition holds

$$\frac{16\eta^2\nu\Delta\Gamma\Omega^2}{\mu^4} \;\ll\; \Gamma\,. \tag{3.57}$$

The expression on the left hand side of Eq. (3.57) is actually the rate with which the y operator coherence evolve on in general as can be inferred from Eqs. (3.43), (3.50) and (3.51). Thus in the weak confinement regime there is a clear separation of timescales with between the y operator coherences and the other coherences that evolve on the

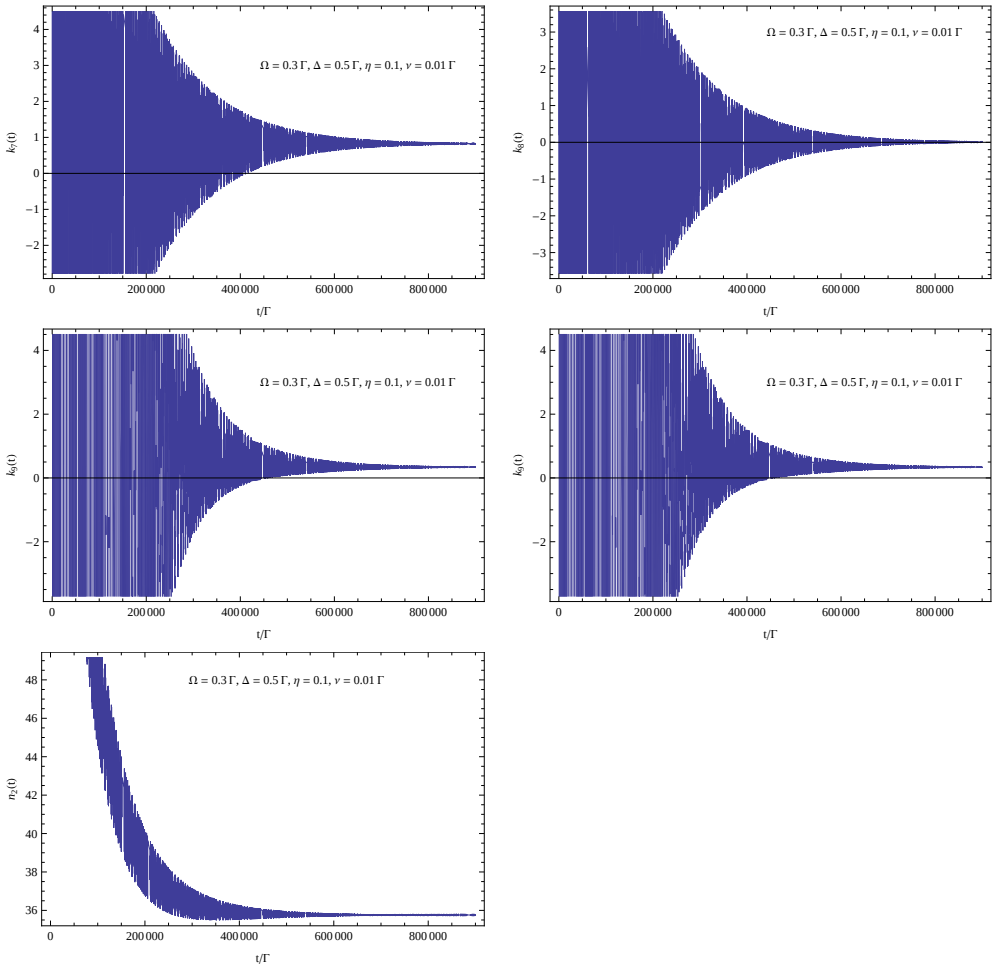

Figure 3.1: Time scale comparison for a numerical solution of k_7 to k_{10}, and n_2 for $\Delta = 0.5\,\Gamma$, $\nu = 0.1\,\Gamma$, $\Omega = 0.3\,\Gamma$, and $d_3 = 0$. Here quasi stationary state expressions for n_1, k_{11} and k_{12} were used with parameters chosen to reflect the weak confinement regime. y particles initially assumed to be in a coherent state.

timescale of Γ. Indeed, it can be clearly seen from Fig. 3.1 that all of the y operator coherences evolve on the same timescale as the y operator population.

3.2.4 Strong confinement regime

Another parameter regime is the one whereby the phonon frequency ν and the detuning Δ exceed the spontaneous decay rate Γ and the Rabi frequency Ω by at least one order of magnitude,

$$\Omega, \Gamma \quad \ll \quad \nu, \Delta, \quad \text{while} \quad \eta \ll 1\,. \tag{3.58}$$

In this case, also known as the strong confinement regime, the time scale separation

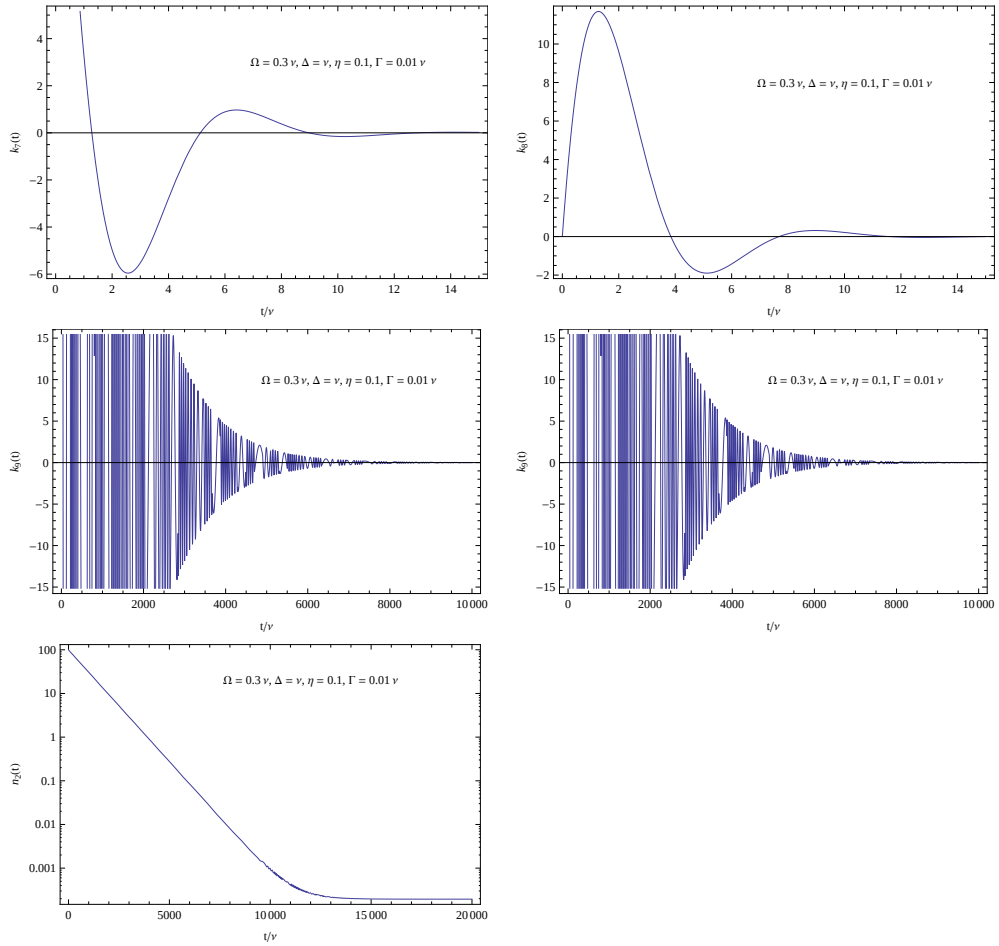

Figure 3.2: Time scale comparison for a numerical solution of k_7 to k_{10}, and n_2 for $\Delta = \nu$, $\Gamma = 0.1\,\nu$, $\Omega = 0.3\,\nu$, and $d_3 = 0$. Here quasi stationary state expressions for n_1, k_{11} and k_{12} were used with parameters chosen to reflect the strong confinement regime. y particles initially assumed to be in a coherent state.

in the dynamics of the trapped particle is different than in the previous subsection. However, at least at the end of the cooling process when n_2 is already relatively small, we can assume that the expectation values n_1, n_4, k_1, k_2, and k_7 to k_{24} evolve much faster than the y operator population n_2. This can clearly be seen from Fig. 3.2 which shows that the y operator coherences reach their respective steady state on a shorter timescale to that experienced by the y operator population.

Remark. Fig. 3.2 seems to show k_9 and k_{10} evolving on the same time scale as n_2. This would seem to violate our assumption of adiabatic elimination for k_9 and k_{10}. However, without even considering adiabatic elimination the rate equations for k_9 and k_{10} can be solved in zeroth order giving $k_9^{(0)} = k_{10}^{(0)} = 0$. Looking at the α form for $\dot{n}_2$ we see

$$\dot{n}_2 = \alpha_{11}^{(2)} n_2^{(0)} + \alpha_{12}^{(1)} k_7^{(1)} + \alpha_{13}^{(1)} k_8^{(1)} + \alpha_{14}^{(2)} k_9^{(0)} + \alpha_{15}^{(2)} k_{10} + \beta_1^{(2)} . \tag{3.59}$$

So for the purposes of finding a steadystate number and cooling rate for n_2 we need only consider zeroth order values for k_9 and k_{10} which are actually zero!

This means, we can simplify the system dynamics via an adiabatic elimination of all expectation values other than n_2. Doing so (cf. App. A.5), we obtain an effective cooling equation of the form

$$\dot{n}_2 = -\gamma_c^{\mathrm{str}} n_2 + c . \tag{3.60}$$

The frequencies γ_c and c in this equation are given by

$$\begin{aligned} \gamma_c^{\mathrm{str}} &= \frac{\eta^2 \Gamma \Omega^2}{4(\Delta - \nu)^2} - \frac{\eta^2 \Gamma \Omega^2}{4(\Delta + \nu)^2} , \\ c &= \frac{\eta^2 \Gamma \Omega^2}{4\Delta^2} \left[\theta + \frac{\Delta^2}{(\Delta + \nu)^2} - 1 \right] \end{aligned} \tag{3.61}$$

up to second order in η. In this case γ_c is actually the effective cooling rate for strongly confined particles. We must also point out here that the cooling rate becomes much larger when the detuning Δ is close to the phonon frequency ν. In this approximation, however, Δ should not be exactly equal to ν as in this case the cooling rate goes infinity which is of course not feasible.

3.3 Stability analysis

In the weak confinement regime we have a set of five linear differential equations that describe the cooling process. As we have just seen these equations are the result of the time scale separation implied by the conditions of the weak confinement regime. The conditions of Eq. (3.42) allowed us to eliminate n_1, k_1, k_2, and k_{13} to k_{24} adiabatically from the system dynamics leaving us with the four y operator coherences and the $y^\dagger y$ population which apply after a relatively short transition time. However what we do not know is whether or not these equations have stationary state solutions. In this section we shall perform a stability analysis on this set of equations. For the case of the strong confinement regime it is not necessary to question stability as $\gamma_c > 0$ always in this regime.

To help our analysis we introduce the shifted y operator expectation values which are defined as

$$\left(\tilde{n}_2, \tilde{k}_7, \tilde{k}_8, \tilde{k}_9, \tilde{k}_{10}\right)^{\mathrm{T}} \equiv \left(n_2, k_7, k_8, k_9, k_{10}\right)^{\mathrm{T}} + M^{-1}\left(\beta_1, \beta_2, \beta_3, \beta_4, \beta_5\right)^{\mathrm{T}}. \quad (3.62)$$

This definition means that the tilde and the non-tilde variables differ only by the stationary state solutions of the non-tilde expectation values. Substituting Eq. (3.62) into Eq. (3.43), we find that

$$\left(\dot{\tilde{n}}_2, \dot{\tilde{k}}_7, \dot{\tilde{k}}_8, \dot{\tilde{k}}_9, \dot{\tilde{k}}_{10}\right)^{\mathrm{T}} = M\left(\tilde{n}_2, \tilde{k}_7, \tilde{k}_8, \tilde{k}_9, \tilde{k}_{10}\right)^{\mathrm{T}}. \quad (3.63)$$

We must also emphasise here that Eq. (3.62) that defines the transformation is just a relabelling of variables to make the plotting of variables in the forthcoming stability analysis more presentable. All of the following calculations can be carried out without the using the transformation. In fact the same calculations that were performed to investigate the existence of steady state solutions were done prior to using the transformation that uses the inverse of M. So, having prior knowledge that the determinant of M was not equal to zero, its inverse could then be used in defining an ansatz for Eq. (3.62).

A stationary state solution exists for this set of equations if all the eigenvalues of M have a negative real part. As we shall see an intuitive approach to understanding the existence of the stationary state resides within the perturbative analysis of the elements of M in terms of the small parameter η.

3.3.1 Time evolution for $\eta = 0$

Noting that $\alpha_{15}^{(2)} = \alpha_{22}^{(2)} = \alpha_{51}^{(2)} = 0$ we can expand Eq. (3.50) up to second order in η by expanding M in powers of η

$$\begin{aligned} M &= M^{(0)} + M^{(1)} + M^{(2)} \\ &= \begin{pmatrix} 0 & 0 & 0 & 0 & 0 \\ 0 & 0 & -\nu & 0 & 0 \\ 0 & \nu & 0 & 0 & 0 \\ 0 & 0 & 0 & 0 & -2\nu \\ 0 & 0 & 0 & 2\nu & 0 \end{pmatrix} + \begin{pmatrix} 0 & \alpha_{12}^{(1)} & \alpha_{13}^{(1)} & 0 & 0 \\ 0 & 0 & 0 & 0 & 0 \\ 0 & 0 & 0 & 0 & 0 \\ 0 & \alpha_{42}^{(1)} & \alpha_{43}^{(1)} & 0 & 0 \\ 0 & \alpha_{52}^{(1)} & \alpha_{53}^{(1)} & 0 & 0 \end{pmatrix} \\ &\quad + \begin{pmatrix} \alpha_{11}^{(2)} & 0 & 0 & \alpha_{14}^{(2)} & \alpha_{15}^{(2)} \\ 0 & \alpha_{22}^{(2)} & \alpha_{23}^{(2)} & 0 & 0 \\ 0 & \alpha_{32}^{(2)} & \alpha_{33}^{(2)} & 0 & 0 \\ \alpha_{41}^{(2)} & 0 & 0 & \alpha_{44}^{(2)} & \alpha_{45}^{(2)} \\ \alpha_{51}^{(2)} & 0 & 0 & \alpha_{54}^{(2)} & \alpha_{55}^{(2)} \end{pmatrix} \end{aligned} \quad (3.64)$$

The first term in Eq. (3.64) is the matrix that contains all the terms which correspond to the time evolution of the y operator expectation values for $\eta = 0$. The eigenvalues of this matrix can be easily shown to be

$$\lambda_1 = 0\,, \quad \lambda_{2,3} = \mp \mathrm{i}\nu\,, \quad \lambda_{4,5} = \mp 2\mathrm{i}\nu\,. \tag{3.65}$$

Taking this into account and solving Eq. (3.63) analytically, we find that

$$\begin{aligned} \tilde{n}_2(t) &= \tilde{n}_2(0)\,, \\ \begin{pmatrix} \tilde{k}_7(t) \\ \tilde{k}_8(t) \end{pmatrix} &= \begin{pmatrix} \cos\nu t & -\sin\nu t \\ \sin\nu t & \cos\nu t \end{pmatrix} \begin{pmatrix} \tilde{k}_7(0) \\ \tilde{k}_8(0) \end{pmatrix}, \\ \begin{pmatrix} \tilde{k}_9(t) \\ \tilde{k}_{10}(t) \end{pmatrix} &= \begin{pmatrix} \cos 2\nu t & -\sin 2\nu t \\ \sin 2\nu t & \cos 2\nu t \end{pmatrix} \begin{pmatrix} \tilde{k}_9(0) \\ \tilde{k}_{10}(0) \end{pmatrix}. \end{aligned} \tag{3.66}$$

The behaviour of Eq. (3.66), the analytic solutions of Eq. (3.63) for $\eta = 0$, can be clearly seen in Fig. 3.3(a) which shows numerical solutions of the effective cooling equations in Eq. (3.63) for the case where the y particles are initially in a coherent state. The first two phase diagrams show $\tilde{k}_8$ and $\tilde{k}_{10}$ as functions of $\tilde{k}_7$ and $\tilde{k}_9$, respectively. As we can see from the diagrams all points lie on a circle which means that the state of the particle remains approximately coherent throughout the cooling process. In fact Fig. 3.3(a) shows that the y particle population $\tilde{n}_2$ and therefore also the mean phonon number m (cf. Eq. (3.36)) in zeroth order in η remains constant in time. This result means that there is no cooling in the zeroth order approximation of η. Of course this fact is obvious when one considers that in zeroth order in η there is no coupling between the electronic and vibrational states of the trapped particle. One must go at least one order higher to encounter terms in the hamiltonian that couple electronic and vibrational operators or in our case the x and y operators.

3.3.2 First order corrections

Calculating the eigenvalues of the matrix M in Eq. (3.50) up to first order in η, we obtain again Eq. (3.65). All of them are either zero or imaginary. This means there are no first order corrections to the eigenvalues. However, since the eigenvalues of M have no real parts, $\tilde{n}_2$ as well as the mean phonon number m in zeroth order in η cannot reach their respective stationary state values. Instead, they remain close to their initial value and no cooling occurs.

3.3.3 Second order corrections

We now take a closer look at the third term in Eq. (3.64). This matrix will allow us to find the second order corrections. In fact all the first order terms are located in different

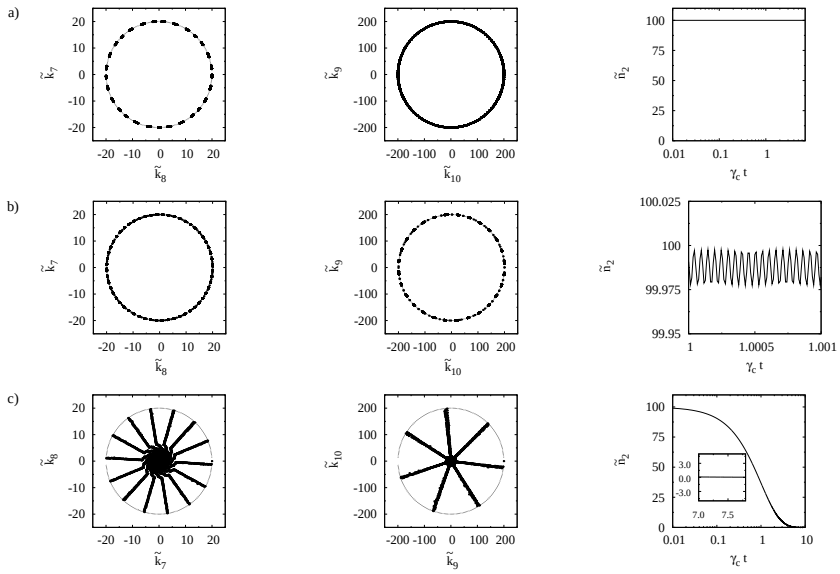

Figure 3.3: Diagrams illustrating the time evolution of the expectation values $\tilde{k}_7$ to $\tilde{k}_{10}$, and $\tilde{n}_2$ for $\Delta = 0.5\Gamma$, $\nu = 0.1\Gamma$, $\Omega = 0.01\Gamma$, and $d_3 = 0$. It is assumed that the y particles are initially in a coherent state. In (a), only terms in zeroth order in η have been taken into account. As expected, we find that the mean phonon number remains constant in time. The coherences $\tilde{k}_7$ to $\tilde{k}_{10}$ evolve such that their points in the respective phase diagrams lie on circles. This means that the y particles remain in a coherent state. In (b), only terms in first order in η have been taken into account. All five eigenvalues of M are still either zero or purely imaginary which is why there is still no reduction of $\tilde{n}_2$. In (c), also the second order terms in η are taken into account. The coherences $\tilde{k}_7$ to $\tilde{k}_{10}$ now evolve towards zero. We now observe an exponential decrease of $\tilde{n}_2$. This implies a reduction of the mean phonon number m in zeroth order in η, ie. cooling.

matrix elements to where the zeroth and second order matrix element terms are. In this way it is easy to see why there are no first order corrections to the eigenvalues of M. Being in the weak confinement regime where $\Gamma \gg \nu$ some second order matrix elements can be neglected as they scale with ν^2 the result of which is evident in Eq. (3.50) and can be deduced from Eqs. (A.60), (A.63), and (A.69). Basically when the first order expression for n_1 and the first and second order expressions for k_{11} and k_{12} are multiplied by $2\eta\nu$ some of the coefficients in front of n_2, k_7, and k_{10} scale with ν^2. Specifically we have $\alpha_{15}^{(2)} = \alpha_{22}^{(2)} = \alpha_{51}^{(2)} = 0$. Then using the fact that $\alpha_{11}^{(2)} = \alpha_{33}^{(2)} = \alpha_{44}^{(2)} = \alpha_{55}^{(2)}$ we find that matrix that will give us our eigenvalues with second order corrections

is

$$\begin{pmatrix} \alpha_{11}^{(2)} & 0 & 0 & \alpha_{14}^{(2)} & 0 \\ 0 & 0 & -\nu & 0 & 0 \\ 0 & \nu & \alpha_{11}^{(2)} & 0 & 0 \\ \alpha_{41}^{(2)} & 0 & 0 & \alpha_{11}^{(2)} & -2\nu \\ 0 & 0 & 0 & 2\nu & \alpha_{11}^{(2)} \end{pmatrix} . \tag{3.67}$$

We can now rearrange rows and columns in Eq. (3.67) to give a block diagonal matrix. The eigenvalues of the individual blocks will then give us the eigenvalues of Eq. (3.67). There are in fact just 2 blocks that we need to find eigenvalues for.

$$\mathcal{K} \equiv \begin{pmatrix} 0 & -\nu \\ \nu & \alpha_{11}^{(2)} \end{pmatrix} \tag{3.68}$$

which has the eigenvalues

$$\lambda_{2,3} \;=\; \frac{1}{2}\,\alpha_{11}^{(2)} \mp \frac{\mathrm{i}}{2}\sqrt{4\nu^2 - \left(\alpha_{11}^{(2)}\right)^2}. \tag{3.69}$$

The other block matrix looks like so

$$\mathcal{M} \equiv \begin{pmatrix} \alpha_{11}^{(2)} & \alpha_{14}^{(2)} & 0 \\ \alpha_{41}^{(2)} & \alpha_{11}^{(2)} & -2\nu \\ 0 & 2\nu & \alpha_{11}^{(2)} \end{pmatrix}$$

and it has the following eigenvalues

$$\lambda_1 \;=\; \alpha_{11}, \quad \lambda_{4,5} \;=\; \alpha_{11}^{(2)} \mp \mathrm{i}\sqrt{4\nu^2 - \alpha_{14}^{(2)}\alpha_{41}^{(2)}}. \tag{3.70}$$

As we are only considering postive values of δ_{eff} the matrix element $\alpha_{11}^{(2)}$ is always negative and so all tilde variables are damped away and tend eventually to zero on the time scale given by $1/\alpha_{11}^{(2)}$. This is illustrated in Fig. 3.3(c) which shows a numerical solution of the effective cooling equations in Eq. (3.63).

Since the y coherences k_7 to k_{10} do not increase in time but oscillate instead with a slowly decreasing amplitude around constant values as is illustrated in Fig. (3.1), the cooling process remains stable and the trapped particle eventually reaches its stationary state. In the following section we use the fact that k_7 to k_{10} oscillate around constant values to analyse the cooling process in more detail. We shall continue our analysis by using time averaged values to replace the coherence variables k_7 to k_{10} at the end of the cooling process. In the weak confinement regime this approximation is applied after a period of time on the order of $1/\alpha_{11}^{(2)}$ as we shall see in the next section.

One can easily check that the time averages of the coherences k_7 to k_{10} are exactly the same as the quasi-stationary state solutions obtained when setting their time derivatives in Eq. (3.43) equal to zero and in fact we shall devote the next subsection to illustrating this neat equivalence.

3.3.4 Time averaged values and quasi - stationary states.

Let us look again at the rate equations for the k_7 and k_8 coherences in Eq. (3.39). Now if we take into account the value of n_1 in zeroth order these equations look like the following.

$$\dot{k}_7 \;=\; \frac{2\eta\nu\Omega^2}{\mu^2} - \nu\, k_8\,, \quad \dot{k}_8 \;=\; \nu\, k_7 - \frac{2\eta\Gamma\Omega^2}{\mu^2}\,. \tag{3.71}$$

Setting both equations equal to zero we easily determine both quasi - stationary states to be

$$k_7^{ss} \;=\; \frac{2\eta\Gamma\Omega^2}{\nu\mu^2}, \quad k_8^{ss} \;=\; \frac{2\eta\Omega^2}{\mu^2}\,. \tag{3.72}$$

Next we can find the solutions of both differential equations. This task is quite doable due to the low number of terms and variables in both equations. Choosing an initial value of 20 for k_7 and an initial value of zero for k_8 (general initial values can also be chosen but to make life easier we've chosen specific values) we get for example the following expressions up to first order in η,

$$\begin{aligned} k_7(t) \;&=\; \frac{\left(20\mu^2\nu - 2\Gamma\eta\Omega^2\right)\cos(\nu\, t) + 2\eta\Omega^2(\Gamma + \nu\sin(\nu\, t))}{\mu^2\nu} \\ k_8(t) \;&=\; \frac{2\eta\nu\Omega^2 - 2\eta\nu\Omega^2\cos(\nu\, t) + \left(20\mu^2\nu - 2\Gamma\eta\Omega^2\right)\sin(\nu t)}{\mu^2\nu}\,. \end{aligned} \tag{3.73}$$

Using these functions we can determine their time averages from the standard definition of such with an arbitrary function $f(t)$ whose average $\bar{f}(t)$ is

$$\bar{f}(t) \equiv \frac{1}{(b-a)} \int_a^b f(t)\, dt \tag{3.74}$$

Taking a to be zero and b to T we find our time averaged value for k_7 to be

$$\bar{k}_7(t) = \frac{2\eta\nu\Omega^2}{T\nu^2\mu^2} + \frac{(20\mu^2\nu - 2\eta\Gamma\Omega^2)\sin(\nu\, T)}{T\nu^2\mu^2} - \frac{2\eta\nu\Omega^2\cos(\nu\, T)}{T\nu^2\mu^2} + \frac{2\eta\Gamma\Omega^2}{\nu\mu^2}\,. \tag{3.75}$$

Towards the end of the cooling process as k_7 reaches its stationary state value the value of T will be much greater then one. Then every term in Eq. (3.75) except the last term

become negligible. Thus the time average becomes

$$\bar{k}_7(t) \approx \frac{2\eta\Gamma\Omega^2}{\nu\mu^2}. \tag{3.76}$$

Therefore in the limit as T goes to infinity the average value becomes the stationary state value

$$k_7^{ss} = \lim_{T\to\infty} \bar{k}_7(t). \tag{3.77}$$

Then for k_8 we find the average value for the function to be

$$\begin{aligned} \bar{k}_8(t) &= \frac{2\left(10\mu^2\nu - \Gamma\eta\Omega^2 + \left(\Gamma\eta\Omega^2 - 10\mu^2\nu\right)\cos(\nu\, T) - \eta\nu\Omega^2\sin(\nu\, T)\right)}{T\mu^2\nu^2} \\ &\quad + \frac{2\eta\Omega^2}{\mu^2} \end{aligned} \tag{3.78}$$

So for a very large value of T we find the first term becomes negligible and we are left with the same expression as we got for the value of k_8's quasi - stationary state, namely

$$\bar{k}_8(t) \approx \frac{2\eta\Omega^2}{\mu^2}. \tag{3.79}$$

Again we have the very nice relationship between the time averaged value and the quasi - stationary state

$$k_8^{ss} = \lim_{T\to\infty} \bar{k}_8(t). \tag{3.80}$$

When a similar analysis is performed for k_9 and k_{10} in first order in η one finds that the average value of the function is actually zero. Indeed this corresponds to the stationary state at this order. One could be tempted to say that Eqs. (3.77) and (3.80) are obvious when one considers that as a function evolves it eventually reaches its steady state. In other words the steady state is the asymptotic value of the function. However this is not always true. In fact this is why this particular example was chosen. From the previous section on stability analysis we have just seen that in first order in η the y operator coherences do not evolve into a steady state. This fact can also be seen when we can numerically integrate Eq. (3.71) the result of which is shown in Fig. 3.4. Here we can see how the functions that represent k_7 and k_8 to first order in η do not evolve to a point for which the function becomes constant. Fortunately for us Eqs. (3.77) and (3.80) imply that towards the end of the cooling process the time averaged values are equivalent to the quasi - stationary state. Thus if we consider our analysis to be towards the end of the cooling process replacing the coherences k_7 to k_{10} with their

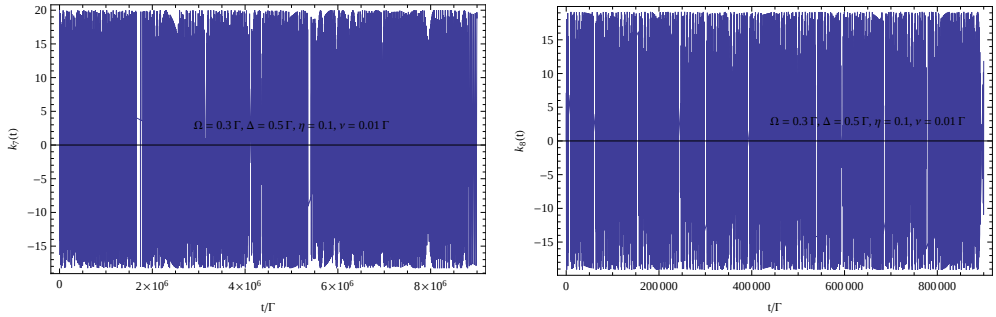

Figure 3.4: The above figures show the evolution of the coherences k_7 and k_8 whose functions are exact up to first order in η. At this order the plots clearly show the absence of a stationary state after a long period of time. Here also for $\Delta = 0.5\,\Gamma$, $\nu = 0.1\,\Gamma$, $\Omega = 0.3\,\Gamma$, and $d_3 = 0$. Here quasi stationary state expressions for n_1, k_{11} and k_{12} were used with parameters chosen to reflect the weak confinement regime. y particles initially assumed to be in a coherent state.

time averaged values would be a reasonable approximation.

Better Argument

The time average value of k_7 over 1 period is actually k_7^{ss}. This is easy to see for $T = 2\pi$ in Eq. (3.75).

$$\begin{aligned}\bar{k}_7 &= \frac{2\eta\nu\Omega^2}{2\pi\nu^2\mu^2} + \frac{(20\mu^2\nu - 2\eta\Gamma\Omega^2)\sin(\nu\,2\pi)}{2\pi\nu^2\mu^2} - \frac{2\eta\nu\Omega^2\cos(\nu\,2\pi)}{2\pi\nu^2\mu^2} + \frac{2\eta\Gamma\Omega^2}{\nu\mu^2} \\ &= \frac{2\eta\nu\Omega^2}{2\pi\nu^2\mu^2} - \frac{2\eta\nu\Omega^2}{2\pi\nu^2\mu^2} + \frac{2\eta\Gamma\Omega^2}{\nu\mu^2} \\ &= \frac{2\eta\Gamma\Omega^2}{\nu\mu^2}. \end{aligned} \tag{3.81}$$

Thus averaging over one period gives the same expression as the quasi-stationary state for k_7. As the time scale of 1 period on the evolution of k_7 is much smaller than the timescale on which n_2 evolves on it is justifiable to use the first order time average value of k_7 in lieu of the k_7 coherence variable in the rate equation for n_2. A similar argument can be used for k_8, k_9 and k_{10}.

3.4 Cooling rates and phonon numbers

Taking the results of the previous section into account and replacing the y operator coherences k_7 to k_{10} by their time averages we now obtain an analytical solution for the closed set of 23 cooling equations which we introduced in this paper. As we have just seen the time averages of the coherences k_7 to k_{10} are exactly the same as the quasi-stationary state solutions obtained when setting their time derivatives in Eq. (3.43)

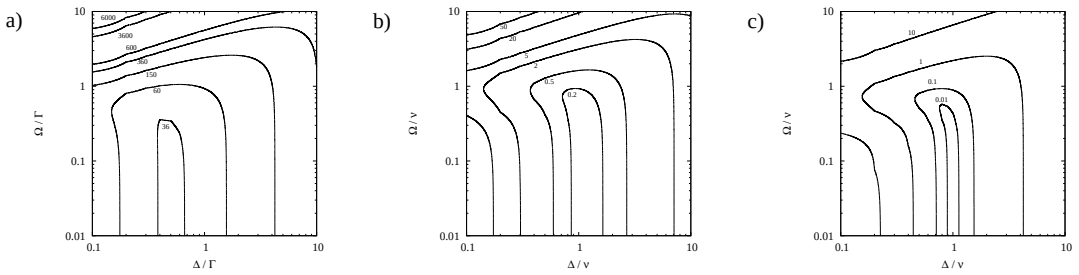

Figure 3.5: Logarithmic contour plot of the stationary state phonon number m_{ss} in Eq. (3.84) as a function of the laser parameters Ω and Δ for a) $\nu = 0.01\,\Gamma$, b) $\Gamma = \nu$, and c) $\Gamma = 0.01\,\nu$.

equal to zero. This means, adiabatically eliminating k_7 to k_{10}, as we did in Section 3.2.4 for the strong confinement regime, and replacing these variables by their time averages yields exactly the same result. Taking this into account and simply eliminating all expectation values other than n_2 adiabatically, we obtain an effective cooling equation which is of exactly the same form as Eq. (3.60). Its solution in zeroth order in η is given by

$$m(t) \;=\; \left[m(0) - m_{ss}\right] \mathrm{e}^{-\gamma_c t} + m_{ss} \tag{3.82}$$

with $m_{ss} = c/\gamma_c$. This equation applies, since n_2 and m are the same in zeroth order in η (c.f. Eq. (3.36)). In the remainder of this section, we derive analytical expressions for the stationary state phonon number m_{ss} and for the effective cooling rate γ_c. We then check that these results are consistent with the effective cooling equations derived in Section 3.2.3 and 3.2.4. Finally, we show that analytical solution for the time evolution of the mean phonon number m in Eq. (3.82) is in very good agreement with a numerical solution of the 23 cooling equations in this thesis which apply as long as $\eta \ll 1$.

3.4.1 Stationary state phonon numbers

Using the cooling equations in Eq. (3.39) and in App. A.4 and setting the time derivatives of all expectation values equal to zero, we obtain the stationary state phonon number

$$m_{ss} \;=\; \frac{1}{16\nu\Delta} \cdot \frac{1}{\xi_1^4} \left[\xi_2^6\,\theta - 2\xi_3^6\right] \tag{3.83}$$

with the frequencies ξ_1, ξ_2, and ξ_3 defined as

$$\begin{aligned}
\xi_1^4 &\equiv (4\Delta^2+\Gamma^2)(\Gamma^2+\nu^2)+2(\Gamma^2+3\nu^2)\Omega^2\,,\\
\xi_2^6 &\equiv (\Gamma^2+\nu^2)\left[(\Gamma^2+4\Delta^2)^2+8(\Gamma^2-4\Delta^2)\nu^2+16\nu^4\right]\\
&\quad +4\left[(\Gamma^2+2\nu^2)(\Gamma^2+4\Delta^2)-8\nu^4\right]\Omega^2+4(\Gamma^2+4\nu^2)\Omega^4\,,\\
\xi_3^6 &\equiv 2(2\Delta+\nu)(\Gamma^2+\nu^2)\left[\Gamma^2+4(\Delta-\nu)^2\right]+\left[3\Gamma^4-(4\Delta^2\right.\\
&\quad \left.-8\Delta\nu-7\nu^2)\Gamma^2-4(\Delta^2-6\Delta\nu+5\nu^2)\nu^2\right]\Omega^2\,. \qquad (3.84)
\end{aligned}$$

This result applies in zeroth order in η without any approximations. Fig. 3.5 shows m_{ss} as a function of the two laser parameters Ω and Δ for three different sets of experimental parameters. In the weak confinement regime one should choose $\Delta = 0.5\,\Gamma$ and for $\nu = \Gamma$ one should choose Δ close to Γ in order to minimise the final kinetic energy of the trapped particle.

Fig. 3.5 also shows that there is a particular dependence for m_{ss} to remain at a constant steady state without further changing its value. This is an interesting result which implies that effective laser cooling is not restricted to laser Rabi frequencies much smaller than Γ as it is often implied in the literature [11–13, 20]. As we shall see below in Section 4.4.3, maximising Ω increases the cooling rate which scales as Ω^2. Our numerical simulations show that Ω can be as large as $0.3\,\Gamma$ in the weak confinement regime and as large as $0.3\,\nu$ in the strong confinement regime without noticeably increasing the final phonon number m_{ss}. Notice also that increasing the value of Ω to larger values rapidly increases the stationary state phonon number thus indicating how cooling changes quickly changes into heating.

3.4.2 Consistency with the standard results

In this section by considering different parameter regimes we show how our results are the same as those results from calculations of previous authors [11–13, 20]. The alternative but consistent analysis of the laser cooling of trapped ions presented in these papers has as its main result a cooling equation of the form

$$\dot{m} = -\eta^2 (A_- - A_+)\, m + A_+\,, \qquad (3.85)$$

where m denotes the mean phonon number. The $A_\pm$ can be interpreted as transition rates between states with different phonon numbers and hence relate to the actual cooling and heating rates. The stationary state phonon rate m_{ss} is consequently given by [10, 11, 13, 20]

$$m_{ss} = \frac{A_+}{A_- - A_+}\,. \qquad (3.86)$$

Using our analysis and taking into account the regime for relatively small Rabi frequencies Ω, Eq. (3.83) whereby we neglect all terms that scale with Ω^2 simplifies to

$$\begin{aligned} m_{ss} &= \frac{\Gamma^4 + 8\Gamma^2(\Delta^2+\nu^2) + 16(\Delta^2-\nu^2)^2}{16\nu\Delta(\Gamma^2+4\Delta^2)}\,\theta \\ &\quad -\frac{(2\Delta+\nu)}{4\Delta(\Gamma^2+4\Delta^2)}\left[\Gamma^2+4(\Delta-\nu)^2\right]. \end{aligned} \tag{3.87}$$

This equation is in good agreement with the stationary state phonon number implied in Refs. [10–13] for $d_3 = 0$. This can be shown using Eqs. (3.86) and (3.41) in this paper and the expressions for $A_\pm$ in Eq. (7) in Ref. [12] which we now do.

The definition of $A_\pm$ taken from Eq. (7) in Ref. [12] is as follows

$$A_\pm = \Gamma\left[\alpha P(\Delta) + P(\Delta \pm \nu)\right] \tag{3.88}$$

and if we work out the algebra such that $P(\Delta)$ is a function of Ω, Γ and Δ then we also get

$$P(\Delta) = \frac{4\Omega^2}{\Gamma^2 + 4\,\Delta^2}. \tag{3.89}$$

Then if we substitute Eq. (3.88) into Eq. (3.87) we find an expression of the following form which is the steadystate as derived by the previous authors.

$$m_{ss} = \frac{\Gamma^2+4(\Delta-\nu)^2}{16\Delta\nu} + \frac{\Gamma^4 + 8\Gamma^2(\Delta^2+\nu^2) + 16(\Delta^2-\nu^2)^2}{16\nu\Delta(\Gamma^2+4\Delta^2)}\,\alpha. \tag{3.90}$$

Now if take Eq. (3.87) which is our result for the steady state in the limit of small Rabi frequencies and using Eq. (3.41) which was determined by incorporating the definition of α as defined in Refs. [10–13] into a rederivation of Eq. (A.55) we find our expression for m_{ss} becomes

$$\begin{aligned} m_{ss} &= \frac{\Gamma^4 + 8\Gamma^2(\Delta^2+\nu^2) + 16(\Delta^2-\nu^2)^2}{16\nu\Delta(\Gamma^2+4\Delta^2)} - \frac{(2\Delta+\nu)}{4\Delta(\Gamma^2+4\Delta^2)}\left[\Gamma^2+4(\Delta-\nu)^2\right] \\ &\quad + \frac{\Gamma^4 + 8\Gamma^2(\Delta^2+\nu^2) + 16(\Delta^2-\nu^2)^2}{16\nu\Delta(\Gamma^2+4\Delta^2)}\left(\alpha - \frac{1}{5}|d_3|^2\right) \end{aligned} \tag{3.91}$$

Noting that previous authors usually consider the case whereby the angular distribution of spontaneous emission is such that $d_3 = 0$ then on adding together the first 2 terms in Eq. (3.91) we find it contracts to the following expression

$$m_{ss} = \frac{\Gamma^2 + 4(\Delta-\nu)^2}{16\Delta\nu} + \frac{\Gamma^4 + 8\Gamma^2(\Delta^2+\nu^2) + 16(\Delta^2-\nu^2)^2}{16\nu\Delta(\Gamma^2+4\Delta^2)}\,\alpha \qquad (3.92)$$

which is of course the standard expression for m_{ss} that has been derived earlier by previous authors.

Weak confinement

In the weak confinement regime, the stationary state phonon number m_{ss} in Eq. (3.83), after neglecting terms that scale with ν^2, simplifies to

$$m_{ss}^{\text{weak}} = \frac{\mu^2}{16\Delta\nu}\,\theta - \frac{(3\Gamma^2-4\Delta^2)\Omega^2}{8\mu^2\nu\Delta}\,. \qquad (3.93)$$

Exactly the same stationary state phonon number is obtained when setting the left hand side of the five effective cooling equations in Eq. (3.39) equal to zero. We now have derived the same result in two different ways thus confirming the consistency of the steady state calculations. As already pointed out above, for small Ω, this expression assumes its minimum if

$$\Delta = \frac{1}{2}\Gamma\,. \qquad (3.94)$$

For this laser detuning and Rabi frequencies $\Omega \ll \Gamma$, which means we neglect all terms that scale with Ω^2, the stationary state phonon number simplifies to

$$m_{ss}^{\text{weak}} = \frac{\Gamma}{4\nu}\,\theta\,. \qquad (3.95)$$

When substituting the detuning $\Delta = \Gamma/2$ into Eq. (3.87) we get this expression for m_{ss}

$$m_{ss} = \frac{\Gamma^4\theta - 2\Gamma^3\nu + 4(-1+\theta)\nu^4 + \Gamma^2 2\nu^2}{4\Gamma^3\nu} \qquad (3.96)$$

Neglecting terms that scale with ν (weak confinement approximation) we get back Eq. (3.93). So, in the optimal case the final phonon number scales essentially as Γ/ν which is much larger than one which is exactly what we saw in the numerical solution of n_2 in Fig. (3.1).

Strong confinement

Using the effective cooling equation derived in Section 3.2.4 and setting it equal to zero, we find that the stationary state phonon number in the strong confinement regimes

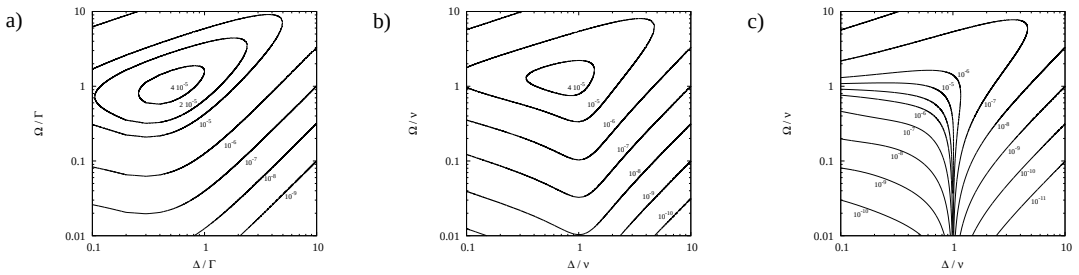

Figure 3.6: Logarithmic contour plot of the cooling rate γ_c in Eq. (3.103) in units of $1/\Gamma$ as a function of the laser parameters Ω and Δ for a) $\nu = 0.01\,\Gamma$ and $\eta = 0.01$, b) $\Gamma = \nu$ and $\eta = 0.1$, and c) $\Gamma = 0.01\,\nu$ and $\eta = 0.1$.

equals

$$m_{\rm ss}^{\rm strong} \;=\; \frac{(\Delta-\nu)^2}{4\nu\Delta^3}\left[(\Delta+\nu)^2\,\theta-(2\Delta+\nu)\nu\right] \tag{3.97}$$

to a very good approximation. Exactly the same result is obtained when neglecting terms proportional to Γ and Ω in Eq. (3.83). This result suggests immediately that one should choose

$$\Delta \;=\; \nu \tag{3.98}$$

in order to minimise the final phonon number $m_{\rm ss}$. Next we substitute this detuning back into Eq. (3.87) which was derived prior to making any approximation with regard to either the strong or weak confinement regime. We now neglect terms which scale with Γ^2 and find the following expression for $m_{\rm ss}$

$$m_{\rm ss}^{\rm strong} \;=\; \frac{\Gamma^2}{16\nu^2}\left[4\theta-3\right]. \tag{3.99}$$

This means, the stationary state phonon number now scales essentially as Γ^2/ν^2 which is much smaller than one [8].

Remark.
We must point out that when we combine Eq. (3.41) with Eqs. (3.94) and (4.46) and set $d_3 = 0$ we get

$$m_{ss}^{strong} = \frac{\Gamma^2}{16\nu^2}(1+\alpha), \quad \text{and} \quad m_{ss}^{weak} = \frac{\Gamma}{4\nu}(1+\alpha) \tag{3.100}$$

It is interesting to note that we found very similar expressions for the m_{ss} in section 2.4.2 when we were considering frequency regimes for the cavity model for which we also called strong and weak confinement. However in those regimes the relevant decay parameter was not the spontaneous decay rate Γ of the atom but instead it was the photon loss rate from tha cavity κ [c.f Eqs. (2.65) and (2.69)] .

If we replace Γ with κ in Eq. (3.100) and set $\alpha = 0$, since the effect of spontaneous emission from the atom is negligible in the cavity model, we we get back the cavity model steady states Eqs. (2.65) and (2.69), thus highlighting the similar cooling mechanisms between the cavity and free particle models.

3.4.3 Effective cooling rates

As we have seen in section (3.2.3) analysing the cooling process for the weak confinement regime gave us an equation of the form

$$\dot{n}_2 = \alpha_{11}\, n_2 + \alpha_{12}\, k_7 + \alpha_{13}\, k_8 + \alpha_{14}\, k_9 + \alpha_{15}\, k_{10} + \beta_1 \tag{3.101}$$

Then in section 3.3.4 we saw how to arrive at our effective cooling equation for n_2 by replacing the coherences k_7 to k_{10} with their time averaged values . In section (3.2.4) for the strong confinement regime we showed the expectation values n_1, n_4, k_1, k_2, and k_7 to k_{24} evolve much faster than the y operator population n_2 thus making it possible to adiabatically eliminate all variables except n_2 to give us an effective cooling equation Eq. (3.60). In both instances the rate at which n_2 decreases is given by the coefficient in front of the n_2 variable in the effective equation. For the weak confinement case this is α_{11} (c.f Eq. (3.52)) and for the strong confinement this is γ_c^{str} (c.f Eq. (3.61)). In fact before any approximation is made with regard to either the strong or weak confinement regimes we can use the equations in App. A.4 specifically Eqs. (A.59), (A.62), (A.64), (A.66), (A.67), and (A.68) to determine, by adiabatic elimination of the variables n_1, n_4, k_1, k_2, and k_{11} to k_{24}, zeroth order and first order expressions for n_1, k_{11} and k_{12}. Substituting these expressions into Eq. (3.39) we find an equation of the form

$$\dot{n}_2 = a_1\, n_2 + a_2\, k_7 + a_3\, k_8 + a_4\, k_9 + a_5\, k_{10} + b_1 \tag{3.102}$$

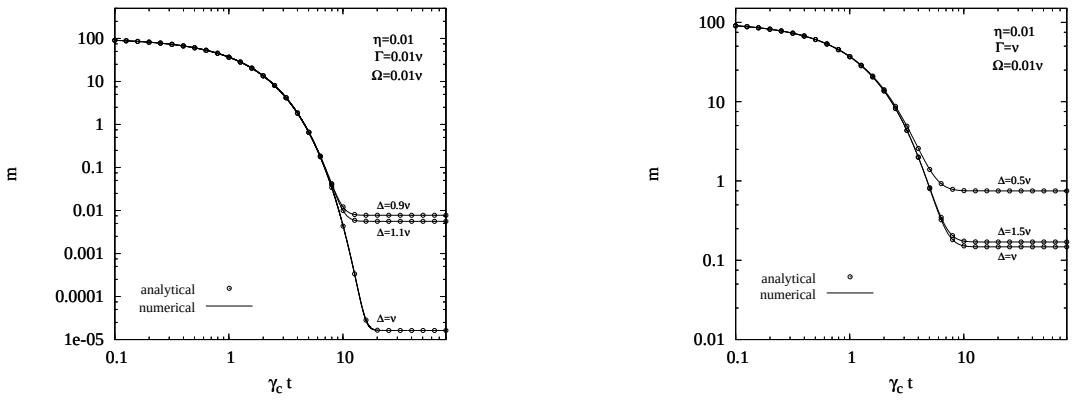

Figure 3.7: Logarithmic plot of the time dependence of the mean phonon number m for the experimental parameters indicated in the figure. The numerical solutions are the result of a numerical integration of 23 cooling equations while the analytical solution represents Eq. (3.82).

Here we are only interested in the rate without regard to the strong or weak confinement regimes and so there is no need to find approximate expressions for the coherences k_7 to k_{10} as we have previously done with time averaging and quasi - stationary approximations. In this case the rate is obviously a_1 and for the sake of simplicity let us instead call this rate γ_c as it is actually the effective cooling rate γ_c in Eq. (3.82) which in second order in η is given by

$$\gamma_c = \frac{16\eta^2\nu\Delta\Gamma\Omega^2}{\mu^2}\cdot\frac{\xi_1^4}{\xi_2^6} \tag{3.103}$$

with ξ_1 and ξ_2 as in Eq. (3.84). Fig. 3.6 shows the dependence of this cooling rate on the laser parameters Ω and Δ. Indeed we find that γ_c increases in general as Ω increases. This confirms that one should choose Ω as large as possible without noticeably decreasing the stationary state phonon number m_{ss} as pointed out already in Section 3.4.1.

For relatively small Rabi frequencies Ω, i.e. for $\Omega \ll \Gamma$, the cooling rate γ_c in Eq. (3.103) simplifies to

$$\gamma_c = \frac{\eta^2\Gamma\Omega^2}{\Gamma^2+4(\Delta-\nu)^2} - \frac{\eta^2\Gamma\Omega^2}{\Gamma^2+4(\Delta+\nu)^2}\,. \tag{3.104}$$

When comparing this result with the expression for $A_- - A_+$ in [10, 12], we find that our cooling rate differs by a factor 4 from the cooling rate reported in these references. The above cooling rate γ_c also differs by a factor $\frac{1}{2}$ from the cooling rate implied in Ref. [11]. However, as Fig. 3.7 confirms, Eq. (3.103) is in very good agreement with

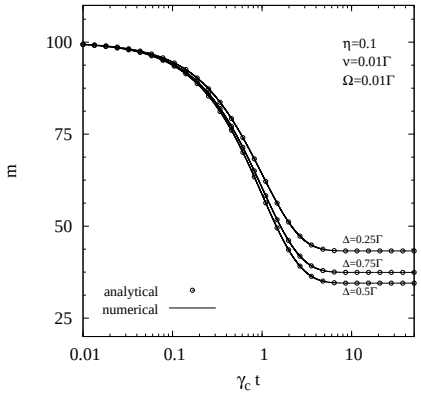

Figure 3.8: Logarithmic plot of the time dependence of m analogously to Fig. 3.7 but for different experimental parameters (weak confinement regime).

numerical solutions of the closed set of 23 cooling equations given in this paper. These numerical solutions of the cooling equations also confirm our analytical solution for the stationary state phonon number m_{ss} in Eq. (3.83).

Weak confinement

For a relatively weakly confined particle, the optimal laser detuning Δ which minimises the stationary state phonon number m_{ss} is given by $\frac{1}{2}\Gamma$ (cf. Eq. (3.94)). Taking this into account, the cooling rate γ_c in Eq. (3.103) simplifies to

$$\gamma_c = \frac{2\eta^2\nu\Omega^2}{\Gamma^2} \tag{3.105}$$

in the limit of weak driving, ie. when neglecting terms proportional to Ω^2. As Fig. 3.8 illustrates, this cooling rate is in good agreement with a numerical solution of the full set of 23 rate equations.

Strong confinement

In the strong confinement regime, terms which scale as Γ or Ω are in general negligible (cf. Eq. (3.58)). Taking this into account and simplifying Eq. (3.103) accordingly, we find that the cooling rate γ_c in this equation is exactly the same as γ_c in Eq. (3.61). The cooling process becomes indeed the most efficient, when the detuning Δ is close to the phonon frequency ν (cf. Eq. (3.98)). The cooling rate is in this case given by

$$\gamma_c = \frac{\eta^2\Omega^2}{\Gamma} \tag{3.106}$$

3.5 Final remarks

We have now analysed the cooling process of a single-trapped particle with red-detuned laser light.In contrast to previous authors [10–13, 27], our analysis avoids the adiabatic elimination of the excited atomic state *prior* to deriving any rate equations for calculating the effective cooling rate γ_c and the stationary state phonon number m_{ss}. Our calculations hence apply to a wider range of laser Rabi frequencies Ω. They show that Ω can be chosen relatively large without affecting the final outcome of the cooling process. For example, in the weak confinement regime with $\nu \ll \Gamma$, Ω can be as large as $0.3\,\Gamma$ and in the strong confinement regime with $\Gamma \ll \nu$, Ω can be as large as $0.4\,\nu$ without changing the stationary state phonon number m_{ss} noticeably. This is an interesting observation, since γ_c scales as Ω^2 and increases rapidly when Ω increases.

The main novelty of our calculations is a transformation of the original Hamiltonian which replaces the atomic lowering operator σ^- and the phonon annihilation operator b by two new operators x and y which commute with each other. The corresponding particles are neither atomic excitations nor phonons but provide a more natural description of the trapped particle in the sense that these operators account for a combined effect of b and σ^-. Our calculations are therefore more straightforward than previous calculations. Since the theory of laser cooling has already been studied in great detail in the literature [10, 13, 26, 27], the main purpose of our approach is to establish and test a framework for the modeling of laser cooling which can be extended relatively easily to more complex cooling scenarios like cavity-mediated laser cooling [14, 69, 84] and possible quantum optical heating mechanisms in sonoluminescence experiments [85]. Indeed, having now developed this approach, the next chapter shall see its application to the cavity model that was explored using the Lamb-Dicke approximation in the previous chapter except now we can use the "sandwich" method

$$D(\mathrm{i}\eta)\, b^\dagger b\, D^\dagger(\mathrm{i}\eta) \quad = \quad b^\dagger b - \mathrm{i}\eta\,(b - b^\dagger) + \eta^2 \tag{3.107}$$

in place of the Lamb-Dicke approximation.

Chapter 4

Cavity Mediated Laser Cooling beyond the Lamb - Dicke Approximation

We now return to the trapped particle in the cavity and apply the techniques we have developed from analysing the case of the free particle. In fact the techniques can be easily adapted to the cavity framework and as we shall see the relevant expressions bear a lot of resemblance to their free particle analogues. Specifically we take the effective Hamiltonian of Eq. (2.37) and determine the groups of rate equations for y operator, x operator and mixed operator expecation values. Having already adiabatically eliminated the excited state we now find our x operators to be bosonic which reduces the number of terms in some rate equations. There is a trade off however in that we now must deal with a nonlinear operator $x^\dagger x x^\dagger x$ which introduces more rate equations. This time also, the rate equations do not feature any θ dependance as we are no longer considering spontaneous emission from the excited state. The analysis of the rate equations once again becomes vastly simpler when considering 2 different frequency regimes of weak and strong confinement which in this case are those first defined in Section 2.4.2 by $\kappa \gg \nu$ and $\kappa \ll \nu$ respectively. It is quite remarkable how we once again discover that in the conditions of weak confinement the x operator expectation values and mixed operator coherences can be adiabatically eliminated leaving us to show the existence of a stationary solution for the y-operator expectation values through a stability analysis. A difference to be noted this time, as we shall see, is that even in the conditions of strong confinement all expectation values of the y operators evolve on the same time scale. Knowing this the subsequent sections will follow similar steps that have been carried out in the previous chapter.

4.1 Theoretical model

Let us look again at Eq. (2.37). Using a similar idea to that of section 3.2.1 we define x to be

$$x \equiv D(i\eta)\, c\,. \tag{4.1}$$

only this time the annihilation operator will be bosonic.

$$\left[x, x^\dagger\right] = 1\,. \tag{4.2}$$

We can again make the interpretation that the operator x differs from c only by the fact that its application not only transforms $|1\rangle$ into $|0\rangle$ but also induces a kick, i.e. it simultaneously displaces the motion of the particle. Eq. (2.37) can now be written as

$$H_I = \hbar g_{\text{eff}}\, x + \text{H.c.} + \hbar\delta_{\text{eff}}\, x^\dagger x + \hbar\nu\, b^\dagger b\,. \tag{4.3}$$

Like before the operators x and b and functions of them do not commute in general. In fact we find the exact same commutators that we found previously in Eqs. (3.28) and (3.29) so we once more introduce another operator y which again can be defined as

$$y \equiv b - i\eta\, x^\dagger x\,. \tag{4.4}$$

Again y is a bosonic operator which obeys the commutator relation

$$\left[y, y^\dagger\right] = 1\,. \tag{4.5}$$

And of course we now have

$$\left[x, y\right] = \left[x^\dagger, y\right] = \left[x, y^\dagger\right] = \left[x^\dagger, y^\dagger\right] = 0 \tag{4.6}$$

which can be checked using the commutator relations in Eqs. (3.28) and (4.5). We can also show that Eq. (4.4) is a unitary transformation since one can show that [105]

$$U \equiv \exp\left[i\eta c^\dagger c\left(b + b^\dagger\right)\right] \tag{4.7}$$

yields y when defining y as $y = U\, b\, U^\dagger$. Proceeding in a similar way one can show that $x = U\, c\, U^\dagger$. Using the x and the y operators therefore does not introduce a new Hilbert space and new physics into the modelling of the cavity cooling process. Using the x and

the y operators, the interaction Hamiltonian $H_{\rm I}$ in Eq. (2.37) can now be written as

$$\begin{aligned} H_{\rm I} &= \hbar g_{\rm eff}\, x + \text{H.c.} + \hbar\delta_{\rm eff}\, x^\dagger x + \hbar\eta^2\nu\, x^\dagger x x^\dagger x \\ &\quad -\mathrm{i}\hbar\eta\nu\, x^\dagger x(y - y^\dagger) + \hbar\nu\, y^\dagger y\,. \end{aligned} \tag{4.8}$$

This Hamiltonian is exact, since the exponential terms in the original Hamiltonian $H_{\rm I}$ in Eq. (2.37) have been removed via a basis transformation and not via an approximation. Unfortunately, the new $H_{\rm I}$ contains non-linear terms which still make it impossible to obtain a closed set of cooling equations. However, as we shall see below, this new form of the interaction Hamiltonian yields simpler equations than the Hamiltonian $H_{\rm I}$ in Eq. (2.37), since x and y commute. In the remainder of this section, we use the interaction Hamiltonian $H_{\rm I}$ to obtain a closed set of cooling equations to model the time evolution of the mean phonon number m.

4.2 Time evolution of expectation values

So once more, instead of solving the master equation in Eq. (2.50), we consider in the following only a finite set of expectation values and derive a closed set of differential equations which show how these evolve in time. Using Eq. (4.1) with Eq. (2.53) we find that the generalised rate equation is given by

$$\langle \dot{A} \rangle = -\frac{\mathrm{i}}{\hbar} \left\langle \left[A, H_{\rm I}\right] \right\rangle - \frac{1}{2}\kappa \left\langle A x^\dagger x + x^\dagger x A \right\rangle + \kappa \left\langle x^\dagger D(\mathrm{i}\eta) A D(\mathrm{i}\eta)^\dagger x \right\rangle . \tag{4.9}$$

In the following, we use this equation to analyse for example the time evolution of the x operator expectation values

$$n_1 \equiv \langle x^\dagger x \rangle\,, \quad n_3 \equiv \langle x^\dagger x x^\dagger x \rangle \tag{4.10}$$

which are identical to the cavity photon expectation values $\langle c^\dagger c \rangle$ and $\langle c^\dagger c c^\dagger c \rangle$. In addition, we consider the y-operator expectation values

$$\begin{aligned} &n_2 \equiv \langle y^\dagger y \rangle\,, \quad k_7 \equiv \langle y + y^\dagger \rangle\,, \quad k_8 \equiv \mathrm{i}\,\langle y - y^\dagger \rangle\,, \\ &k_9 \equiv \langle y^2 + y^{\dagger 2} \rangle\,, \quad k_{10} \equiv \mathrm{i}\,\langle y^2 - y^{\dagger 2} \rangle\,. \end{aligned} \tag{4.11}$$

Finally, we also need to consider the mixed operator expectation values

$$k_{11} \equiv \langle x^\dagger x (y + y^\dagger) \rangle\,, \quad k_{12} \equiv \mathrm{i}\,\langle x^\dagger x (y - y^\dagger) \rangle\,. \tag{4.12}$$

The definitions of the other expectation values which are used to derive the remaining rate equations can be found in App. B.1. Combining $m \equiv \langle b^\dagger b \rangle$ with the definitions of

x and y in Eqs. (4.1) and (4.4), we find that m can also be written as

$$m \equiv n_2 - \eta\, k_{12} + \eta^2\, n_3\,. \tag{4.13}$$

Note that in the free particle case the last term was the population n_1. So once again m and n_2 are the same for $\eta = 0$. Then applying Eq. (4.9) to the y operator expectation values in Eq. (4.11), we find that their time derivatives are without any approximations given by

$$\begin{aligned}
\dot{n}_2 &= \eta\nu\, k_{11} - \eta\kappa\, k_{12} + \eta^2\kappa\, n_1\,,\\
\dot{k}_7 &= 2\eta\nu\, n_1 - \nu\, k_8\,,\\
\dot{k}_8 &= \nu\, k_7 - 2\eta\kappa\, n_1\,,\\
\dot{k}_9 &= -2\nu\, k_{10} + 2\eta\nu\, k_{11} + 2\eta\kappa\, k_{12} - 2\eta^2\kappa\, n_1\,,\\
\dot{k}_{10} &= 2\nu\, k_9 + 2\eta\nu\, k_{12} - 2\eta\kappa\, k_{11}\,.
\end{aligned} \tag{4.14}$$

Like their free particle analogues these five differential equations depend only on the y operator expectation values themselves as well as on n_1, k_{11}, and k_{12}. The time derivatives of other expectation values can be found in App. B.2 where we also perform an adiabatic elimination of all these equations as they are the equations that define the relatively fast evolving variables.

4.2.1 Weak confinement regime

We now look again at the case where the trapped particle experiences a relatively weak trapping potential and where the Lamb-Dicke parameter η is much smaller than one. More concretely we assume in the following that

$$\nu \ll \kappa \;\text{ and }\; \eta \ll 1\,. \tag{4.15}$$

A closer look at the cooling equations in App. B.2 shows that this choice of parameters causes the y operator expectation values n_2 and k_7 to k_{10} to evolve on a much slower time scale than all other relevant expectation values. The reason for this is that these variables are all x or mixed operator expectation values which decay with the cavity decay rate κ. Taking this into account and eliminating n_1, n_3, k_1, k_2, and k_{13} to k_{24} adiabatically from the system dynamics, we obtain a closed set of five effective cooling equations which applies after a relatively short transition time and which can be written in similar matrix form to Eq. (3.43) of the free particle analysis.

$$\left(\dot{n}_2, \dot{k}_7, \dot{k}_8, \dot{k}_9, \dot{k}_{10}\right)^{\mathrm{T}} = M\left(n_2, k_7, k_8, k_9, k_{10}\right)^{\mathrm{T}} + \left(\beta_1, \beta_2, \beta_3, \beta_4, \beta_5\right)^{\mathrm{T}}\,. \tag{4.16}$$

Eq. (4.14) shows that the time derivatives of the y operator expectation values n_2, and k_7 to k_{10} depend only on n_1, k_{11}, and k_{12} just like their free particle counterparts. The calculation of the 5×5 matrix M therefore only requires the calculation of n_1, k_{11}, and k_{12} which can be found in App. B.2. Substituting Eqs. (B.4), (B.7), (B.9), and (B.12) into Eq. (4.14), and using the α notation like in the free particle example, M can again be written as

$$M = \begin{pmatrix} \alpha_{11}^{(2)} & \alpha_{12}^{(1)} & \alpha_{13}^{(1)} & \alpha_{14}^{(2)} & 0 \\ 0 & 0 & -\nu & 0 & 0 \\ 0 & \nu & \alpha_{33}^{(2)} & 0 & 0 \\ \alpha_{41}^{(2)} & \alpha_{42}^{(1)} & \alpha_{43}^{(1)} & \alpha_{44}^{(2)} & -2\nu \\ 0 & \alpha_{52}^{(1)} & \alpha_{53}^{(1)} & 2\nu & \alpha_{55}^{(2)} \end{pmatrix}. \tag{4.17}$$

This time, the first order matrix elements $\alpha_{ij}^{(1)}$ in these equations are given by

$$\begin{aligned} &\alpha_{12}^{(1)} = -\frac{8\eta\nu g_{\text{eff}}^2}{\mu^4}(\kappa^2 - 4\delta_{\text{eff}}^2), \quad \alpha_{13}^{(1)} = -\frac{4\eta\kappa g_{\text{eff}}^2}{\mu^2}, \\ &\alpha_{42}^{(1)} = \frac{32\eta\nu g_{\text{eff}}^2\kappa^2}{\mu^4}, \quad \alpha_{43}^{(1)} = \frac{8\eta\kappa g_{\text{eff}}^2}{\mu^2}, \\ &\alpha_{52}^{(1)} = -\alpha_{43}^{(1)}, \quad \alpha_{53}^{(1)} = \alpha_{42}^{(1)} \end{aligned} \tag{4.18}$$

with μ^2 defined as in Eq. (B.5). The non-zero matrix elements $\alpha_{ij}^{(2)}$ of M in second order in η and first order in ν are given by

$$\begin{aligned} &\alpha_{11}^{(2)} = \alpha_{33}^{(2)} = \alpha_{44}^{(2)} = \alpha_{55}^{(2)} = -\frac{64\eta^2\nu\delta_{\text{eff}}\kappa g_{\text{eff}}^2}{\mu^4}, \\ &\alpha_{14}^{(2)} = \frac{8\eta^2\nu\delta_{\text{eff}}\kappa g_{\text{eff}}^2}{\mu^4}, \quad \alpha_{41}^{(2)} = \frac{32\eta^2\nu\delta_{\text{eff}}\kappa g_{\text{eff}}^2}{\mu^4}. \end{aligned} \tag{4.19}$$

We can now show that β_1 up to second order in η is given by $\beta_1 = \beta_1^{(2)}$ with

$$\beta_1^{(2)} = \frac{4\eta^2\kappa g_{\text{eff}}^2}{\mu^2} + \frac{32\eta^2 g_{\text{eff}}^4\kappa\left(3\kappa^2 - 4\delta_{\text{eff}}^2\right)}{\mu^6}. \tag{4.20}$$

Moreover, we find that the coefficients β_2 to β_5 in Eq. (3.43) are in first order in η given by

$$\begin{aligned} &\beta_2^{(1)} = \frac{8\eta\nu g_{\text{eff}}^2}{\mu^2}, \quad \beta_3^{(1)} = -\frac{8\eta\kappa g_{\text{eff}}^2}{\mu^2}, \\ &\beta_4^{(1)} = \beta_5^{(1)} = 0. \end{aligned} \tag{4.21}$$

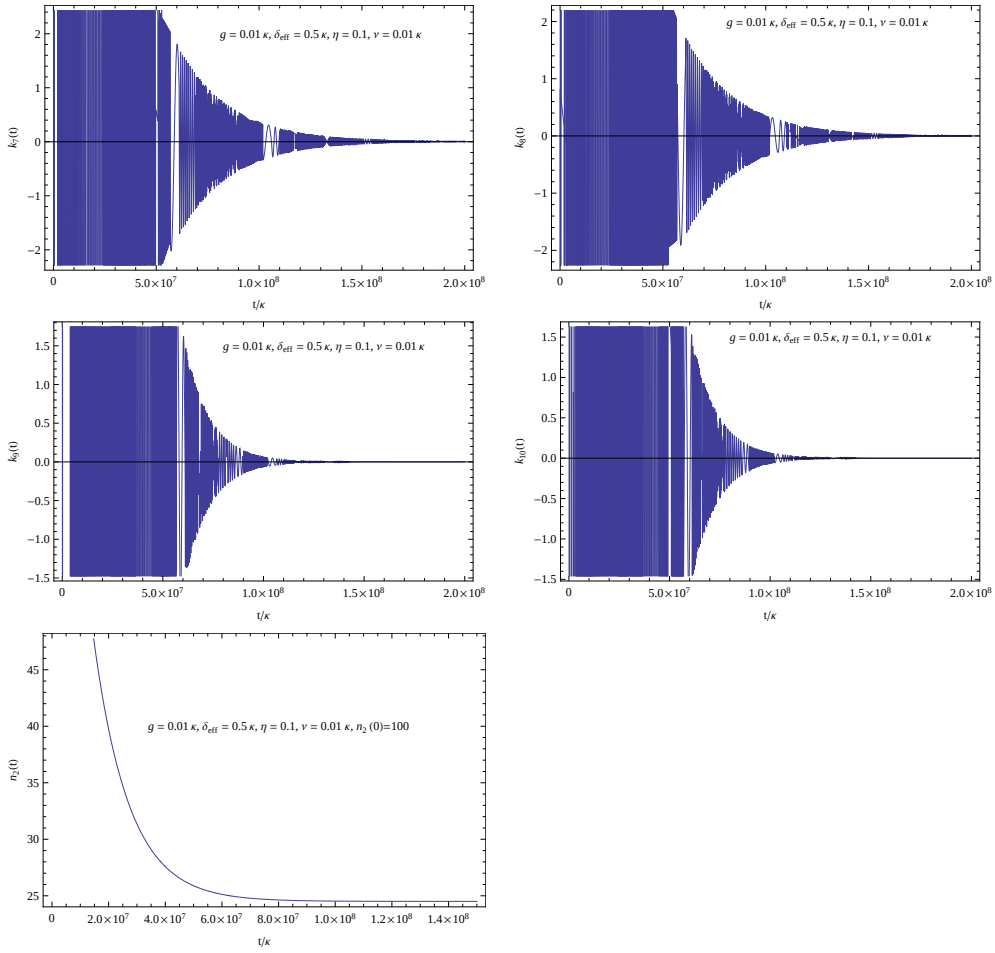

Figure 4.1: Time scale comparison for a numerical solution of k_7 to k_{10}, and n_2 for $\delta_{\text{eff}} = \kappa/2$, $\nu = 0.1\,\kappa$ and $g_{\text{eff}} = 0.01\,\kappa$. Here quasi stationary state expressions for n_1, k_{11} and k_{12} were used with parameters chosen to reflect the weak confinement regime. y particles initially assumed to be in a coherent state.

Using this closed set of five differential equations we can now analyse the time evolution of the y operator expectation values analytically and numerically just like we did for the case of the free particle. Here we can see from Fig. 4.1 that all of the y operator coherences evolve on the same timescale as the y operator population n_2. So once again the weak confinement regime which we introduced in Eq. (3.42) does not allow for the adiabatic elimination of the y operator coherences k_7 to k_{10},

4.2.2 Strong confinement regime

Let us now have a closer look at the parameter regime where the phonon frequency ν and the detuning δ_{eff} exceed the spontaneous decay rate κ and g_{eff} by at least one order

of magnitude,

$$g_{\text{eff}}, \kappa \;\ll\; \nu, \delta_{\text{eff}}, \;\text{ while }\; \eta \ll 1\,. \tag{4.22}$$

Using Eq. (4.16) in this regime we find that the corresponding matrix for M has the following form

$$M \;=\; \begin{pmatrix} \alpha_{11}^{(2)} & \alpha_{12}^{(1)} & \alpha_{13}^{(1)} & \alpha_{14}^{(2)} & \alpha_{15}^{(2)} \\ 0 & \alpha_{22}^{(2)} & -\nu & 0 & 0 \\ 0 & \nu & \alpha_{33}^{(2)} & 0 & 0 \\ \alpha_{41}^{(2)} & \alpha_{42}^{(1)} & \alpha_{43}^{(1)} & \alpha_{44}^{(2)} & -2\nu + \alpha_{45}^{(2)} \\ \alpha_{51}^{(2)} & \alpha_{52}^{(1)} & \alpha_{53}^{(1)} & 2\nu - \alpha_{45}^{(2)} & \alpha_{55}^{(2)} \end{pmatrix}. \tag{4.23}$$

The calculation of the above 5×5 matrix only required the calculation of n_1, k_{11} and k_{12} which can be found in App. B.3. The matrix elements can then be found by substituting Eqs. (B.13), (B.14, (B.15) and (B.16) into Eq. (4.14). The first order matrix elements $\alpha_{ij}^{(1)}$ are given by

$$\begin{aligned} \alpha_{12}^{(1)} &= -\frac{2\eta g_{\text{eff}}^2 \nu}{\delta_{\text{eff}}^2 - \nu^2}\,, \;\; \alpha_{13}^{(1)} = -\frac{\eta g_{\text{eff}}^2 \kappa \left(\delta_{\text{eff}}^2 + \nu^2\right)}{\left(\delta_{\text{eff}}^2 - \nu^2\right)^2}\,, \\ \alpha_{42}^{(1)} &= \frac{4\eta g_{\text{eff}}^2 \nu}{\delta_{\text{eff}}^2 - \nu^2}\,, \;\; \alpha_{43}^{(1)} = \frac{2\eta g_{\text{eff}}^2 \kappa \left(3\delta_{\text{eff}}^2 - 5\nu^2\right)}{\left(\delta_{\text{eff}}^2 - \nu^2\right)^2}\,, \\ \alpha_{52}^{(1)} &= -\alpha_{43}^{(1)}\,, \;\; \alpha_{53}^{(1)} = \alpha_{42}^{(1)}\,. \end{aligned} \tag{4.24}$$

The non-zero matrix elements $\alpha_{ij}^{(2)}$ of M in second order in η are given by

$$\begin{aligned} \alpha_{11}^{(2)} &= \alpha_{33}^{(2)} = -\frac{4\eta^2 g_{\text{eff}}^2 \delta_{\text{eff}}^2 \kappa \nu}{\left(\delta_{\text{eff}}^2 - \nu^2\right)^2}\,, \\ \alpha_{44}^{(2)} &= \alpha_{55}^{(2)} = -\frac{4 g_{\text{eff}}^2 \delta_{\text{eff}} \eta^2 \kappa \nu}{\xi^8} \left[5\delta_{\text{eff}}^4 - 34\delta_{\text{eff}}^2 \nu^2 + 38\nu^4\right], \\ \alpha_{22} &= -\frac{4\eta^2 g_{\text{eff}}^2 \nu^3}{\delta_{\text{eff}}^3 \kappa - \delta_{\text{eff}} \kappa \nu^2} \\ \alpha_{14}^{(2)} &= \frac{2 g_{\text{eff}}^2 \delta_{\text{eff}} \eta^2 \kappa \nu}{\xi^8} \left[\delta_{\text{eff}}^4 + 4\delta_{\text{eff}}^2 \nu^2 - 14\nu^4\right], \;\; \alpha_{41}^{(2)} = \frac{8\eta^2 g_{\text{eff}}^2 \kappa \nu \left(\delta_{\text{eff}}^2 - 2\nu^2\right)}{\delta_{\text{eff}} \left(\delta_{\text{eff}}^2 - \nu^2\right)^2} \\ \alpha_{45} &= -\alpha_{54} = \frac{12 g^2 \delta \eta^2 \nu^2}{\xi^4}\,, \\ \alpha_{51}^{(2)} &= \frac{8\eta^2 g_{\text{eff}}^2 \nu^2}{\delta_{\text{eff}}(\delta_{\text{eff}}^2 - \nu^2)}), \alpha_{15}^{(2)} = \frac{2 g_{\text{eff}}^2 \delta_{\text{eff}} \eta^2 \kappa \nu}{\xi^8} \left[\delta_{\text{eff}}^4 + 4\delta_{\text{eff}}^2 \nu^2 - 14\nu^4\right] \end{aligned} \tag{4.25}$$

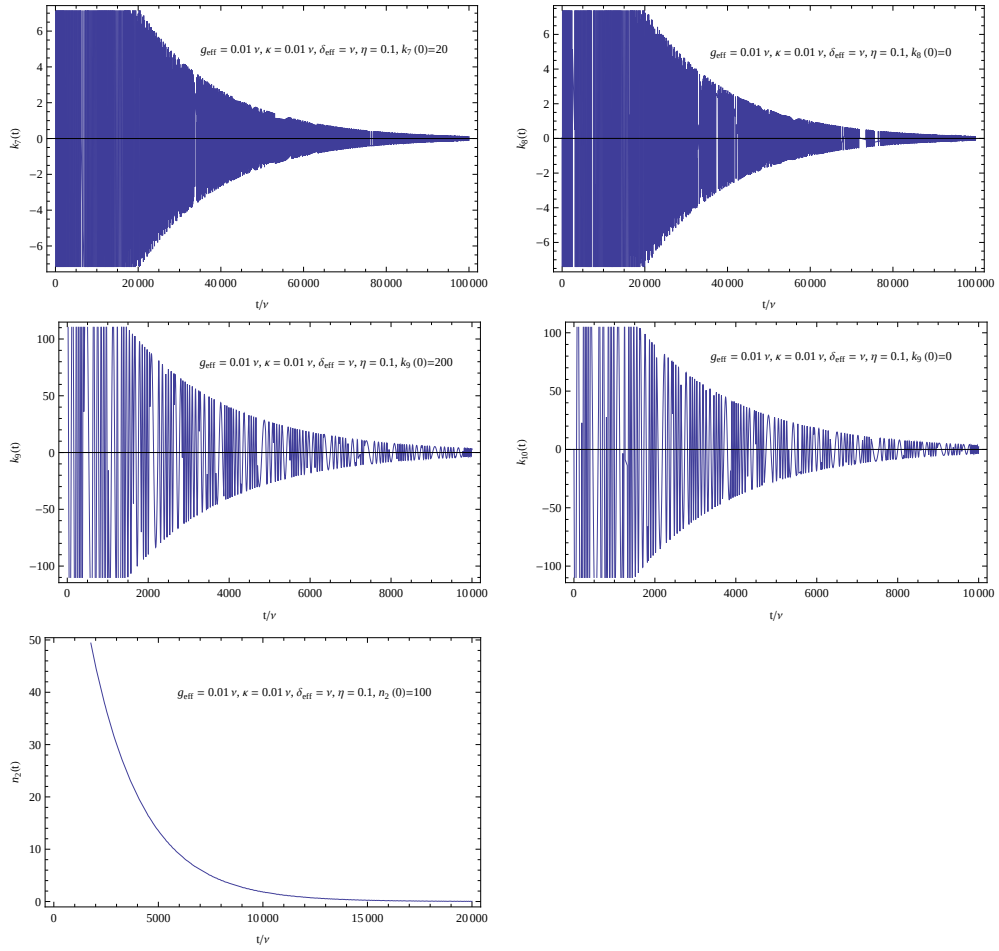

Figure 4.2: Time scale comparison for a numerical solution to k_7 to k_{10}, and n_2 for $\delta_{\text{eff}} = \nu$, $\kappa = 0.1\,\nu$ and $g_{\text{eff}} = 0.01\,\nu$. Here quasi stationary state expressions for n_1, k_{11} and k_{12} were used with parameters chosen to reflect the strong confinement regime. y particles initially assumed to be in a coherent state.

with ξ^4 defined as in Eq. (B.17). We can also show that β_1 in second order is given by

$$\beta_1 = \frac{4\eta^2 g_{\text{eff}}^2 \kappa}{\mu^4} + \frac{8 g_{\text{eff}}^4 \eta^2 \kappa \left(-4\delta_{\text{eff}}^2 + 12\nu^2\right)}{\delta_{\text{eff}}^2 \left(16\delta_{\text{eff}}^4 + \kappa^4\right)}. \tag{4.26}$$

The other coefficients β_2 to β_5 are found to be

$$\beta_2^{(1)} = \frac{2\eta\nu g_{\text{eff}}^2}{\delta_{\text{eff}}^2}, \quad \beta_3^{(1)} = -\frac{2\eta\kappa g_{\text{eff}}^2}{\delta_{\text{eff}}^2},$$
$$\beta_4^{(1)} = \beta_5^{(1)} = 0. \tag{4.27}$$

We thus have, in the strong confinement, a closed set of five equations. Fig. 4.2 shows the evolution of the numerical solution of these 5 equations. Fig. 4.2 is the result of plotting the numerical solution of Eq. (4.14). These equations were used after substituting in the quasi-stationary state values for n_1, k_{11} and k_{12}. However, and this is important, the expressions for n_1, k_{11} and k_{12} are those for which no approximation was made with regard to either the weak or strong confinement regimes. The choice of parameters for ν and κ in the numerical integration reflect this distinction. As can clearly be seen from Fig. 4.2 all y operator expectation values evolve towards a steady state on the same time scale. This is in contrast to the case of strong confinement in the free particle case (c.f. Fig. 3.2). There all the expectation values of all y operator *coherences* reach a steady state in a much shorter time to that of the y operator population. So if we adiabatically eliminate all y operator coherences here it would *not* be a reasonable approximation as they evolve on the same time scale as the y operator population. Thus, it is not clear whether an analytic solution for the steady state exists for the case of strong confinement. We must therefore perform a stability analysis on the Eq. (4.14) for the conditions of weak confinement. Proving that a stationary state exists will allow us to replace the relevant expectation values with their time average values (c.f. Section 3.3.4).

4.3 Stability analysis

Using our perturbative analysis to derive equations to second order in η for the case of the trapped particle in the cavity has left us with the five y operator differential equations of Eq. (4.14) for which it is not clear whether a stationary state solution exists. This applies to both the weak and strong confinement regimes. We shall now perform a stability analysis for both these cases and show that a stationary state solution does in fact exist.

4.3.1 Weak confinement regime

Looking at Eq. (4.17) it is easy to see that M has the same form as Eq. (3.50) that represented the five slowly evolving equations of the free particle. Then the same steps apply as before for the zeroth, first and second order matrices that were carried out in sections 3.3.1, 3.3.2 and 3.3.3. Therefore the zeroth and first order matrices have eigenvalues whose real part is zero, thus proving that the zeroth and first order approximations of Eq. (4.14) have no stationary state solution. So the second order matrix elements must be taken into account. Doing so of course results in the same eigenvalues as Eqs. (3.69), (3.70). Here the values for the alphas are those of Eqs. (4.18), (4.19) and (4.20). As in the case of the free particle, since the matrix element $\alpha_{11}^{(2)}$ is always negative, the variables of Eq. (4.14) are damped away and asymptotically approach zero on the timescale

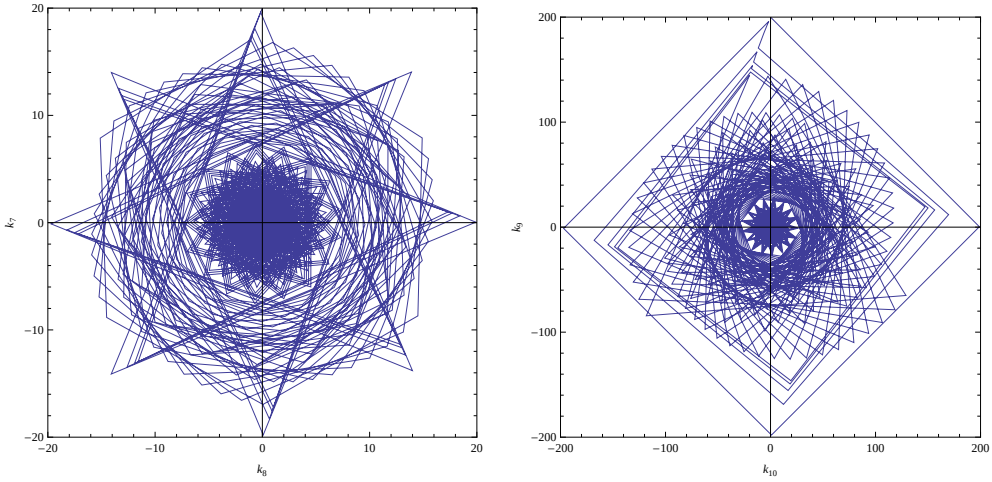

Figure 4.3: Phase portraits from a numerical solution of k_8 against k_7 and k_{10} against k_9 for $\delta_{\text{eff}} = \kappa/2$, $\nu = 0.1\,\kappa$ and $g_{\text{eff}} = 0.01\,\kappa$. Here quasi stationary state expressions for n_1, k_{11} and k_{12} were used with parameters chosen to reflect the weak confinement regime. y particles initially assumed to be in a coherent state.

given by $1/\alpha_{11}$. Fig. 4.3 illustrates how the expectation values of the y operator coherences evolve towards zero thus indicating that they do not increase in time but instead oscillate around constant values with a slowly decreasing amplitude. This enables us to replace the coherence variables k_7 to k_{10} with their time averaged values after a period of time on the order of $1/\alpha_{11}$.

4.3.2 Strong Confinement

In the strong confinement regime we have five differential equations that describe the cooling process. These five equations are those of Eq. (4.16) whose corresponding matrix M is defined by Eq. (4.23). Our numerical solution of these 5 equations has been plotted in Fig. 4.2 and shows that the coherences oscillate and asymptotically approach a fixed value. We can determine the eigenvalues of Eq. (4.23) and by showing that their real parts have a negative value we will have proven the existence of a stationary (stable) solution for the 5 equations. The matrix consisting of just zeroth order terms and the matrix consisting of just first order terms have the exact same form as those we met previously in Eq. (3.64). Then these matrices have the exact same eigenvalues as Eq. (3.65), whose real parts are not negative. Thus the second order matrix elements must once more be taken into account. Using the same idea as in section 3.3.3 where we only consider k_7 and k_8 from the set of 5 as by themselves they form a closed set. In

this case this closed set has the corresponding matrix

$$\tilde{\mathcal{K}} \equiv \begin{pmatrix} \alpha_{22}^{(2)} & -\nu \\ \nu & \alpha_{11}^{(2)} \end{pmatrix} \tag{4.28}$$

which has the eigenvalues

$$\lambda_{2,3} = \frac{1}{2}\left(\alpha_{11}^{(2)} + \alpha_{22}^{(2)}\right) \mp \frac{\mathrm{i}}{2}\sqrt{4\nu^2 - \left(\alpha_{11}^{(2)} - \alpha_{22}^{(2)}\right)^2}. \tag{4.29}$$

So if k_7 and k_8 reach a stationary state when

$$\frac{1}{2}\left(\alpha_{11}^{(2)} + \alpha_{22}^{(2)}\right) < 0 \tag{4.30}$$

which is true if α_{11} and α_{22} are negative (c.f. Eq. (4.25)) which in turn can only be true if $\delta_{\text{eff}} > \nu$. Finding the eigenvalues of the matrix that corresponds to the evolution of n_2, k_9 and k_{10}

$$\tilde{\mathcal{M}} \equiv \begin{pmatrix} \alpha_{11}^{(2)} & \alpha_{14}^{(2)} & \alpha_{15}^{(2)} \\ \alpha_{41}^{(2)} & \alpha_{44}^{(2)} & -2\,\nu - \alpha_{45}^{(2)} \\ \alpha_{51}^{(0)} & 2\nu - \alpha_{45}^{(2)} & \alpha_{44}^{(2)} \end{pmatrix}$$

is not straightforward. However, finding the characteristic polynomial and solving to find the cubic roots results in a 3 long expressions involving different permutations and functions of α_{11}, α_{15}, α_{51}, α_{44} and α_{45}. Since permutations of the alphas will have expressions that go above second order in η we can make the approximation of neglecting such terms. Doing so, we find that the following conditions are necessary for the real part of the eigenvalues to be negative

$$\alpha_{11} < 0, \quad 2\alpha_{44} < 0\,. \tag{4.31}$$

These conditions will be true as long as δ_{eff} does not fall between the following values approximately for the case of the strong confinement regime.

$$2.3\nu > \delta_{\text{eff}} > 1.2\nu\,. \tag{4.32}$$

This is so as Eq. (4.25) shows that α_{11} and α_{44} are always negative when

$$\left[5\delta_{\text{eff}}^4 - 34\delta_{\text{eff}}^2\nu^2 + 38\nu^4\right] > 0\,. \tag{4.33}$$

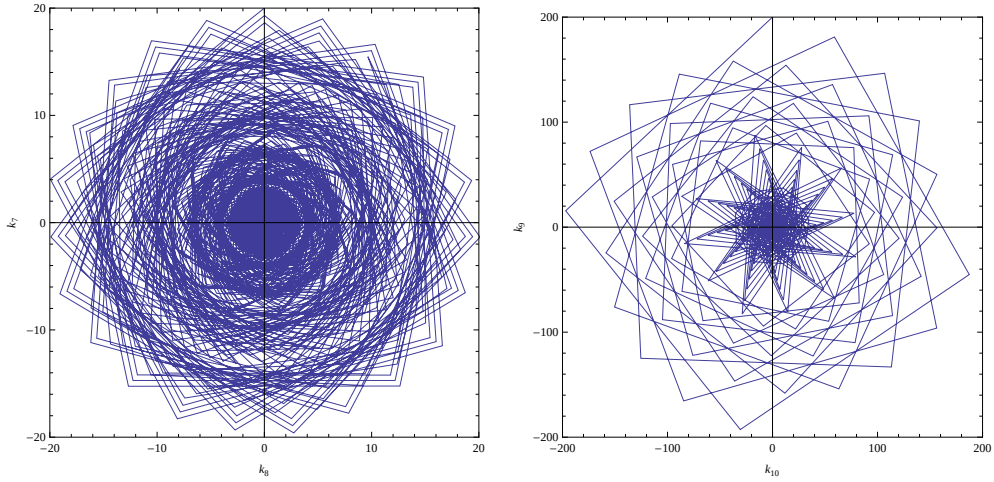

Figure 4.4: Phase portraits from a numerical solution of k_8 against k_7 and k_{10} against k_9 for $\delta_{\text{eff}} = \nu$, $\kappa = 0.1\nu$ and $g_{\text{eff}} = 0.01\nu$. Here quasi stationary state expressions for n_1, k_{11} and k_{12} were used with parameters chosen to reflect the strong confinement regime. y particles initially assumed to be in a coherent state.

So in the strong confinement regime the five eigenvalues of M have negative real parts thus proving that all variables are damped away and eventually tend to zero on the timescale given by $1/\alpha_{11}$. Fig. 4.4 which plots the numerical solution of Eq. (4.14) for the strong confinement regime clearly illustrates how the coherences k_7 to k_{10} evolve towards zero. Since the y coherences do not increase but oscillate with a slowly decreasing amplitude around constant values, the cooling process remains stable and the trapped particle eventually reaches its stationary state. This observation enables us to replace the coherences by their time averaged values. This means the calculations in the following section apply only towards the end of the cooling process after a transition time of the order $1/\alpha_{11}^{(2)}$ for both the weak and strong confinement regimes.

4.4 Cooling rates and phonon numbers

Using the same form of the rate equation for n_2 as Eq. (3.101) we can determine the effective n_2 rate equation for both the weak confinement regime using the values of the α_{ij}'s in Eq. (4.19) and the strong confinement regime using the values of the α_{ij}'s in Eq. (4.25). Since n_2 and the mean phonon number are identical in zeroth order in η, this equation allows us to calculate the effective cooling rate γ_{c} and the stationary state phonon number m_{ss} for the cooling process illustrated in Fig. 2.1. As we shall see below, these are exactly the same as the cooling rate and the stationary state phonon number which we obtained previously when applying the Lamb-Dicke approximation [15–18, 69]. This section also shows that our current analysis of the cavity cooling process is

consistent with earlier results.

4.4.1 Time averaging of k_7 to k_{10}

In this subsection we derive approximate solutions for the y operator coherences k_7 to k_{10} in first order in η. Taking only terms in first order in η into account, we find for example that the time derivatives of k_7 and k_8 are given by

$$\begin{pmatrix} \dot{k}_7 \\ \dot{k}_8 \end{pmatrix} = \begin{pmatrix} 0 & -\nu \\ \nu & 0 \end{pmatrix} \begin{pmatrix} k_7 \\ k_8 \end{pmatrix} + \begin{pmatrix} \beta_2 \\ \beta_3 \end{pmatrix}. \tag{4.34}$$

As we have seen in the previous section, these equations describe relatively fast oscillations around constant values whose amplitudes decrease in time. This allows us to approximate k_7 and k_8 by their time averages which are given by

$$k_7 = \frac{8\eta\kappa g_{\rm eff}^2}{\nu(\kappa^2 + 4\delta_{\rm eff}^2)}, \quad k_8 = \frac{8\eta g_{\rm eff}^2}{\kappa^2 + 4\delta_{\rm eff}^2} \tag{4.35}$$

up to first order in η. Moreover, we find that the time derivatives of k_9 and k_{10} equal

$$\begin{aligned} \dot{k}_9 &= -2\nu\, k_{10}\,, \\ \dot{k}_{10} &= 2\nu\, k_9 \end{aligned} \tag{4.36}$$

in zeroth order in η. These coherences also oscillate relatively rapidly. This allows us to replace k_9 and k_{10} by the average values of these oscillations and assume that

$$k_9 = k_{10} = 0 \tag{4.37}$$

in zeroth order in η. Substituting the expressions for the α_{ij}'s in Eq. (4.19) and using the time average values we find that the effective rate equation for n_2 in the weak confinement regime becomes

$$\dot{n}_2 = -\frac{64\eta^2 g_{\rm eff}^2 \delta_{\rm eff}\kappa\nu}{\left(4\delta_{\rm eff}^2 + \kappa^2\right)^2} n_2 + \frac{4\eta^2 g_{\rm eff}^2 \kappa}{4\delta_{\rm eff}^2 + \kappa^2}. \tag{4.38}$$

In a similiar manner the effective rate equation for n_2 in the strong confinement regime becomes

$$\dot{n}_2 = -\left(\frac{\eta^2\kappa g_{\rm eff}^2}{(\delta_{\rm eff} - \nu)^2} - \frac{\eta^2\kappa g_{\rm eff}^2}{(\delta_{\rm eff} + \nu)^2}\right) n_2 + \frac{\eta^2\kappa g_{\rm eff}^2}{(\delta_{\rm eff} + \nu)^2} \tag{4.39}$$

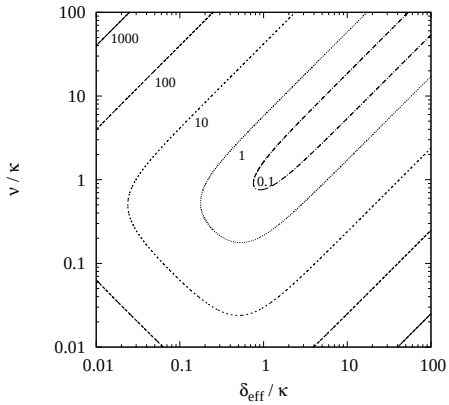

Figure 4.5: Logarithmic contour plot of the stationary state phonon number m_{ss} in Eq. (4.40) as a function of the relative phonon frequency ν/κ and the relative effective detuning $\delta_{\text{eff}}/\kappa$.

In the following two sections section we shall show how to derive an analytic expression for the steady state m_{ss} and cooling rate γ_c without making any approximation to either the weak or strong confinement regimes. We will then show that both the steady state and cooling rate reduce to the expressions that are consistent with the weak and strong confinement regimes.

4.4.2 Stationary state phonon numbers

Using the cooling equations in Eq. (4.14) and in App. B.2 and setting the time derivatives of all expectation values equal to zero, we obtain the stationary state phonon number

$$m^{ss} = \frac{\kappa^2 + 4(\nu - \delta_{\text{eff}})^2}{16\nu\delta_{\text{eff}}} \tag{4.40}$$

This result applies in zeroth order in η without any approximations with respect to either the weak or strong confinement regimes. Fig. 4.5 shows m_{ss} as a function of the two laser parameters ν and δ_{eff} . In the weak confinement regime one should choose $\delta_{\text{eff}} = 0.5\,\kappa$ and for $\nu \gg \kappa$ one should choose δ_{eff} close to ν in order to minimise the final kinetic energy of the trapped particle. To see this more clearly consider the following example

Example.
Consider $\nu/\kappa = 10$. This is in the strong confinement regime as $\nu \gg \kappa$. So if we let $\delta_{\text{eff}} = \nu$ then $\delta_{\text{eff}} = 10\kappa/\kappa = 10$ which means m_{ss}, according to Fig. 4.5, is less than 0.1. On the other hand if we consider the weak confinement regime and choose $\nu/\kappa = 0.1$ then $\delta_{\text{eff}} = 0.5$ which corresponds to a steady state of about 5 when checking Fig. 4.5.

Noting Eq. (4.40)'s consistency with Eq. (2.62) from the earlier chapter we can now apply the approximations that correspond to the weak and strong confinement regimes and show that we get the same expressions that can be found from Eq. (4.38) and Eq. (4.39) respectively.

Weak confinement

In the weak confinement regime, the stationary state phonon number m_{ss} in Eq. (4.40) simplifies to

$$m^{\text{ss}} = \frac{\kappa^2 + 4\delta_{\text{eff}}^2}{16\nu\delta_{\text{eff}}} \tag{4.41}$$

Exactly the same stationary state phonon number is obtained when setting the left hand side of Eq. (4.38) equal to zero. This confirms the consistency of the calculations in this paper. This expression assumes its minimum if

$$\delta_{\text{eff}} = \frac{1}{2}\kappa\,. \tag{4.42}$$

For this laser detuning the stationary state phonon number simplifies to

$$m_{\text{ss}}^{\text{weak}} = \frac{\kappa}{4\nu}\,. \tag{4.43}$$

This means, in the optimal case the final phonon numbers scales essentially as κ/ν which is much larger than one.

Strong confinement

Using the effective cooling equation derived in Eq. (4.39) and setting it equal to zero, we find that the stationary state phonon number in the strong confinement regime equals

$$m_{\text{ss}}^{\text{strong}} = \frac{(\delta_{\text{eff}} - \nu)^2}{4\delta_{\text{eff}}\nu} \tag{4.44}$$

to a very good approximation. Exactly the same result is obtained when neglecting terms proportional to κ in Eq. (4.40). This result suggests immediately that one should

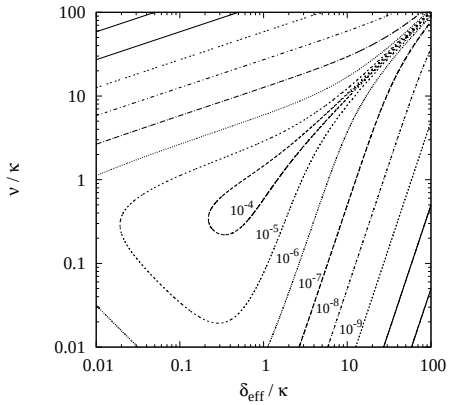

Figure 4.6: Logarithmic contour plot of the effective cooling rate γ_c in Eq. (4.47) in units of $2g_{\text{eff}}^2/\kappa$ as a function of the relative phonon frequency ν/κ and the relative effective detuning $\delta_{\text{eff}}/\kappa$ for $\eta = 0.01$.

choose

$$\delta_{\text{eff}} \quad = \quad \nu \tag{4.45}$$

in order to minimise the final phonon number m_{ss}. When substituting this detuning back into Eq. (4.40), we find that the stationary state phonon number for cavity laser sideband cooling in the strong confinement regime is to a very good approximation given by

$$m_{\text{ss}}^{\text{strong}} \quad = \quad \frac{\kappa^2}{16\nu^2}\,. \tag{4.46}$$

This means, the stationary state phonon number now scales essentially as κ^2/ν^2 which is much smaller than one.

4.4.3 Effective cooling rates

We now use cooling equations in App. B.2 and determine the first and second order expressions for n_1, k_{11} and k_12 and substitute them into the rate equation for n_2 in Eq. (4.14). Doing so will allow us to extract the cooling rate before making approximations with regard to either the weak or strong confinement regimes. In this case we do not need to know what functions the y operator coherences are as the rate will simply be the coefficient in front of the n_2 variable which in second order in η, is given by

$$\gamma_c \quad = \quad \frac{64\eta^2\nu\,\delta_{\text{eff}}\kappa\,g_{\text{eff}}^2}{\left[\kappa^2+4(\delta_{\text{eff}}+\nu)^2\right]\cdot\left[\kappa^2+4(\delta_{\text{eff}}-\nu)^2\right]}\,. \tag{4.47}$$

We can also express γ_c in the form of the popular $A^- - A^+$ transition rate notation in the following way

$$\gamma_c = \frac{4\eta^2\kappa g_{\text{eff}}^2}{\kappa^2 + 4(\delta_{\text{eff}} - \nu)^2} - \frac{4\eta^2\kappa g_{\text{eff}}^2}{\kappa^2 + 4(\delta_{\text{eff}} + \nu)^2}. \tag{4.48}$$

Fig. 4.6 shows a contour plot of the cooling rate γ_c of Eq. (4.47) in units of $2g_{\text{eff}}^2/\kappa$ as a function of ν/κ and δ_{eff}. The figure illustrates how the cooling rate varies between the weak and strong confinement regimes. Consider again the following example.

> **Example.** Suppose that we are in the strong confinement regime so that $\nu = 10\kappa$. Then for the cooling rate to be minimised $\delta_{\text{eff}} = \nu = 10$. This means that the cooling rate will be of the order of 10^{-4}. In fact for any value of δ_{eff} the cooling rate will be of this order as all values will lie along the diagonal in the figure. Now if we move to the weak confinement regime and have $\nu = 0.1\kappa$ then for $\delta_{\text{eff}} = \kappa/2$ we get the cooling rate to be of the order of 10^{-5}.

So as one moves between the weak and strong confinement regimes the cooling rate increases by an order of magnitude depending on parameters.

Weak confinement

For a relatively weakly confined particle, the optimal laser detuning δ_{eff} which minimises the stationary state phonon number m_{ss} is given by $\frac{1}{2}\kappa$ (cf. Eq. (4.42)). Taking this into account, the cooling rate γ_c in Eq. (4.47) simplifies to

$$\gamma_c = \frac{8\eta^2 g_{\text{eff}}^2 \nu\kappa^2}{\kappa^4 + 4\nu^4}. \tag{4.49}$$

which is the same result we found in Eq. (2.80) for the first order Lamb-Dicke approximation.

Strong confinement

In the strong confinement regime, terms which scale as κ^2 are in general negligible (cf. Eq. (4.22)). The cooling process becomes indeed the most efficient, when the detuning δ_{eff} is close to the phonon frequency ν (cf. Eq. (4.45)). The cooling rate is in this case given by

$$\gamma_c = \frac{64\eta^2 g_{\text{eff}}^2 \nu^2}{\kappa(\kappa^2 + 16\nu^2)}. \tag{4.50}$$

which is the same result that we found in Eq. (2.81) for the first order Lamb-Dicke approximation.

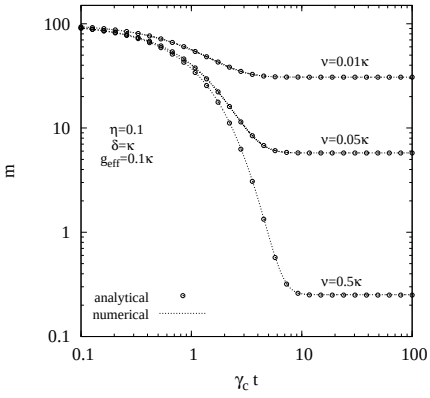

Figure 4.7: Plot showing a numerical integration of all 25 cooling equations (c.f. Eqs. (4.14), (B.3), (B.6), (B.8), (B.10), and (B.11)) compared with the analytic solution of Eq. (4.52) which includes all terms up to η^2.

4.5 Numerical Results

Summarising the results of the previous section we note that in both weak and strong confinement cases we have a single effective cooling equation of the form

$$\dot{n}_2 \quad = \quad -\gamma_c n_2 + c\,. \tag{4.51}$$

As previously discussed, n_2 and the stationary state phonon number m_{ss} are identical in zeroth order (c.f. Eq. (4.13)). Therefore an analytic solution for the steady state $m(t)$ will have the form

$$m(t) \quad = \quad \left[m(0) - m_{ss}\right] \mathrm{e}^{-\gamma_c t} + m_{ss} \tag{4.52}$$

with $m_{ss} = c/\gamma_c$. This equation applies, since n_2 and m are the same in zeroth order in η. Let us emphasise that Eq. (4.52) applies independent of the relative size of ν, i.e. in the strong and in the weak confinement regime but only after a transition time of $1/\gamma_c$. As we shall, in spite of the time average approximation which is only reasonable after a transition time of $1/\gamma_c$, Eq. (4.52) agrees well with a numerical solution of all 25 expectation value rate equations. Fig. 4.7 illustrates nicely how the cooling process changes as the choice of parameters transitions between the weak and strong confinement regimes. The figure compares a numerical integration of all 25 cooling equations (c.f. Eqs. (4.14), (B.3), (B.6), (B.8), (B.10), and (B.11)) to the analytic solution of Eq. (4.52) which includes all terms up to η^2. Here we see that for a choice of $\nu = 0.01\kappa$ we find ourselves deep in the weak confinement regime. We can also see that the cooling rate is very gradual and eventually reaches a steady state not much lower from the initial phonon number. Choosing $\nu = 0.05\kappa$ we remain within the weak

confinement regime whilst the cooling rate increases and the steady state drops. The next choice of parameter, $\nu = 0.5\kappa$ moves us an order higher to previously and brings us to the boundary of the strong confinement regime ($\nu \simeq \kappa$). Here we have the steepest cooling rate and the lowest phonon number steady state. The comparison with the analytic solution shows agreement for all parameter choices. This is very encouraging as the approximations performed with respect to the time averaging of the y operator coherences could only be justified if applied towards the end of the cooling process on the order of $1/\gamma_c$. This would correspond to 1 on the time axis of Fig. 4.7 but as can clearly be seen the analytic curves match very well with the numerical ones at times less than 1. It must also be pointed out here that in the analytic solution for $m(t)$ the expressions used for γ_c and m_{ss} are those of Eqs. (4.47) and (4.40) respectively which make no approximation regarding either the weak or strong confinement regimes.

4.6 Final Remarks

In this chapter we revisited one of the standard scenarios for cavity cooling [15, 16, 69]. The main difference compared to previous calculations [14–18, 69] is that instead of expanding the Hamiltonian H_I in Eq. (3.16) in η, we solve the cooling equations for small Lamb-Dicke parameters η perturbatively. This is possible after replacing the phonon and the cavity photon annihilation operators b and c in the initial interaction Hamiltonian H_I by two new bosonic operators x and y (q.v Eqs. (3.26), (4.4) and (4.6)). The operator x annihilates cavity photons while giving a kick to the motion of the respective particle. The operator y annihilates phonons but not without affecting the state of the cavity photons as well. Using this method a total of 25 rate equations were needed to determine a set of 5 equations (c.f. Eq. (4.14)) that described the cooling of the system to second order in η. A numerical integration of these 5 equations was performed with parameters chosen so as to show the behaviour of the 5 equations with respect to both the weak and strong confinement regimes. In both cases all 5 equations evolved on the same time scale and as such it was necessary to perform a stability analysis to determine the existence of a stable solution. Time averaging of the variables in the set of 5 equations that described the cooling process was shown to be justified on determining said stable solution for this group of 5 equations. Looking at the two extreme cases of the weak and strong confinement regimes vastly simplified the analysis of the 25 rate equations and resulted in a single effective equation for both cases. Solving said equation resulted in a simple analytic function that could be plotted against a numerical integration of all 25 equations. Doing so revealed good agreement between the analytic result and the numerical result over a range of parameter choices that reflected the transition from the weak to the strong confinement regime. All analytic results were also shown to be consistent with the earlier results found in chapter 2

using the Lamb-Dicke approximation.

Chapter 5

Conclusions

We have now reached the conclusion of the present analysis and at this point we would like to gather together all that we have learned over the course of the investigation. We undertook the task of establishing a quantum approach to cavity mediated laser cooling. We set out to understand a cooling mechanism for single particles that could be explained by using the concept of discretised energy loss. Such energy loss was described as the removal of quanta of vibrational energy of the particle incurred from the interaction between the different elements of the systems considered. We considered 2 types of systems. The first system consisted of a laser driven trapped particle interacting with the single mode of a cavity field from which photons could escape through the cavity mirrors. The second system considered consisted of a laser driven trapped particle interacting with a free radiation field. Both systems used different forms of the quantum optical master equation to model the change of vibrational quanta and loss within its system.

In chapter 2 we presented the model through which we could investigate the interaction between the trapped particle and the single mode of the cavity. We found that in the parameter regime of a tightly confined particle inside a relatively leaky optical cavity described by Eq. (2.22), the cavity cooling scenario in Figure 2.1 has many similarities with ordinary laser cooling [8, 10, 11, 13]. The reason is that the atomic 0–1 transition and the cavity are so strongly detuned that the electronic states of the trapped particle can be adiabatically eliminated from the system dynamics (q.v Section 2.2). The remaining master equation (q.v Eq. (2.50)) with the interaction Hamiltonian H_{I} in Eq. (2.37) is almost the same as in laser cooling. One only needs to replace the cavity annihilation operator c by the atomic lowering operator $|0\rangle\langle 1|$, the cavity decay rate κ by the atomic decay rate Γ, and the effective coupling constant g_{eff} by the cooling laser Rabi frequency Ω, and so on.

As in laser cooling, we found that it is useful to distinguish between two different parameter regimes: the strong confinement regime and the weak confinement regime.

In the strong confinement regime, where the relevant spontaneous decay rate (κ or Γ) is much smaller than the phonon frequency ν, one should choose the relevant laser detuning equal to ν (q.v Eq. (2.68)) in order to minimise the stationary state phonon number m^{ss}. In laser cooling, this case is known as *laser sideband cooling*. The stationary state phonon number m^{ss} for cavity cooling in the strong confinement regime is essentially given by $\kappa^2/16\nu^2$ (q.v Eq. (2.62)) while scaling as Γ^2/ν^2 in laser sideband cooling [13]. This means, it is possible to cool to phonon numbers well below one (ground state cooling), although realising $\kappa \ll \nu$ in cavity cooling is experimentally very demanding.

We adopted a different approach to analysing the cooling process and firstly applied the method to the case of the trapped particle interacting with the free radiation field and then to trapped particle in the cavity. The motivation for a new approach was made in response to realising the naivety of adiabatically eliminating all rate equations except the phonon number rate equation. A subgroup of the 14 rate equations that described the cooling process in Chapter 2 were assumed to have quasi-stationary states. These equation are only exact up to first order in η. This subgroup of equations could easily be shown to have no stationary state solution (q.v section 2.5). By adiabatically eliminating this subgroup of equations we were inadvertently determining the time averaged values of the relevant variables which were equivalent to the quasi-stationary state values (q.v section 3.3.4). So we determined the correct expressions inadvertently!

It was realised that to have a stable solution for this subgroup of equations it would be necessary to use equations that were exact up to second order in η. Doing so we found that we had no control in determining which coherence expectation values could be used to form closed sets of rate equations. In response to this situation we developed the novel method of using the algebra of the commutator between the displacement operator $D(i\eta)$ and the phonon annihilation and creation operators in the rate equation derivations. In addition 2 unitary transformations (q.v Eqs. (3.26) and (3.30)) were employed to make the rate derivations more straightforward.

In chapter 3 we found that we could greatly simplify the calculations by considering the cases of weak ($\Gamma \gg \nu$) and strong ($\Gamma \ll \nu$) confinement once more. In the weak confinement case the y operator rate equations were found to evolve on the same timescale whilst in the strong confinement regime the y operator coherences and the y operator population evolved on different timescales. Steady states and cooling rates were derived that agreed with their cavity counterparts (q.v Eq. 3.100)). We were then able to further simplify the analysis by considering the limit of weak driving $\Omega \ll \Gamma$. Using this approximation we recovered the results of previous authors [10–13]. This method also provided an alternative approach to adiabatically eliminating the excited state of the particle.

In chapter 4 we applied the transformation method to the Hamiltonian describing

trapped particle and cavity interaction. Here we found that the x annihilation operator could be easily defined with the bosonic annihilation operator in place of the fermionic σ^- Pauli operator. Indeed, this provided a nice example of the crucial difference between a purely bosonic system (cavity) and bosonic plus fermionic system (free particle). Here the difference lay in the commutators of Eqs. (3.27) and (4.4). So it is quite remarkable then, that when considering this fundamental difference, that expressions derived for the cooling rate and steady states have the exact same form as their free particle analogues.

Feynman pointed out in his classic paper "Space time Approach to Non-relativistic Quantum Mechanics " [106] how curious it was that there were 2 differing but equivalent approaches to the mathematical formulation of quantum mechanics to which his paper became a third. He himself thought that there was something special about nature in the sense it could be described using quantum mechanics in completely different ways. In some sense this could be the take home message of this thesis. The quantum formalism that was developed to describe the cooling of trapped ions [10–13] and later, cavity mediated laser cooling ,[14–19] used a transition rate formalism that could be applied equally well to both frameworks. In our work we have shown that the exact same results can be produced by using the transformation formalism. Its usefulness can be captured in the definition of the x unitary transformation which can be used for both free particle and cavity systems.

Appendix A

Free Particle Model

A.1 Derivation of conditional Hamiltonian H_{cond}

To clarify our use of the quantum jump approach to determine Eqs. (3.19), (3.20) and the form of the master equation Eq. (3.21) the following section shall give a brief description of the concepts involved and a short derivation of the central expressions.

Previously, in section (3.1.4), we briefly described the ensemble description of a single particle system. Here we shall elaborate on this concept some more. To adhere to the necessary condition of the observation of sequential photon emission we must impose a requirement on the the length of time Δt between observations on the single system. If we suppose the single particle to be a 2 level system with an optical transition frequency of ω_0 with a spontaneous decay rate of Γ then Δt must not be smaller than the time it takes for the particle to become excited, $1/\omega_0$, but much smaller than the lifetime of the excited state. As otherwise with respect to the former we would encounter the quantum zeno effect [107] (a sort of "freezing" of the systems dynamics) and with respect to latter we would risk the possibility of not detecting a sequential emission event. Thus we have

$$\frac{1}{\omega_0} \ll \Delta t \ll \frac{1}{\Gamma}. \tag{A.1}$$

The trick that is used in this approach of applying an ensemble description to a single particle system is to consider an ensemble $\mathcal{E}$ of many particles and their associated quantised free radiation fields. The single particle system then is a member of the ensemble $\mathcal{E}$

The initial state of the ensemble at $t_0 = 0$ is then described by the state $|0_{ph}\rangle|\psi_{\text{par}}\rangle$. Then each member of the $\mathcal{E}$ ensemble is a measurement for photon detection performed at times $t_1 = \Delta t, \ldots t_n = n\Delta t, \ldots$. Next, for $n = 1, 2, \ldots,$ we denote by $\mathcal{E}_0^{(n\Delta t)}$ the subensemble which consists of all systems of $\mathcal{E}$ for which at times $\Delta t, \ldots n\Delta t, \ldots$

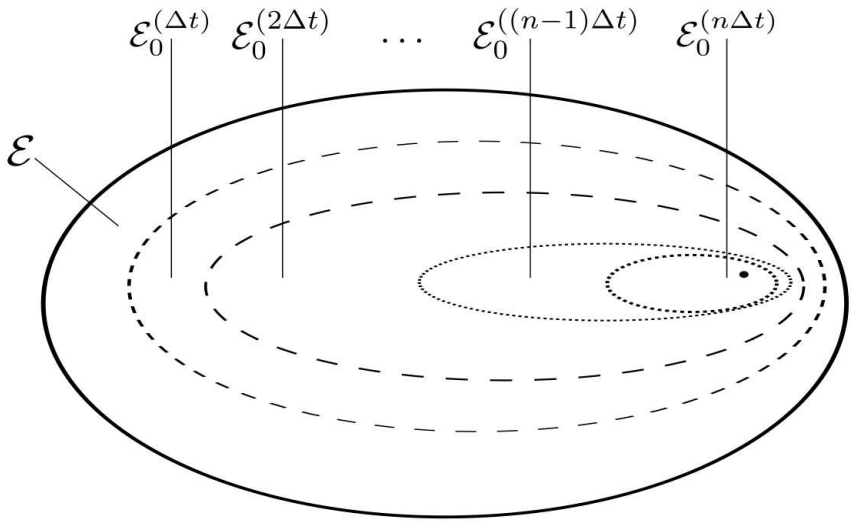

Figure A.1: The ensemble of 2 level systems $\mathcal{E}$ with the subensembles $\mathcal{E}^{(\Delta t)}$. The single particle system is denoted by the dot contained within the subensembles $\mathcal{E}^{(n\Delta t)}$

no photon was detected. This is illustrated in Fig. (A.1) where we denote our single particle system of particle plus free radiation field as a dot $\cdot$ within the subensemble $\mathcal{E}_0^{(n\Delta t)}$. Using the von Neumann - Lüders projection postulate [108] we let $\mathcal{P}_0$ be the projector onto the no - photon subspace,

$$\mathcal{P}_0 \equiv |0_{ph}\rangle\langle 0_{ph}| \otimes \mathbf{1}_{\text{par}} \tag{A.2}$$

and let $U(t, t_0)$ be the unitary operator that describes the complete time developement of the laser driving, the particle field interaction and the particles external motion (c.f Eqs. (3.2) and (3.4)). Then after a time Δt the state of the subensemble $\mathcal{E}_0^{(\Delta t)}$ is described by

$$\mathcal{P}_0 U(t_1, t_0)|0_{ph}\rangle|\psi_{\text{par}}\rangle \equiv |0_{ph}\rangle|\psi_{\text{par}}(\Delta t)\rangle\,. \tag{A.3}$$

After a time $2\Delta t$ the subensemble $\mathcal{E}_0^{(2\Delta t)}$ is described by

$$\mathcal{P}_0 U(t_2, t_1)\mathcal{P}_0 U(\Delta t, 0)|0_{ph}\rangle|\psi_{\text{par}}\rangle \equiv |0_{ph}\rangle|\psi_{\text{par}}(2\Delta t)\rangle\,. \tag{A.4}$$

After a time $(n-1)\Delta t$ the subensemble $\mathcal{E}_0^{((n-1)\Delta t)}$ is described by

$$\mathcal{P}_0 U(t_{n-1}, t_{n-2})\mathcal{P}_0 \ldots \mathcal{P}_0 U(t_1, t_0)|0_{ph}\rangle|\psi_{\text{par}}\rangle \equiv |0_{ph}\rangle|\psi_{\text{par}}((n-1)\Delta t)\rangle \tag{A.5}$$

and after a time $n\Delta t$ the subensemble $\mathcal{E}_0^{(n\Delta t)}$ is described by

$$\mathcal{P}_0 U(t_n, t_{n-1})\mathcal{P}_0 \ldots \mathcal{P}_0 U(t_1, t_0)|0_{ph}\rangle|\psi_{\rm par}\rangle \equiv |0_{ph}\rangle|\psi_{\rm par}(n\Delta t)\rangle\,. \tag{A.6}$$

It is now quite simple to see how this approach can account for the detection of sequential emission events. As we stated earlier $\mathcal{E}$ is the ensemble of many particles with its own quantised radiation field. So if a photon is detected at a time $2\Delta t$ then this means that no photon has been detected during the time Δt. Therefore a member of $\mathcal{E}$ will also be a member of the subensemble $\mathcal{E}_0^{(\Delta t)}$. In a different case if a photon is detected at a time $3\Delta t$ then this means that no photon has been detected during the time $2\Delta t$ and so the member of $\mathcal{E}$ will now be a member of the subensemble $\mathcal{E}_0^{(2\Delta t)}$. More precisely for some timedependent function $f(t)$

$$\mathcal{E}_0^{(n\Delta t)} \;=\; \{f(t') \in \mathcal{E} : (n-1)\,\Delta t \le t' < n\,\Delta t\} \tag{A.7}$$

So in general if photon is detected *after* a time $n\Delta t$ then this means that no photon has been detected *up to* the time $n\Delta t$ and so the member of $\mathcal{E}$ will now be a member of the subensemble $\mathcal{E}_0^{(n\Delta t)}$.Thus the probability of finding a member of $\mathcal{E}$ in the subensemble $\mathcal{E}_0^{(n\Delta t)}$ is the same as the probability of not detecting a photon up to the time $n\Delta t$. Now the probability of finding a member of $\mathcal{E}$ in the subensemble $\mathcal{E}_0^{(n\Delta t)}$ is actually the relative size of $\mathcal{E}_0^{(n\Delta t)}$ which is given by

$$P_0(n\Delta t) \;\equiv\; \|\,|\psi_{\rm par}(n\Delta t)\rangle\,\|\,. \tag{A.8}$$

To determine $|\psi_{\rm par}(n\Delta t)\rangle$ redefine Eq. (A.6) to be

$$\mathcal{P}_0 U((n)\Delta t, (n-1)\Delta t)\mathcal{P}_0 \ldots \mathcal{P}_0 U(\Delta t, 0)|0_{ph}\rangle|\psi_{\rm par}\rangle \equiv |0_{ph}\rangle U_{\rm cond}(n\Delta t,\, 0)|\psi_{\rm par}(0)\rangle \tag{A.9}$$

so that

$$U_{\rm cond}(n\Delta t,\, 0)|\psi_{\rm par}(0)\rangle \equiv |\psi_{\rm par}(n\Delta t)\rangle \tag{A.10}$$

From Eqs. (A.4),(A.5) and (A.6) it is easy to see that

$$\mathcal{P}_0 U(t' + \Delta t, t)\mathcal{P}_0 \;=\; |0_{ph}\rangle\langle 0_{ph}|U(t' + \Delta t, t')|0_{ph}\rangle\langle 0_{ph}|. \tag{A.11}$$

Expanding the inner expression $\langle 0_{ph}|U(t'+\Delta t, t')|0_{ph}\rangle$ using second order perturbation theory and using the fact that

$$U_{\rm cond}(t, 0) \;=\; \prod_1^n \langle 0_{ph}|U(t_i, t_{i-1})|0_{ph}\rangle \tag{A.12}$$

and where we are saying that $t = t_n = n\Delta t$ we can find an expression for the conditional Hamilitonian H_{cond} which we now do so with respect to Eq. (3.16), the interaction Hamiltonian H_{I}

A.1.1 2nd order perturbation calculation of $U_{cond}(t,0)$

We first expand $\langle 0_{ph}|U(t_i,t_{i-1}))|0_{ph}\rangle$ up to second order [109] where $t_i - t_{i-1} = \Delta t$

$$\begin{aligned}\langle 0_{ph}|U_I(t_i,t_{i-1})|0_{ph}\rangle &= \mathbf{1} - \frac{i}{\hbar}\int_{t_{i-1}}^{t_i} dt'\langle 0_{ph}|H_I(t')|0_{ph}\rangle \\ &\quad -\frac{1}{\hbar^2}\int_{t_{i-1}}^{t_i}\int_{t_{i-1}}^{t'} dt''\langle 0_{ph}|H_I(t')H_I(t'')|0_{ph}\rangle \end{aligned} \tag{A.13}$$

The first term remains unaffected by the operation. The second term only has contributions from the particle, laser and phonon terms of Eq. (3.16)

$$\frac{\mathrm{i}}{\hbar}\int_{t_{i-1}}^{t_i} dt\,\langle 0_{ph}|H_I(t')|0_{ph}\rangle = -\frac{\mathrm{i}}{\hbar}\int_{t_{i-1}}^{t_i} dt'\left(\frac{1}{2}\hbar\Omega\, D(\mathrm{i}\eta)\sigma^- + \text{H.c.} + \hbar\Delta\sigma^+\sigma^- + \hbar\nu\, b^\dagger b\right) \tag{A.14}$$

Expanding out the third term we neglect all terms that contribute in Δt^2. All terms with $\langle 0_{ph}|a^\dagger|0_{ph}\rangle$ vanish. This then leaves us with

$$-\frac{1}{\hbar^2}\int_{t_{i-1}}^{t_i}\int_{t_{i-1}}^{t'} dt''\langle 0_{ph}|H_{\text{dip}}(t')H_{\text{dip}}(t'')|0_{ph}\rangle \tag{A.15}$$

where H_{dip} is the first term in Eq. (3.16) which as we recall is

$$\begin{aligned}H_{\text{dip}}(t) &= \sum_{\mathbf{k}\lambda}\hbar g_{\mathbf{k}\lambda}\,\sigma^- a^\dagger_{\mathbf{k}\lambda}\, D\left(\frac{\mathrm{i}\eta k\cos\vartheta}{k_{\text{L}}}\right)\mathrm{e}^{-\mathrm{i}k\sin\vartheta\left[R_x\cos\varphi + R_y\sin\varphi\right]}\,\mathrm{e}^{\mathrm{i}(\omega_k-\omega_{\text{L}})t} \\ &\quad +\text{H.c}\,. \end{aligned} \tag{A.16}$$

Evaluation of Eq. (A.15) gives us four terms but obviously the 2 terms involving $\sigma^-\sigma^-$ and $\sigma^+\sigma^+$ vanish. This leaves 2 terms. One of which has $\langle 0_{ph}|a^\dagger_{\mathbf{k}\lambda}a_{\mathbf{k}\lambda}|0_{ph}\rangle$. However

$$\langle 0_{ph}|a^\dagger_{\mathbf{k}\lambda}a_{\mathbf{k}\lambda}|0_{ph}\rangle = 0 \tag{A.17}$$

This just leaves one term that has $\langle 0_{ph}|a_{\mathbf{k}\lambda}a^\dagger_{\mathbf{k}\lambda}|0_{ph}\rangle$ which we can easily show is equal to one

$$\langle 0_{ph}|a_{\mathbf{k}\lambda}a^\dagger_{\mathbf{k}\lambda}|0_{ph}\rangle = 1\,. \tag{A.18}$$

We thus have

$$\frac{1}{\hbar^2}\int_{t_{i-1}}^{t_i} dt' \int_{t_{i-1}}^{t'} dt'' \langle 0_{ph}|H_{\rm dip}(t')H_{\rm dip}(t'')|0_{ph}\rangle = \sum_{\mathbf{k}\lambda}\int_{t_{i-1}}^{t_i} dt' \int_{t_{i-1}}^{t'} dt''|g_{\mathbf{k}\lambda}|^2 \times e^{\mathrm{i}(\omega_0-\omega_k)(t'-t'')}\sigma^+\sigma^- . \quad \text{(A.19)}$$

From Eq. (A.1) we know that Δt is much larger than the inverse optical frequency ω_0 and since $t'-t_{i-1} \leq \Delta t$ we can extend the inner integral to infinity allowing us to make use of the identity

$$\lim_{\Delta t\to\infty}\int_0^{\Delta t} dt'' e^{\mathrm{i}(\omega_0-\omega_k)(t'-t'')} = \frac{1}{2}\left(\pi\delta(\omega_0-\omega_k) - \mathrm{i}\frac{\mathcal{P}}{\omega_0-\omega_k}\right). \quad \text{(A.20)}$$

Following the time honoured tradition of treating the principal value part as a level shift and rescaling the energy scale so as to start the energy measurement from where the level shift ends, thereby neglecting it, and also substituting the expression for $g_{\mathbf{k}\lambda}$ we find that Eq. (A.19) becomes

$$-\frac{1}{2}\pi\Delta t\sum_{\mathbf{k}\lambda}\frac{e^2\omega_k}{2\epsilon_0\hbar V}|\mathbf{D}_{01}\cdot\mathbf{e}_{\mathbf{k}\lambda}|^2\delta(\omega_0-\omega_k)\sigma^+\sigma^- . \quad \text{(A.21)}$$

In order to proceed further it will be necessary to convert the following expression to an integral in ω_k

$$\sum_{\mathbf{k}}\sum_{\lambda}|\mathbf{D}_{01}\cdot\mathbf{e}_{\mathbf{k}\lambda}|^2 . \quad \text{(A.22)}$$

Firstly we convert the summation over $\mathbf{k}$ to an integration over ω_k

$$\begin{aligned}\sum_{\mathbf{k}} &\rightarrow \frac{V}{(2\pi)^3}\int d\mathbf{k} \\ &= \frac{V}{(2\pi)^3}\int_0^\infty\int_0^\pi\int_0^{2\pi} k^2\sin\vartheta dk d\vartheta d\varphi \\ &= \frac{V}{(2\pi)^3}\int_0^\infty\int_0^\pi\int_0^{2\pi}\frac{\omega_k^2}{c^2}\sin\vartheta\frac{d\omega_k}{c}d\vartheta d\varphi \\ &= \frac{V}{8\pi^3c^3}\int_0^\infty\int_0^\pi\int_0^{2\pi}\omega_k^2\sin\vartheta d\omega_k d\vartheta d\varphi . \end{aligned} \quad \text{(A.23)}$$

Next let us denote the vector that describes the normalised dipole $\hat{\mathbf{D}}_{01} \equiv \mathbf{D}_{01}/|\mathbf{D}_{01}|$ as

$$\hat{\mathbf{D}}_{01} = (d_1, d_2, d_3)^{\mathrm{T}} . \quad \text{(A.24)}$$

Now we express the sum over polarisations of the vector product of the Dipole moment and the vector that defines the direction of the free radiation field in terms of the spherical polar variables ω_k, ϑ and φ using the fact that $\mathbf{e}_{\mathbf{k}\lambda}\cdot\mathbf{k}=0$, and $\mathbf{e}_{\mathbf{k}1}\cdot\mathbf{e}_{\mathbf{k}2}=0$ we can express the sum over λ in the following manner.

$$\begin{aligned}\sum_{\lambda}|\mathbf{D}_{01}\cdot\mathbf{e}_{\mathbf{k}\lambda}|^2 &= |D_{01}|^2-|\mathbf{D}_{01}\cdot\hat{\mathbf{k}}|^2\\ &= |D_{01}|^2-|D_{01}|^2\,|d_1\,\sin\vartheta\cos\varphi+d_2\,\sin\vartheta\sin\varphi+d_3\,\cos\vartheta|^2\\ &= |D_{01}|^2\left(1-\left|\sin\vartheta\left(d_1\cos\varphi+d_2\sin\varphi\right)+d_3\,\cos\vartheta\right|^2\right). \quad \text{(A.25)}\end{aligned}$$

If we now expand out the square in Eq. (A.25) we get the following terms.

$$\begin{aligned}\sum_{\lambda}|\mathbf{D}_{01}\cdot\mathbf{e}_{\mathbf{k}\lambda}|^2 &= |D_{01}|^2-|D_{01}|^2|d_1^2\,\sin^2\vartheta\cos^2\varphi+d_2^2\,\sin^2\vartheta\sin^2\varphi+d_3^2\,\cos^2\vartheta\\ &\quad +2d_1\,d_2\,2\sin^2\vartheta\sin\varphi\cos\varphi+2d_1\,d_3\sin\vartheta\cos\vartheta\cos\varphi\\ &\quad +2d_2\,d_3\sin\vartheta\cos\vartheta\sin\varphi|\,. \quad \text{(A.26)}\end{aligned}$$

Making use of the fact that $\omega_0^3=2\int_0^\infty\omega_k^3\delta(\omega_0-\omega_k)d\omega_k$ and using Eq. (A.21) with Eq. (A.25) we find that Eq. (A.21) becomes a series of 5 integrals.

$$\left(\frac{e^2\omega_0^3}{8\pi^2c^3\hbar}\right)\int_0^{2\pi}\mathrm{d}\varphi\int_0^{\pi}\sin\vartheta\sigma^+\sigma^-|D_{01}|^2 = \frac{3\Gamma}{2}\sigma^+\sigma^-, \quad \text{(A.27)}$$

$$-\left(\frac{e^2\omega_0^3}{8\pi^2c^3\hbar}\right)\int_0^{2\pi}\mathrm{d}\varphi\left(d_1^2\cos^2\varphi+d_2^2\sin^2\varphi\right)\int_0^{\pi}\mathrm{d}\vartheta\sin^3\vartheta|D_{01}|^2 = -\frac{3\Gamma}{2}\left(d_1^2+d_2^2\right)\times\sigma^+\sigma^-, \quad \text{(A.28)}$$

$$-\left(\frac{e^2\omega_0^3}{8\pi^2c^3\hbar}\right)\int_0^{2\pi}\mathrm{d}\varphi\,d_3^2\int_0^{\pi}\mathrm{d}\vartheta\sin\vartheta\,\cos^2\vartheta\sigma^+\sigma^-|D_{01}|^2 = -\frac{\Gamma}{2}d_3^2\times\sigma^+\sigma^-, \quad \text{(A.29)}$$

$$-2\left(\frac{e^2\omega_0^3}{8\pi^2c^3\hbar}\right)d_1^2\,d_2^2\int_0^{2\pi}\mathrm{d}\varphi\cos\varphi\sin\varphi\int_0^{\pi}\mathrm{d}\vartheta\sin\vartheta\sigma^+\sigma^-|D_{01}|^2 = 0, \quad \text{(A.30)}$$

$$\left(\frac{e^2\omega_0^3}{4\pi^2c^3\hbar}\right)\int_0^{2\pi}\mathrm{d}\varphi\,\left(d_1\cos\varphi+d_2\sin\varphi\right)\int_0^{\pi}\mathrm{d}\vartheta d_3\sin\vartheta\cos\vartheta\sigma^+\sigma^-|D_{01}|^2=0\,. \quad \text{(A.31)}$$

Noting that $d_1^2+d_2^2=1-d_3^2$ and defining $\Gamma=e^2|D_{01}|^2\omega_0^3/3\pi\hbar c^3$, we add together the nonvanishing integrals Eqs (A.27), (A.28) and (A.29) to get

$$\left(\frac{3\Gamma}{2}-\frac{\Gamma}{2}\left(1-d_3^2\right)-\frac{\Gamma}{2}d_3^2\right)\sigma^+\sigma^- \;=\; \frac{\Gamma}{2}\sigma^+\sigma^-\,. \quad \text{(A.32)}$$

Collecting all terms together we find that Eq. (A.13) becomes

$$\begin{aligned}\langle 0_{ph}|U_I(t_i,t_{i-1})|0_{ph}\rangle \;&=\; \mathbf{1}-\frac{\mathrm{i}}{\hbar}\int_{t_{i-1}}^{t_i}dt'\left(\frac{1}{2}\hbar\Omega\,D(\mathrm{i}\eta)\sigma^-+\mathrm{H.c.}+\hbar\Delta\sigma^+\sigma^-+\hbar\nu\,b^\dagger b\right)\\ &\quad-\frac{1}{2}\Gamma\Delta t\sigma^+\sigma^-\,. \quad \text{(A.33)}\end{aligned}$$

Next we integrate so that $\int_{t_{i-1}}^{t_i}dt'\,\Gamma/2\;\sigma^+\sigma^-=\Gamma/2\;\sigma^+\sigma^-\,\Delta t$ and make use of the fact that $e^\epsilon\approx 1-\epsilon$ for small ϵ to get

$$\langle 0_{ph}|U_I(t_i,t_{i-1})|0_{ph}\rangle=\mathrm{e}^{-\frac{\mathrm{i}}{\hbar}\int_{t_{i-1}}^{t_i}dt'\left(H^{\rm I}_{\rm par}+H^{\rm I}_{\rm phn}+H^{\rm L}-\frac{1}{2}\Gamma\sigma^+\sigma^-\right)}\,. \quad \text{(A.34)}$$

and where we have defined the interaction Hamiltonians $H^{\rm I}_{\rm par}$, $H^{\rm I}_{\rm phn}$ and $H^{\rm L}$ to be the particle, phonon and laser interaction Hamiltonians respectively from Eqs. (3.16) and (A.33). We should point out that these Hamiltonians are also time independent this being due of course to Eqs. (3.14) and (3.15) Going back to Eq. (A.10) and using the following properties of products, sums and exponential

$$\begin{aligned}\prod_{i=1}^{n}\exp\left[\int_{t_{i-1}}^{t_i}dt'f(t')\right] \;&=\; \exp\left[\int_0^{t_1}dt'f(t')+\cdots+\int_{t_{n-1}}^{t_n}dt'f(t')\right]\\ &=\; \mathcal{T}\exp\left[\int_0^{n\Delta t}dtf(t')\right] \quad \text{(A.35)}\end{aligned}$$

and using the time ordering property $\mathcal{T}$ to mean $t_1<\cdots<t_n$ we finally arrive at the expression for the conditional unitary operator $U_{\rm cond}(n\Delta t,0)$

$$U_{\rm cond}(n\Delta t,0) \;=\; \mathcal{T}\mathrm{e}^{-\frac{\mathrm{i}}{\hbar}\int_0^{n\Delta t}dt'\left(H^{\rm I}_{\rm par}+H^{\rm I}_{\rm phn}+H^{\rm L}-\frac{1}{2}\Gamma\sigma^+\sigma^-\right)} \quad \text{(A.36)}$$

Thus we deduce that $H_{\rm cond}$ is

$$H_{\rm cond} = \frac{1}{2}\hbar\Omega\, D(\mathrm{i}\eta)\sigma^- + \mathrm{H.c.} + \hbar\Delta\,\sigma^+\sigma^- + \hbar\nu\, b^\dagger b - \frac{\mathrm{i}}{2}\hbar\Gamma\,\sigma^+\sigma^-. \qquad \text{(A.37)}$$

A.1.2 Coarse graining

If we consider our ensemble of states for which there has been no photon emission to be described by the density operator $\rho^0(n\Delta t)$ and using the fact that $H_{\rm cond}$ is time independent then

$$\begin{aligned}
\rho^0(n\Delta t) &= \left(\mathbf{1} - \frac{i}{\hbar}H_{cond}\int_0^{n\Delta t} dt\right)\rho(0)\left(\mathbf{1} + \frac{i}{\hbar}H_{cond}^\dagger\int_0^{n\Delta t} dt\right) \\
&= \left(\rho(0) - \frac{i}{\hbar}H_{\rm cond}\rho(0)\, n\Delta t\right)\left(\mathbf{1} + \frac{i}{\hbar}H_{cond}\, n\Delta t\right) \\
&= \rho(0) - \frac{i}{\hbar}\left[H_{\rm cond}\rho(0) - \rho(0)H_{cond}^\dagger\right] n\Delta t + O(\Delta t^2) \qquad \text{(A.38)}
\end{aligned}$$

Next we denote the density operator that describes the part of the ensemble for which a photon has been detected as $\rho^>(n\Delta t)$ and consider the derivative of the density operator that describes on the full ensemble.

$$\begin{aligned}
\dot\rho(t) &= \lim_{n\Delta t\to 0}\frac{\rho(n\Delta t) - \rho(0)}{n\Delta t} \\
&= \lim_{n\Delta t\to 0}\frac{\rho^0(n\Delta t) + \rho^>(n\Delta t) - \rho(0)}{n\Delta t} \\
&= \lim_{n\Delta t\to 0}\frac{\rho^0(n\Delta t) - \rho(0)}{n\Delta t} + \lim_{n\Delta t\to 0}\frac{\rho^>(n\Delta t)}{n\Delta t} \\
&= \lim_{n\Delta t\to 0}\frac{-i/\hbar\left[H_{\rm cond}\rho(0) - \rho(0)H_{\rm cond}^\dagger\right] n\Delta t}{n\Delta t} + \lim_{n\Delta t\to 0}\frac{\mathcal{R}(\rho)\, n\Delta t}{n\Delta t}
\end{aligned} \qquad \text{(A.39)}$$

Here we have also defined $\rho^>(n\Delta t) \equiv \mathcal{R}(\rho)n\Delta t$ where $R(\rho)$ is the density operator that the particle density operator is "reset" to after a photon detection. Thus on the coarse-grained timescale as $n\Delta t \to 0$ we recover the usual master equation that describes the ensemble of systems $\rho(t)$ from Eq. (3.21).

A.2 Derivation of the reset state $\mathcal{R}(\rho)$

This can be considered as the second part of the quantum jump approach, namely the construction of the density operator $\rho^>(n\Delta t)$ through which we shall determine the

reset operator. As before the initial state of the ensemble is $|0_{ph}\rangle|\psi\rangle$ but now we seek the state of the subsystem with one photon emission at time $t_{n+1} = t_n + \Delta t$ where $t_n = n\Delta t$ as before. Let $\mathcal{P}_1$ be the projector onto the photon emission subspace. Then

$$\mathcal{P}_1 = \mathbf{1} - \mathcal{P}_0 = \sum_{\mathbf{k}\lambda} |1_{\mathbf{k}\lambda}\rangle\langle 1_{\mathbf{k}\lambda}| \otimes \mathbf{1}_{\text{par}} \tag{A.40}$$

The unnormalised state of the subensemble for which a photon has been detected is then given by

$$\begin{aligned} \rho^{>}(t_{n+1}) &= \mathcal{P}_1\rho(t_{n+1})\mathcal{P}_1 \\ &= \sum_{\mathbf{k}\lambda} |1_{\mathbf{k}\lambda}\rangle\langle 1_{\mathbf{k}\lambda}|U_I(t_{n+1},t_n)|0_{ph}\rangle \\ &\quad \times|\psi\rangle\langle\psi|\langle 0_{ph}|U_I^{\dagger}(t_{n+1},t_n)\sum_{\mathbf{k'}\lambda}|1_{\mathbf{k'}\lambda}\rangle\langle 1_{\mathbf{k'}\lambda}| \end{aligned} \tag{A.41}$$

We next follow the argument laid out in reference [101] which states that after a photon detection by absorption no photons are present any longer and the resulting reset state is obtained by a partial trace over the free radiation field. After taking the partial trace with respect to the free radiation field we find Eq. (A.41) changes to

$$\rho^{>}_{\text{par}}(t_{n+1}) = \sum_{\mathbf{k}\lambda}\langle 1_{\mathbf{k}\lambda}|U_I(t_{n+1},t_n)|0_{ph}\rangle|\psi\rangle\langle\psi|\langle 0_{ph}|U_I^{\dagger}(t_{n+1,t_n})|1_{\mathbf{k}\lambda}\rangle \tag{A.42}$$

As a first step in determining (A.42) we use a first order perturbation expansion on the amplitudes within (A.42) which gives us the following integral form.

$$\begin{aligned} \langle 1_{\mathbf{k}\lambda}|U_I(\Delta t,0)|0_{ph}\rangle &= -\frac{\mathrm{i}}{\hbar}\int_0^{\Delta t} dt' \sum_{\mathbf{k}\lambda} e^{-\mathrm{i}(\omega_k-\omega_0)t'}\hbar g_{\mathbf{k}\lambda} D\left(\frac{\mathrm{i}\eta k\cos\vartheta}{k_{\mathrm{L}}}\right) \\ &\quad \times \mathrm{e}^{-\mathrm{i}k\sin\vartheta\left[R_x\cos\varphi + R_y\sin\varphi\right]}\sigma^{-}. \end{aligned} \tag{A.43}$$

The other amplitude can then be found by taking the complex conjugate of Eq. A.43. We can now determine an expression for the density operator $\rho^{>}_{\text{par}}(t_{n+1})$ which is

$$\begin{aligned} \rho^{>}_{par}(t_{n+1}) &= \sum_{\mathbf{k}\lambda}\int_0^{\Delta t} dt' \int_0^{\Delta t} dt'' \sum_{\mathbf{k}\lambda} e^{-\mathrm{i}(\omega_{\mathrm{k}}-\omega_0)(\mathrm{t}'-\mathrm{t}'')}|g_{\mathbf{k}\lambda}|^2 \\ &\quad \times\sigma^{-} D\left(\frac{\mathrm{i}\eta k\cos\vartheta}{k_{\mathrm{L}}}\right)\rho(0)D^{\dagger}\left(\frac{\mathrm{i}\eta k\cos\vartheta}{k_{\mathrm{L}}}\right)\sigma^{+}. \end{aligned} \tag{A.44}$$

Notice that the exponentials on the last line of Eq. (A.43) have now vanished. This is because we are making the approximation that R_x and R_y now represent numbers since we are only considering the motion quantised in the direction of the laser. We now decompose the double integral over t and t' for the rectangular integration domain into two triangular integration domains which gives

$$\int_0^{\Delta t'} dt' \int_0^{\Delta t} dt'' = \int_0^{\Delta t} dt' \int_0^{t'} dt'' + \int_0^{\Delta t} dt' \int_{t'}^{\Delta t} dt'' \tag{A.45}$$

Using the following integration relation we interchange the order of integration in the second double integral

$$\int_0^{\Delta t} dt' \int_t^{\prime\Delta t} dt'' \;=\; \int_0^{\Delta t} dt'' \int_0^{t''} dt' . \tag{A.46}$$

Then, by making the replacements $t'' \to t'$ and $t'' \to t'$ in the second double integral Eq. (A.45) contracts to the following double integral. [109]

$$\begin{aligned} \rho^{>}_{par}(t_{n+1}) \;=\; & 2\sum_{\mathbf{k}\lambda} \int_0^{\Delta t} dt' \int_0^{t} dt'' \sum_{\mathbf{k}\lambda} e^{-\mathrm{i}(\omega_\mathrm{k}-\omega_0)(\mathrm{t}'-\mathrm{t}'')} |g_{\mathbf{k}\lambda}|^2 \\ & \times \sigma^- D\left(\frac{\mathrm{i}\eta k\cos\vartheta}{k_\mathrm{L}}\right) \rho(0) D^\dagger \left(\frac{\mathrm{i}\eta k\cos\vartheta}{k_\mathrm{L}}\right) \sigma^+ . \end{aligned} \tag{A.47}$$

Next we use the identity of Eq. (A.20), neglect the principal value, integrate over t', substitute for $g_{\mathbf{k}\lambda}$ and make the sum to integral replacement in the large volume as in Eq. (A.23) to get the following expression for $R(\rho)$ noting of course that $\rho^{>}_{par}(t_{n+1}) = R(\rho)\Delta t$.

$$\begin{aligned} \mathcal{R}(\rho) \;=\; & 2\pi \int_0^{\pi} \mathrm{d}\vartheta \sin\vartheta \int_0^{2\pi} \mathrm{d}\varphi \sum_{\lambda=1,2} |\mathbf{D}_{01}\cdot\mathbf{e}_{\mathbf{k}\lambda}|^2 \int_0^{\infty} \mathrm{d}\omega_k\, \omega_k^2 \left(\frac{L}{2\pi c}\right)^3 \left(\frac{e^2\omega_k}{2\epsilon_0\hbar V}\right) \\ & \times \frac{1}{2}\delta(\omega_0-\omega_k)\sigma^- D\left(\frac{\mathrm{i}\eta k\cos\vartheta}{k_\mathrm{L}}\right) \rho(0) D^\dagger \left(\frac{\mathrm{i}\eta k\cos\vartheta}{k_\mathrm{L}}\right) \sigma^+ . \end{aligned} \tag{A.48}$$

Now we must account for the recoil factors which are included through the wave vector that defines the direction of the free radiation field (c.f Eq. (3.13)). We substitute Eq. (A.26) back into Eq. (A.48) and also use the delta function property and cancel constants to get the factor $e^2\omega_0^3/8\pi^2c^3\hbar$. Previously when we were performing the same operation in the calculation of Eq. (A.21) we were able to integrate out both the φ and ϑ variables. This was because of the form of the second order perturbation

with respect to the displacement operators. In that case the displacement operators vanished due to their unitary multiplication property. In the present case however, this is no longer possible due to the form of the operators in Eq. (A.48) . To illustrate this point we shall label the operator form as function a $F(\varphi)$

$$F(\vartheta) \;=\; \sigma^{-} D\left(\frac{i\eta k\cos\vartheta}{k_{\mathrm{L}}}\right)\rho(0)D^{\dagger}\left(\frac{i\eta k\cos\vartheta}{k_{\mathrm{L}}}\right)\sigma^{+}. \tag{A.49}$$

We can now only integrate out the φ variable. After substituting Eq. (A.26) into Eq. (A.48) the penultimate expression for $\mathcal{R}(\rho)$ becomes a matter of solving the following integrals and adding together all terms.

$$\left(\frac{e^2\omega_0^3}{8\pi^2c^3\hbar}\right)\int_0^{2\pi}\mathrm{d}\varphi\int_0^{\pi}\sin\vartheta|D_{01}|^2F(\vartheta) \;=\; \frac{3\Gamma}{4}\int_0^{\pi}\mathrm{d}\vartheta\sin\vartheta F(\vartheta), \tag{A.50}$$

$$\begin{aligned} &-\left(\frac{e^2\omega_0^3}{8\pi^2c^3\hbar}\right)\int_0^{2\pi}\mathrm{d}\varphi\left(d_1^2\cos^2\varphi+d_2^2\sin^2\varphi\right)\int_0^{\pi}\mathrm{d}\vartheta\sin^3\vartheta|D_{01}|^2F(\vartheta)\\ =\quad &-\frac{3\Gamma}{8}\left(d_1^2+d_2^2\right)\int_0^{\pi}\mathrm{d}\vartheta\sin^3\vartheta F(\vartheta), \end{aligned} \tag{A.51}$$

$$\begin{aligned} -\left(\frac{e^2\omega_0^3}{8\pi^2c^3\hbar}\right)\int_0^{2\pi}\mathrm{d}\varphi\, d_3^2\int_0^{\pi}\mathrm{d}\vartheta\sin\vartheta\,\cos^2\vartheta|D_{01}|^2F(\vartheta) \;=\; &-\frac{3\Gamma}{4}d_3^2\int_0^{\pi}\mathrm{d}\vartheta\sin\vartheta\\ &\times\cos^2\vartheta F(\vartheta), \end{aligned} \tag{A.52}$$

$$-2\left(\frac{e^2\omega_0^3}{8\pi^2c^3\hbar}\right)d_1^2\,d_2^2\int_0^{2\pi}\mathrm{d}\varphi\cos\varphi\sin\varphi\int_0^{\pi}\mathrm{d}\vartheta\sin\vartheta F(\vartheta)|D_{01}|^2 \;=\; 0, \tag{A.53}$$

$$\left(\frac{e^2\omega_0^3}{4\pi^2c^3\hbar}\right)\int_0^{2\pi}\mathrm{d}\varphi\left(d_1\cos\varphi+d_2\sin\varphi\right)\int_0^{\pi}\mathrm{d}\vartheta d_3\sin\vartheta\cos\vartheta F(\vartheta)|D_{01}|^2=0. \tag{A.54}$$

Lastly we note that $d_1^2+d_2^2=1-d_3^2$ and set $\zeta=\cos\vartheta$ to finally arrive at the expression for the reset operator $\mathcal{R}(\rho)$

$$\mathcal{R}(\rho) \;=\; \frac{3\Gamma}{8}\int_{-1}^{1}\mathrm{d}\zeta\,\sigma^{-}D(i\eta\zeta)\,\rho\,D(i\eta\zeta)^{\dagger}\sigma^{+}\left[\,1+|d_3|^2+\left(1-3|d_3|^2\right)\zeta^2\,\right] \tag{A.55}$$

The spontaneous decay rate Γ in this equation is the same as Γ in Eq. (3.24). Notice that d_3 denotes the component of the normalised dipole moment $\hat{\mathbf{D}}_{01}$ in the direction of the cooling laser.

A.3 Relevant expectation values

The calculations in the following two appendices require in addition to the expectation values defined in Section 3.2.2 the x operator expectation values

$$k_1 \equiv \langle x + x^\dagger \rangle\,, \quad k_2 \equiv \mathrm{i}\,\langle x - x^\dagger \rangle\,. \tag{A.56}$$

Moreover we employ the mixed operator expectation values

$$\begin{aligned}
&n_4 \equiv \langle x^\dagger x y^\dagger y \rangle\,, \quad k_{13} \equiv \langle (x + x^\dagger) y^\dagger y \rangle\,,\\
&k_{14} \equiv \mathrm{i}\,\langle (x - x^\dagger) y^\dagger y \rangle\,, \quad k_{15} \equiv \langle (x - x^\dagger)(y - y^\dagger) \rangle\,,\\
&k_{16} \equiv \mathrm{i}\,\langle (x + x^\dagger)(y - y^\dagger) \rangle\,, \quad k_{17} \equiv \langle (x + x^\dagger)(y + y^\dagger) \rangle\,,\\
&k_{18} \equiv \mathrm{i}\,\langle (x - x^\dagger)(y + y^\dagger) \rangle\,,
\end{aligned} \tag{A.57}$$

and

$$\begin{aligned}
k_{19} &\equiv \langle (x - x^\dagger)(y^2 - y^{\dagger 2}) \rangle\,,\\
k_{20} &\equiv \mathrm{i}\,\langle (x + x^\dagger)(y^2 - y^{\dagger 2}) \rangle\,,\\
k_{21} &\equiv \langle (x + x^\dagger)(y^2 + y^{\dagger 2}) \rangle\,,\\
k_{22} &\equiv \mathrm{i}\,\langle (x - x^\dagger)(y^2 + y^{\dagger 2}) \rangle\,,\\
k_{23} &\equiv \langle x^\dagger x (y^2 + y^{\dagger 2}) \rangle\,,\\
k_{24} &\equiv \mathrm{i}\,\langle x^\dagger x (y^2 - y^{\dagger 2}) \rangle\,.
\end{aligned} \tag{A.58}$$

The time derivatives of these and other expectation values which we defined in Sec. 3.2.2 can be found in App. A.4.

A.4 n_1, k_{11}, and k_{12} in the weak confinement regime

Setting $\eta = 0$ and substituting the x operator expectation values n_1, k_1, and k_2 into Eq. (3.34), we find that they evolve according to

$$\begin{aligned} \dot{n}_1 &= \frac{1}{2}\Omega k_2 - \Gamma n_1 , \\ \dot{k}_1 &= -\Delta k_2 - \frac{1}{2}\Gamma k_1 , \\ \dot{k}_2 &= \Omega(1-2n_1) + \Delta k_1 - \frac{1}{2}\Gamma k_2 \end{aligned} \tag{A.59}$$

in zeroth order in η. These equations form a closed set of differential equations. Eliminating all x-operator expectation values adiabatically which change on the relatively fast time scale given by Γ and adopting a notation where $x = x^{(0)} + x^{(1)} + x^{(2)} + ...$, with the superscript indicating the scaling of the respective term with respect to η, we find for example that n_1 is in zeroth order in η given by

$$n_1^{(0)} = \frac{\Omega^2}{\mu^2} . \tag{A.60}$$

The constant μ^2 in this equation is given by

$$\mu^2 \equiv 2\Omega^2 + \Gamma^2 + 4\Delta^2 . \tag{A.61}$$

In addition to $n^{(0)}$, we obtain solutions for $k_1^{(0)}$ and $k_2^{(0)}$. These will be used in the next subsection to calculate the coherences k_{11} and k_{12} up to first order in η.

Setting $\eta = 0$ and using again Eq. (3.34), we find that the time evolution of the mixed operator coherences k_{11} and k_{12} and k_{15} to k_{18} is in zeroth order in η given by

$$\begin{aligned} \dot{k}_{11} &= \frac{1}{2}\Omega k_{18} - \nu k_{12} - \Gamma k_{11} , \\ \dot{k}_{12} &= -\frac{1}{2}\Omega k_{15} + \nu k_{11} - \Gamma k_{12} , \\ \dot{k}_{15} &= -\Omega(k_8 - 2k_{12}) - \Delta k_{16} - \nu k_{18} - \frac{1}{2}\Gamma k_{15} , \\ \dot{k}_{16} &= \Delta k_{15} + \nu k_{17} - \frac{1}{2}\Gamma k_{16} , \\ \dot{k}_{17} &= -\Delta k_{18} - \nu k_{16} - \frac{1}{2}\Gamma k_{17} , \\ \dot{k}_{18} &= \Omega(k_7 - 2k_{11}) + \Delta k_{17} + \nu k_{15} - \frac{1}{2}\Gamma k_{18} . \end{aligned} \tag{A.62}$$

All six expectation values evolve on the relatively fast time scale given by the spontaneous decay rate Γ. Taking this into account and eliminating them adiabatically in the

weak coupling regime, i.e. for relatively small ν, we find that

$$\begin{aligned} k_{11}^{(0)} &= \frac{\Omega^2}{\mu^4\Gamma}\left[\mu^2\Gamma\, k_7 - (3\Gamma^2 - 4\Delta^2)\nu\, k_8\right], \\ k_{12}^{(0)} &= \frac{\Omega^2}{\mu^4\Gamma}\left[(3\Gamma^2 - 4\Delta^2)\nu\, k_7 + \mu^2\Gamma\, k_8\right] \end{aligned} \tag{A.63}$$

to a very good approximation. The constant μ^2 is given in Eq. (A.61) above. In addition to $k_{11}^{(0)}$ and $k_{12}^{(0)}$ we obtain expressions for $k_{15}^{(0)}$ and $k_{16}^{(0)}$. These are used in the next subsection to calculate n_1 up to first order in η.

Proceeding as above but taking terms up to first order in η into account we find that the first order in η contributions of the x operator expectation values n_1, k_1, and k_2 in Eq. (4.10) evolve according to

$$\begin{aligned} \dot{n}_1^{(1)} &= \frac{1}{2}\Omega\, k_2^{(1)} - \Gamma\, n_1^{(1)}, \\ \dot{k}_1^{(1)} &= -\eta\nu\, k_{15}^{(0)} - \Delta\, k_2^{(1)} - \frac{1}{2}\Gamma\, k_1^{(1)}, \\ \dot{k}_2^{(1)} &= -2\Omega n_1^{(1)} - \eta\nu\, k_{16}^{(0)} + \Delta\, k_1^{(1)} - \frac{1}{2}\Gamma\, k_2^{(1)}. \end{aligned} \tag{A.64}$$

These equations form a closed set of cooling equations, when the results for $k_{15}^{(0)}$ and $k_{16}^{(0)}$ which we obtained in App. A.4 are taken into account. Eliminating n_1, k_1 and k_2 adiabatically

$$n_1^{(1)} = \frac{8\eta\nu\Delta\Omega^2}{\mu^4}\, k_8 \tag{A.65}$$

in the weak confinement regime which we introduced in Section 3.2.3. This means terms proportional to ν^2 have been neglected.

In order to calculate k_{11} and k_{12} up to first order in η, we need a closed set of cooling equations which holds correctly up to this order. Applying Eq. (3.34) again to

k_{11} and k_{12} and k_{15} to k_{18}, we find that

$$\begin{aligned}
\dot{k}_{11}^{(1)} &= \frac{1}{2}\Omega\, k_{18}^{(1)} - \nu\, k_{12}^{(1)} + 2\eta\nu\, n_1^{(0)} - \Gamma\, k_{11}^{(1)}\,, \\
\dot{k}_{12}^{(1)} &= -\frac{1}{2}\Omega\, k_{15}^{(1)} + \nu\, k_{11}^{(1)} - \Gamma\, k_{12}^{(1)}\,, \\
\dot{k}_{15}^{(1)} &= 2\Omega\, k_{12}^{(1)} - \Delta\, k_{16}^{(1)} - \nu\, k_{18}^{(1)} + \eta\nu \left(k_1^{(0)} + 2k_{13}^{(0)} \right. \\
&\quad \left. -k_{21}^{(0)}\right) - \frac{1}{2}\Gamma\, k_{15}^{(1)}\,, \\
\dot{k}_{16}^{(1)} &= \Delta\, k_{15}^{(1)} + \nu\, k_{17}^{(1)} + \eta\nu \left(k_2^{(0)} + 2k_{14}^{(0)} - k_{22}^{(0)}\right) \\
&\quad -\frac{1}{2}\Gamma\, k_{16}^{(1)}\,, \\
\dot{k}_{17}^{(1)} &= -\Delta\, k_{18}^{(1)} - \nu\, k_{16}^{(1)} + \eta\nu \left(k_1^{(0)} - k_{19}^{(0)}\right) - \frac{1}{2}\Gamma\, k_{17}^{(1)}\,, \\
\dot{k}_{18}^{(1)} &= -2\Omega\, k_{11}^{(1)} + \Delta\, k_{17}^{(1)} + \nu\, k_{15}^{(1)} + \eta\nu \left(k_2^{(0)} - k_{20}^{(0)}\right) \\
&\quad -\frac{1}{2}\Gamma\, k_{18}^{(1)}\,.
\end{aligned} \tag{A.66}$$

Substituting the definitions of the mixed-particle expectation values n_4, k_{13} and k_{14} and k_{19} to k_{22} into Eq. (3.34) and setting $\eta = 0$, we find that

$$\begin{aligned}
\dot{n}_4 &= \frac{1}{2}\Omega\, k_{14} - \Gamma\, n_4\,, \\
\dot{k}_{13} &= -\Delta\, k_{14} - \frac{1}{2}\Gamma\, k_{13}\,, \\
\dot{k}_{14} &= \Omega\,(n_2 - 2n_4) + \Delta\, k_{13} - \frac{1}{2}\Gamma\, k_{14}\,,
\end{aligned} \tag{A.67}$$

while

$$\begin{aligned}
\dot{k}_{19} &= -\Omega(k_{10} - 2k_{24}) - \Delta\, k_{20} - 2\nu\, k_{22} - \frac{1}{2}\Gamma\, k_{19}\,, \\
\dot{k}_{20} &= \Delta\, k_{19} + 2\nu\, k_{21} - \frac{1}{2}\Gamma\, k_{20}\,, \\
\dot{k}_{21} &= -\Delta\, k_{22} - 2\nu\, k_{20} - \frac{1}{2}\Gamma\, k_{21}\,, \\
\dot{k}_{22} &= \Omega(k_9 - 2k_{23}) + \Delta\, k_{21} + 2\nu\, k_{19} - \frac{1}{2}\Gamma\, k_{22} \\
\dot{k}_{23} &= \frac{1}{2}\Omega\, k_{22} - 2\nu\, k_{24} - \Gamma\, k_{23}\,, \\
\dot{k}_{24} &= -\frac{1}{2}\Omega\, k_{19} + 2\nu\, k_{23} - \Gamma\, k_{24}\,.
\end{aligned} \tag{A.68}$$

These final six differential equations hold in zeroth order in η. Setting the right hand side of these and of the cooling equations in Eq. (A.66) equal to zero, we finally find

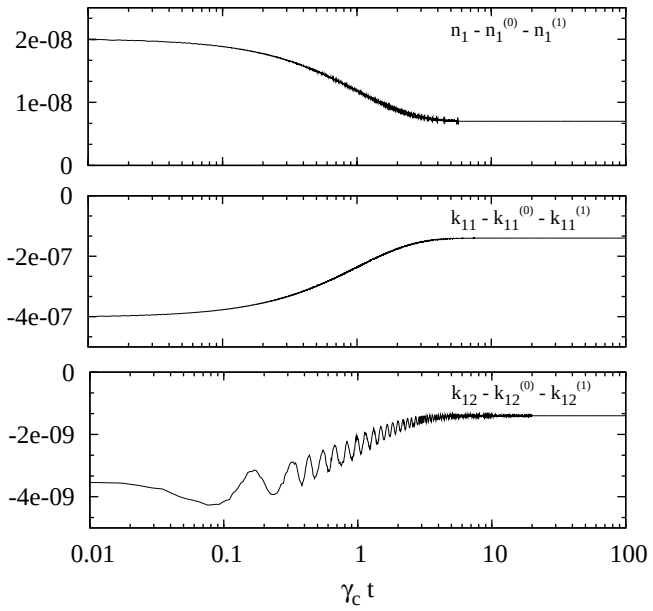

Figure A.2: A comparison of the analytical results for n_1, k_{11}, and k_{12} in Eqs. (A.60), (A.63), (A.65), and (A.69) with the results of a numerical solution of the above cooling equations for $\eta = 0.1$, $\Omega = \nu = 0.01\,\Gamma$, and $\Delta = 0.5\,\Gamma$.

that

$$\begin{aligned} k_{11}^{(1)} &= \frac{4\eta\nu\Omega^2}{\mu^4}\left[2\Delta\, k_{10} + \Gamma\right], \\ k_{12}^{(1)} &= \frac{8\eta\nu\Delta\Omega^2}{\mu^4}\left[2n_2 - k_9 + 1\right] \end{aligned} \tag{A.69}$$

in the weak confinement regime. This means, terms of order ν^2 have again been neglected. Fig. A.2 compares the above analytical results for n_1, k_{11}, and k_{12} with the result of a numerical solution of the above cooling equations. Very good agreement between both solutions is found which suggests that the effective cooling equations in Eq. (3.43) apply after a very short transition time of the order $1/\Gamma$.

A.5 n_1, k_{11} and k_{12} in the strong confinement regime

The calculation of n_1 in zeroth order in η is the same as in App. A.4. However, in the strong coupling regime, the expression in Eq. (A.60) simplifies to

$$n_1^{(0)} = \frac{\Omega^2}{4\Delta^2}. \tag{A.70}$$

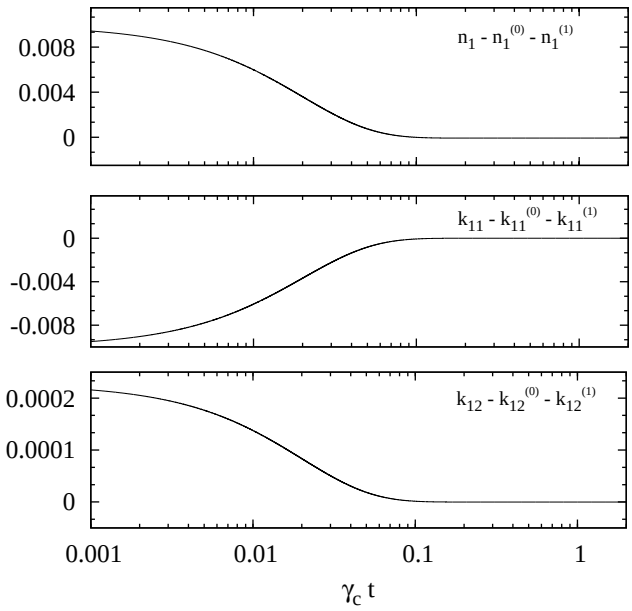

Figure A.3: A comparison of the analytical results for n_1, k_{11}, and k_{12} in Eqs. (B.13), (A.72), and (A.74) with the results of a numerical solution of the above cooling equations for $\eta = 0.01$, $\Omega = \Gamma = 0.01\,\nu$, and $\Delta = \nu$.

Setting $\eta = 0$ and eliminating the y operator coherences adiabatically from the system dynamics we immediately find that k_7 to k_{10} all equal zero in zeroth order in η,

$$k_7^{(0)} = k_8^{(0)} = k_9^{(0)} = k_{10}^{(0)} = 0\,. \tag{A.71}$$

Taking this into account when eliminating the mixed operator expectation values whose time derivatives are given in Eq. (A.62), we moreover find that

$$k_{11}^{(0)} = k_{12}^{(0)} = 0\,. \tag{A.72}$$

To calculate the coherences k_{11} and k_{12} up to first order in η, we have a look at the time derivatives of k_{11}, k_{12}, and k_{15} to k_{18} in first order in η which can be found in Eq. (A.66). Combining Eqs. (A.68) and (A.71), we immediately see that

$$k_{19}^{(0)} = k_{20}^{(0)} = k_{21}^{(0)} = k_{22}^{(0)} = 0\,. \tag{A.73}$$

Taking this and the expressions for $k_1^{(0)}$, $k_2^{(0)}$, $k_{13}^{(0)}$, and $k_{14}^{(0)}$ obtained in App. A.4 into account, when setting the time derivatives of the relatively fast evolving variables in

Eq. (A.66) equal to zero, we therefore find that

$$\begin{aligned} k_{11}^{(1)} &= \frac{\eta\nu\Gamma\Omega^2}{4(\Delta+\nu)^2\Delta^2}\left[1-\frac{4\nu\Delta}{(\Delta-\nu)^2}\,n_2\right], \\ k_{12}^{(1)} &= \frac{\eta\nu\Omega^2}{2(\Delta+\nu)\Delta^2}\left[1+\frac{2\Delta}{\Delta-\nu}\,n_2\right]. \end{aligned} \tag{A.74}$$

These coherences are different from the coherences in Eq. (A.69), since they apply only in the strong confinement regime. As Fig. A.3 shows there is again very good agreement the analytical and the numerical solutions for n_1, k_{11}, and k_{12}. This means that the effective cooling equation for the strong confinement regime in Eq. (3.60) too applies after a relatively short transition time.

Appendix B

Trapped Particle In a Cavity

B.1 Expectation values

The following appendices shall calculate x operator and mixed operator expectation values in similar manner to that performed in appendix A.4 and A.5 except this time we have more rate equations for the x operator expectation values

$$\begin{aligned} &k_1 \equiv \langle x + x^\dagger \rangle\,, \;\; k_2 \equiv \mathrm{i}\,\langle x - x^\dagger \rangle\,, \\ &k_3 \equiv \langle x^2 + x^{\dagger 2} \rangle\,, \;\; k_4 \equiv \mathrm{i}\,\langle x^2 - x^{\dagger 2} \rangle\,, \\ &k_5 \equiv \langle x^\dagger (x + x^\dagger) x \rangle\,, \;\; k_6 \equiv \mathrm{i}\,\langle x^\dagger (x - x^\dagger) x \rangle\,. \end{aligned} \tag{B.1}$$

and less rate equations for the mixed

$$\begin{aligned} k_{13} &\equiv \langle (x + x^\dagger) y^\dagger y \rangle\,, \\ k_{14} &\equiv \mathrm{i}\,\langle (x - x^\dagger) y^\dagger y \rangle\,, \\ k_{15} &\equiv \langle (x - x^\dagger)(y - y^\dagger) \rangle\,, \\ k_{16} &\equiv \mathrm{i}\,\langle (x + x^\dagger)(y - y^\dagger) \rangle\,, \\ k_{17} &\equiv \langle (x + x^\dagger)(y + y^\dagger) \rangle\,, \\ k_{18} &\equiv \mathrm{i}\,\langle (x - x^\dagger)(y + y^\dagger) \rangle\,, \\ k_{19} &\equiv \langle (x - x^\dagger)(y^2 - y^{\dagger 2}) \rangle\,, \\ k_{20} &\equiv \mathrm{i}\,\langle (x + x^\dagger)(y^2 - y^{\dagger 2}) \rangle\,, \\ k_{21} &\equiv \langle (x + x^\dagger)(y^2 + y^{\dagger 2}) \rangle\,, \\ k_{22} &\equiv \mathrm{i}\,\langle (x - x^\dagger)(y^2 + y^{\dagger 2}) \rangle\,. \end{aligned} \tag{B.2}$$

Their time derivatives can be found in App. B.2.

B.2 Calculation of n_1, k_{11}, and k_{12} for the weak confinement regime

Setting $\eta = 0$ and substituting the x operator expectation values in Eq. (4.10) into Eq. (4.9), we find that these evolve according to

$$\begin{aligned}
\dot{n}_1 &= g_{\text{eff}} k_2 - \kappa n_1 , \\
\dot{n}_3 &= g_{\text{eff}} \left(k_2 + 2k_6\right) + \kappa \left(n_1 - 2n_3\right) , \\
\dot{k}_1 &= -\delta_{\text{eff}} k_2 - \frac{1}{2}\kappa k_1 , \\
\dot{k}_2 &= 2g_{\text{eff}} + \delta_{\text{eff}} k_1 - \frac{1}{2}\kappa k_2 , \\
\dot{k}_3 &= -2g_{\text{eff}} k_2 - 2\delta_{\text{eff}} k_4 - \kappa k_3 , \\
\dot{k}_4 &= 2g_{\text{eff}} k_1 + 2\delta_{\text{eff}} k_3 - \kappa k_4 , \\
\dot{k}_5 &= g_{\text{eff}} k_4 - \delta_{\text{eff}} k_6 - \frac{3}{2}\kappa k_5 , \\
\dot{k}_6 &= g_{\text{eff}} \left(4n_1 - k_3\right) + \delta_{\text{eff}} k_5 - \frac{3}{2}\kappa k_6 .
\end{aligned} \tag{B.3}$$

These equations form a closed set of differential equations. Eliminating all x-operator expectation values adiabatically which change on the relatively fast time scale given by κ and adopting a notation where $x = x^{(0)} + x^{(1)} + x^{(2)} + ...$, with the superscript indicating the scaling of the respective term with respect to η, we find for example that n_1 is in zeroth order in η given by

$$n_1^{(0)} = 4\frac{g_{\text{eff}}^2}{\mu^2} . \tag{B.4}$$

The constant μ^2 in this equation is given by

$$\mu^2 \equiv \kappa^2 + 4\delta_{\text{eff}}^2 . \tag{B.5}$$

In addition to $n_1^{(0)}$, we obtain solutions for $k_1^{(0)}$ and $k_2^{(0)}$. These will be used in the next subsection to calculate the coherences k_{11} and k_{12} up to first order in η.

In addition we obtain expressions for the zeroth order in η solutions $k_1^{(0)}$, $k_2^{(0)}$, $k_5^{(0)}$, $k_6^{(0)}$, and $n_3^{(0)}$. These will be used in the next subsection to calculate the coherences k_{11} and k_{12} up to first order in η.

Setting $\eta = 0$ and using again Eq. (4.9), we moreover find that the time evolution of the mixed operator coherences k_{11} and k_{12} and k_{15} to k_{18} is in zeroth order in η

given by

$$\begin{aligned}
\dot{k}_{11} &= g_{\rm eff}\, k_{18} - \nu\, k_{12} - \kappa\, k_{11}\,, \\
\dot{k}_{12} &= -g_{\rm eff}\, k_{15} + \nu\, k_{11} - \kappa\, k_{12}\,, \\
\dot{k}_{15} &= -2g_{\rm eff}\, k_8 - \delta_{\rm eff}\, k_{16} - \nu\, k_{18} - \frac{1}{2}\kappa\, k_{15}\,, \\
\dot{k}_{16} &= \delta_{\rm eff}\, k_{15} + \nu\, k_{17} - \frac{1}{2}\kappa\, k_{16}\,, \\
\dot{k}_{17} &= -\delta_{\rm eff}\, k_{18} - \nu\, k_{16} - \frac{1}{2}\kappa\, k_{17}\,, \\
\dot{k}_{18} &= 2g_{\rm eff}\, k_7 + \delta_{\rm eff}\, k_{17} + \nu\, k_{15} - \frac{1}{2}\kappa\, k_{18}\,. \qquad \text{(B.6)}
\end{aligned}$$

These six equations too form a closed set of cooling equations which describe a time evolution on the time scale of the spontaneous cavity decay rate κ. Taking this into account and eliminating k_{11} and k_{12} and k_{15} to k_{18} adiabatically in the weak coupling regime, i.e. for relatively small ν, we find that

$$\begin{aligned}
k_{11}^{(0)} &= \frac{4g_{\rm eff}^2}{\mu^4\kappa}\left[\mu^2\kappa\, k_7 - (3\kappa^2 - 4\delta_{\rm eff}^2)\nu\, k_8\right]\,, \\
k_{12}^{(0)} &= \frac{4g_{\rm eff}^2}{\mu^4\kappa}\left[(3\kappa^2 - 4\delta_{\rm eff}^2)\nu\, k_7 + \mu^2\kappa\, k_8\right] \qquad \text{(B.7)}
\end{aligned}$$

to a very good approximation. The constant μ^2 is given in Eq. (B.5) above. In addition to $k_{11}^{(0)}$ and $k_{12}^{(0)}$ we obtain expressions for $k_{15}^{(0)}$ and $k_{16}^{(0)}$. These are used in the next subsection to calculate n_1 up to first order in η.

Proceeding as above but taking terms up to first order in η into account we find that the first order in η contributions of the x operator expectation values n_1, k_1, and k_2 in Eq. (4.10) evolve according to

$$\begin{aligned}
\dot{n}_1^{(1)} &= \frac{1}{2}\Omega\, k_2^{(1)} - \Gamma\, n_1^{(1)}\,, \\
\dot{k}_1^{(1)} &= -\eta\nu\, k_{15}^{(0)} - \Delta\, k_2^{(1)} - \frac{1}{2}\Gamma\, k_1^{(1)}\,, \\
\dot{k}_2^{(1)} &= -2\Omega n_1^{(1)} - \eta\nu\, k_{16}^{(0)} + \Delta\, k_1^{(1)} - \frac{1}{2}\Gamma\, k_2^{(1)}\,. \qquad \text{(B.8)}
\end{aligned}$$

These equations form a closed set of cooling equations, when the results for $k_{15}^{(0)}$ and $k_{16}^{(0)}$ which we obtained in App. B.2 are taken into account. Eliminating n_1, k_1 and k_2 adiabatically

$$n_1^{(1)} = \frac{32\eta\nu\,\delta_{\rm eff} g_{\rm eff}^2}{\mu^4}\, k_8 \qquad \text{(B.9)}$$

in the weak confinement regime which we introduced in Section 3.2.3. This means terms proportional to ν^2 have been neglected.

In order to calculate k_{11} and k_{12} up to first order in η, we need a closed set of cooling equations which holds correctly up to this order. Applying Eq. (3.34) again to k_{11} and k_{12} and k_{15} to k_{18}, we find that

$$\begin{aligned}
\dot{k}_{11}^{(1)} &= g_{\text{eff}}\, k_{18}^{(1)} - \nu\, k_{12}^{(1)} + 2\eta\nu\, n_3^{(0)} - \kappa\, k_{11}^{(1)}\,, \\
\dot{k}_{12}^{(1)} &= -g_{\text{eff}}\, k_{15}^{(1)} + \nu\, k_{11}^{(1)} + 2\eta\kappa \left[n_1^{(0)} - n_3^{(0)}\right] - \kappa\, k_{12}^{(1)}\,, \\
\dot{k}_{15}^{(1)} &= -\delta_{\text{eff}}\, k_{16}^{(1)} - \nu\, k_{18}^{(1)} + \eta\nu \left[k_1^{(0)} + 2k_{13}^{(0)} - k_{21}^{(0)}\right] \\
&\quad + 2\eta\kappa\, k_6^{(0)} - \frac{1}{2}\kappa\, k_{15}^{(1)}\,, \\
\dot{k}_{16}^{(1)} &= \delta_{\text{eff}}\, k_{15}^{(1)} + \nu\, k_{17}^{(1)} + \eta\nu \left[k_2^{(0)} + 2k_{14}^{(0)} - k_{22}^{(0)}\right] \\
&\quad - 2\eta\kappa\, k_5^{(0)} - \frac{1}{2}\kappa\, k_{16}^{(1)}\,, \\
\dot{k}_{17}^{(1)} &= -\delta_{\text{eff}}\, k_{18}^{(1)} - \nu\, k_{16}^{(1)} + \eta\nu \left[k_1^{(0)} + 2k_5^{(0)} - k_{19}^{(0)}\right] \\
&\quad - \frac{1}{2}\kappa\, k_{17}^{(1)}\,, \\
\dot{k}_{18}^{(1)} &= \delta_{\text{eff}}\, k_{17}^{(1)} + \nu\, k_{15}^{(1)} + \eta\nu \left[k_2^{(0)} + 2k_6^{(0)} - k_{20}^{(0)}\right] \\
&\quad - \frac{1}{2}\kappa\, k_{18}^{(1)}\,.
\end{aligned} \tag{B.10}$$

Substituting the definitions of the mixed-particle expectation values k_{13} and k_{14} and k_{19} to k_{22} into Eq. (4.9) and setting $\eta = 0$, we find moreover that

$$\begin{aligned}
\dot{k}_{13} &= -\delta_{\text{eff}}\, k_{14} - \frac{1}{2}\kappa\, k_{13}\,, \\
\dot{k}_{14} &= 2g_{\text{eff}}\, n_2 + \delta_{\text{eff}}\, k_{13} - \frac{1}{2}\kappa\, k_{14}\,, \\
\dot{k}_{19} &= -2g_{\text{eff}}\, k_{10} - \delta_{\text{eff}}\, k_{20} - 2\nu\, k_{22} - \frac{1}{2}\kappa\, k_{19}\,, \\
\dot{k}_{20} &= \delta_{\text{eff}}\, k_{19} + 2\nu\, k_{21} - \frac{1}{2}\kappa\, k_{20}\,, \\
\dot{k}_{21} &= -\delta_{\text{eff}}\, k_{22} - 2\nu\, k_{20} - \frac{1}{2}\kappa\, k_{21}\,, \\
\dot{k}_{22} &= 2g_{\text{eff}}\, k_9 + \delta_{\text{eff}}\, k_{21} + 2\nu\, k_{19} - \frac{1}{2}\kappa\, k_{22}\,.
\end{aligned} \tag{B.11}$$

These final six differential equations hold in zeroth order in η. Setting the right hand side of these and of the cooling equations in Eq. (B.10) equal to zero, we finally find

that

$$\begin{aligned} k_{11}^{(1)} &= \frac{16\eta\nu g_{\text{eff}}^2}{\mu^4}\left[2\delta_{\text{eff}}k_{10}+\kappa\right]+\frac{64\eta g_{\text{eff}}^4\nu\left(16\delta_{\text{eff}}^4+16\delta_{\text{eff}}^2\kappa^2-5\kappa^4\right)}{\kappa\mu^8}, \\ k_{12}^{(1)} &= \frac{8\eta\nu\Delta\Omega^2}{\mu^4}\left[2n_2-k_9+1\right]-\frac{32\eta g_{\text{eff}}^4\left(3\kappa^2-4\delta_{\text{eff}}^2\right)}{\mu^6} \end{aligned} \tag{B.12}$$

in the weak confinement regime. This means, terms of order ν^2 have again been neglected.

B.3 n_1, k_{11} and k_{12} in the strong confinement regime

The calculation of n_1 in zeroth order in η is the same as in App. B.2. However, in the strong coupling regime, the expression in Eq. (A.60) simplifies to

$$n_1^{(0)} = \frac{g_{\text{eff}}^2}{\delta_{\text{eff}}^2}. \tag{B.13}$$

For $\eta = 0$ we can also use Eq. (B.6) to determine the zeroth order expressions for k_{11} and k_{12}. These equations still evolve on the relatively fast timescale given by the cavity decay rate κ which means we can still perform an adiabatic elimination of the mixed operator expectation values in Eq. (B.6). Also, since we are in the strong confinement regime we can use the approximation $\kappa \ll \nu$ to neglect terms that scale with κ^2. Doing so we find that

$$\begin{aligned} k_{11}^{(0)} &= \frac{g_{\text{eff}}^2}{\nu\left[\delta_{\text{eff}}^2-\nu^2\right]^2}\left(2\nu\left(\delta_{\text{eff}}^2-\nu^2\right)k_7+\kappa\left(\delta_{\text{eff}}^2-3\nu^2\right)k_8\right], \\ k_{12}^{(0)} &= -\frac{g_{\text{eff}}^2}{\nu\left(\delta_{\text{eff}}^2-\nu^2\right)^2}\left[\kappa\left(\delta_{\text{eff}}^2-3\nu^2\right)k_7+2\nu\left(-\delta_{\text{eff}}^2+\nu^2\right)k_8\right]. \end{aligned} \tag{B.14}$$

The expressions for $k_{15}^{(0)}$ and $k_{16}^{(0)}$ that are also obtained are used next with the first order equations of Eq. (B.8) to calculate n_1 to first order in η. Eliminating n_1, k_1 and k_2 adiabatically

$$n_1^{(1)} = \frac{2\eta g_{\text{eff}}^2\nu}{\kappa\delta_{\text{eff}}\left(\delta_{\text{eff}}^2-\nu^2\right)^2}\left[\nu\left(-\delta_{\text{eff}}^2+\nu^2\right)k_7+\kappa\delta_{\text{eff}}^2k_8\right] \tag{B.15}$$

in the strong confinement regime. This means that we have made the approximation of

neglecting terms proportional to κ^2. Adiabatically eliminating the zeroth order equations of Eq. (B.11) we substitute the respective quasi-stationary state values into the first order equations of Eq. (B.10). Finally we adiabatically eliminate Eq. (B.10) to find the first order expressions for k_{11} and k_{12} to be

$$\begin{aligned}
k_{11}^{(1)} &= -\frac{2\eta g_{\text{eff}}^2 \delta_{\text{eff}} \kappa}{\xi^8}\left[2\delta_{\text{eff}}^4 - 19\delta_{\text{eff}}^2\nu^2 + 26\nu^4\right] k_9 \\
&\quad + \frac{6\eta g_{\text{eff}}^2 \delta_{\text{eff}} \nu}{\xi^4} k_{10} - \frac{4\eta g_{\text{eff}}^2 \kappa \nu^2}{\delta_{\text{eff}}\left(\delta_{\text{eff}}^2 - \nu^2\right)^2} n_2 \\
&\quad - \frac{g_{\text{eff}}^2 \eta \kappa}{\delta_{\text{eff}}^4 \nu\left(\delta_{\text{eff}}^2 - \nu^2\right)^2}\left[-\delta_{\text{eff}}^2(\delta_{\text{eff}} - \nu)^2\nu^2 + g_{\text{eff}}^2\left(4\delta_{\text{eff}}^4 - 6\delta_{\text{eff}}^2\nu^2 - 2\nu^4\right)\right], \\
k_{12}^{(1)} &= \frac{6 g_{\text{eff}}^2 \delta_{\text{eff}} \eta \nu}{\xi^4} k_9 - \frac{2 g_{\text{eff}}^2 \delta_{\text{eff}} \eta \kappa}{\xi^8}\left[2\delta_{\text{eff}}^4 - 19\delta_{\text{eff}}^2\nu^2 + 26\nu^4\right] k_{10} \\
&\quad - \frac{4 g_{\text{eff}}^2 \eta \nu}{\delta_{\text{eff}}(\delta_{\text{eff}}^2 - \nu^2)} n_2 \\
&\quad - \frac{32\eta g_{\text{eff}}^2}{\mu^4\left(\delta_{\text{eff}}^2 - \nu^2\right)}\left[\delta_{\text{eff}}^2\nu(-\delta_{\text{eff}} + \nu) + g_{\text{eff}}^2\left(\delta_{\text{eff}}^2 + \nu^2\right)\right].
\end{aligned} \tag{B.16}$$

Here

$$\xi \equiv \delta_{\text{eff}}^4 - 5\delta_{\text{eff}}^2\nu^2 + 4\nu^4 \tag{B.17}$$

and μ^4 is defined as in Eq. (B.5). These coherences can now be used to determine the expressions for the matrix elements of Eq. (4.23)

Bibliography

1. Hänsch, T. & Schawlow, A. *Opt. Comm* **13,** 68 (1975).
2. Wineland, D. & Dehmelt, H. *Bull. Am. Phys. Soc.* **20,** 637 (1975).
3. Phillips, W. D. *Rev. Mod. Phys.* **70,** 721 (1998).
4. Chu, S. *Rev. Mod. Phys.* **70,** 685 (1998).
5. Cohen-Tannoudji, C. N. *Rev. Mod. Phys.* **70,** 685 (1998).
6. Cohen-Tannoudji, C. & Philips, W. *Phys. Today* **43,** 33 (1990).
7. Ketterle, W. & VanDruten, N. J. *Adv. in Atom. and Mol. Phys.* **37,** 181 (1996).
8. Wineland, D. J. & Itano, W. M. *Phys. Rev. A* **20,** 1521 (1979).
9. A.Aspect, E.Arimondo, R.Kaiser, Vansteenkiste, N. & C.Cohen-Tannoudji. *Phys. Rev. Lett* **61,** 826 (1988).
10. S.Stenholm. *Rev. Mod. Phys* **58,** 699 (1986).
11. Cirac, J. I., Blatt, R., Zoller, P. & Phillips, W. D. *Phys. Rev. A* **46,** 2668 (1992).
12. S.Stenholm. *J. Opt. Soc. Am. B* **2,** 1743 (1985).
13. Eschner, J., Morigi, G., Schmidt-Kaler, F. & Blatt, R. *J. Opt. Soc. Am. B* **20,** 1003 (2003).
14. Beige, A., Knight, P. L. & Vitiello, G. *New J. Phys* **7,** 96 (2005).
15. Cirac, J. I., Parkins, A. S., Blatt, R. & Zoller, P. *Opt. Comm* **97,** 353 (1993).
16. Cirac, J. I., Lewenstein, M. & Zoller, P. *Phys. Rev. A* **51,** 1650 (1995).
17. Zippilli, S. & Morigi, G. *Phys. Rev. Lett* **95,** 143001 (2005).
18. Zippilli, S. & Morigi, G. *Phys. Rev. A* **72,** 053408 (2005).
19. Vuletić, V., Chan, H. W. & Black, A. T. *Phys. Rev. A* **64,** 033405 (2001).
20. Lindberg, M. & Stenholm, S. *J. Phys. B* **17,** 3375 (1984).
21. Stenholm, S. *Appl. Phys.* **15,** 287 (1978).
22. Lindberg, M. *J. Phys. B* **17,** 2129 (1984).
23. J. Javanainen, M. L. & Stenholm, S. *J. Opt. Soc. Am. B* **1,** 111 (1984).

24. Dalibard, J. & Cohen-Tannoudji, C. *J. Phys. B* **18,** 1661 (1985).
25. Raab, C. *et al. Phys. Rev. Lett* **85,** 538541 (2000).
26. Horvath, G. Z. K., Thompson, R. C. & Knight, P. L. *Contemp. Phys.* **38,** 27 (1997).
27. Leibfried, D., Blatt, R., Monroe, C. & Wineland, D. *Rev. Mod. Phys* **75,** 281 (2003).
28. Anderson, M. H., Ensher, J. R., Matthews, M. R., Wieman, C. E. & Cornell, E. A. *Science* **269,** 1995 (1995).
29. Davis, K. B. *et al. Phys. Rev. Lett* **3969,** 1995 (1995).
30. Myatt, C. J., Burt, E. A., Ghrist, R. W., Cornell, E. A. & Wieman, C. E. *Phys. Rev. Lett* **78,** 586 (1997).
31. DeMarco, B. & Jin, D. S. *Science* **285,** 1703 (1999).
32. Purcell, E. M. *Phys. Rev* **69,** 681 (1946).
33. Vigneron, K. *Etude d'effets de bistabilite optique induits par des atomes froids places dans une cavite optique* (Maters thesis, Ecole Superieure d' Optique, 1995).
34. Roch, J. F. *et al. Phys. Rev. Lett* **78,** 634 (1997).
35. Pinkse, P. W. H., Fischer, T., Maunz, P. & Rempe, G. *Nature* **404,** 365 (2000).
36. Maunz, P. *et al. Nature* **50,** 428 (2004).
37. Nussmann, S. *et al. Nature Phys.* **1,** 122 (2005).
38. Kubanek, A. *et al. Nature* **462,** 898 (2009).
39. Black, A. T., Chan, H. W. & Vuletic, V. *Phys. Rev. Lett* **91,** 203001 (2003).
40. Chan, H. W., Black, A. T. & Vuletić, V. *Phys. Rev. Lett* **90,** 063003 (2003).
41. Leibrandt, D. R., Labaziewicz, J., Vuletic, V. & Chuang, I. L. *Phys. Rev. Lett* **103,** 103001 (2009).
42. Schleier-Smith, M. H. *et al. arXiv:1104.4623, Optomechanical Cavity Cooling of an Atomic Ensemble* (2011).
43. McKeever, J. *et al. Phys. Rev. Lett* **90,** 133602 (2003).
44. Gibbons, M. J., Kim, S. Y., Fortier, K. M., Ahmadi, P. & Chapman, M. S. *Phys. Rev. A* **78,** 043418 (2008).
45. Nagorny, B., Elsässer, T. & Hemmerich, A. *Phys. Rev. Lett* **91,** 055025 (2003).
46. Elsässer, T., Nagorny, B. & Hemmerich, A. *Phys. Rev. A* **91,** 051401 (2003).
47. Trupke, M. *et al. Phys. Rev. Lett* **99,** 06360 (2007).
48. Colombe, Y. *et al. Nature* **450,** 272 (2007).
49. Khudaverdyan, M. *et al. New J. Phys.* **10,** 073023 (2008).

50. Kampschulte, T. *et al. arXive,* 1004.5348 (2010).

51. Herskind, P. F., Dantan, A., Marler, J. P., Albert, M. & Drewsen, M. *Nature Phys.* **5,** 494 (2009).

52. A. Wickenbrock, P. P. & Renzoni, F. *J. Mod. Opt,* Collective strong coupling in a lossy optical cavity (in press).

53. Mossberg, T. W., Lewenstein, M. & Gauthier, D. J. *Phys. Rev. Lett* **67,** 1723 (1991).

54. Zaugg, T., Wilkens, M., Meystre, P. & Lenz, G. *Opt. Comm.* **97,** 189 (1993).

55. Domokos, P. & Ritsch, H. *Phys. Rev. Lett* **89,** 253003 (2002).

56. Domokos, P. & Ritsch, H. *J. Opt. Soc. Am. B* **20,** 1098 (2003).

57. Horak, P., Hechenblaikner, G., Gheri, K. M., Stecher, H. & Ritsch, H. *Phys. Rev. Lett* **79,** 4974 (1997).

58. Hechenblaikner, G., Gangl, M., P, P. H. & Ritsch, H. *Phys. Rev. A* **58,** 3030 (1998).

59. Domokos, P., Horak, P. & Ritsch, H. *J. Phys. B* **34,** 187 (2001).

60. Vuletić, V. & Chu, S. *Phys. Rev. Lett* **84,** 3787 (2000).

61. Murr, K. *Phys. Rev. Lett* **96,** 253001 (2006).

62. Murr, K. *et al. Phys. Rev. A* **73,** 063415 (2006).

63. Murr, K. *et al. Phys. Rev. A* **74,** 043412 (2006).

64. Tan, L., Liu, L.-W. & Sun, Y.-F. *arXiv,* 1002.4036 (2010).

65. Barker, P. F. & Shneider, M. N. *Phys. Rev. A* **81,** 023826 (2010).

66. J.Schulze, R., Genes, C. & Ritsch, H. *Phys. Rev. A* **81,** 063820 (2010).

67. Barker, P. F. *Phys. Rev. Lett* **105,** 073002 (2010).

68. Xuereb, A., Domokos, P., Asboth, J., Horak, P. & Freegarde, T. *Phys. Rev. A* **79,** 053810 (2009).

69. Blake, T., Kurcz, A. & Beige, A. *J. Mod. Opt* **58,** 1317 (2011).

70. Kowalewski, M., Morigi, G., Pinkse, P. W. H. & Rielde, R. V. *Phys. Rev. A* **84,** 033408 (2011).

71. Bienert, M. & Morigi, G. *arXiv:1109.1666, Cavity cooling of a trapped atom using Electromagnetically–Induced Transparency* (2011).

72. Bethlem, H. L., Berden, G. & Meijer, G. *Phys. Rev. Lett* **83,** 1558 (1999).

73. Weinstein, J., deCarvalho, R., Guillet, T., Friedrich, B. & Doyle, J. *Nature* **395,** 148 (1998).

74. Van Buuren, L. D. *et al. Phys. Rev. Lett* **102,** 033001 (2009).

75. Köhler, T., Goral, K. & Julienne, P. S. *Rev. Mod. Phys* **78,** 1311 (2006).

76. Wang, D. *et al. Phys. Rev. Lett* **93,** 243005 (2004).

77. Sage, J. M., Sainis, S., Bergeman, T. & DeMille, D. *Phys. Rev. Lett* **94,** 203001 (2005).

78. Shuman, E. S., Barry, J. F. & DeMille, D. *Nature* **467,** 820 (2010).

79. Zeppenfeld, M., Motsch, M., Pinkse, P. & Rempe, G. *Phys. Rev. A* **80,** 041401, (2009).

80. Lev, B. L. *et al. Phys. Rev. A* **77,** 023402 (2008).

81. Kowalewski, M., Morigi, G., Pinkse, P. W. H. & Rielde, R. V. *Appl. Phys. B* **89,** 459 (2007).

82. Morigi, G., Pinkse, P. W. H., Kowalewski, M. & Rielde, R. V. *Phys. Rev. Lett.* **99,** 073001 (2007).

83. Vogel, W. & de Matos Filho, R. L. *Phys. Rev. A* **52,** 4214 (1995).

84. Blake, T., Kurcz, A. & Beige, A. *arXiv:1103.0410* (2010).

85. Kurcz, A., Capolupo, A. & Beige, A. *New J. Phys.* **11,** 053001 (2009).

86. Haken, H. *Rev. Mod. Phy* **47,** 1 (1975).

87. Walls, D. F. & Millburn, G. J. *Quantum Optics* (Springer, New York, USA, 2008).

88. Zee, A. *Quantum Field Theory in a Nutshell* (Princeton University Press, Princeton, USA, 2000).

89. Nayfeh, A. H. *Perturbation Methods* (Wiley, New York, USA, 1973).

90. Bogoliubov, N. N. & Mitropolskii, Y. A. *Asymptotic Methods in the Theory of Non-linear Oscillations* (Gordon Breach, New York, USA, 1967).

91. Gardiner, C. W. & Zoller, P. *Quantum Noise* (Springer, Berlin, Germany, 2000).

92. Volosov, V. M. *Soviet Math. Dokl* **12,** 221 (1961).

93. Berman, P. *Cavity Quantum Electrodynamics* (Academic, San Diego CA, 1994).

94. Haroche, S. & Raimond, J. M. *Exploring the Quantum* (Oxford Graduate Texts, Oxford, UK, 2006).

95. Itano, W. M. & Wineland, D. J. *Phys. Rev. A* **25,** 1 (1981).

96. Takamoto, M. & Katori, H. *Phys. Rev. Lett* **91,** 223001 (2003).

97. Gerry, C. C. & Knight, P. L. *Introductory Quantum Optics* (Cambridge University Press, Cambridge, UK, 2003).

98. Carrmichael, H. *An Open Systems Approach to Quantum Optics* (Springer Verlag, London, UK, 1993).

99. Breur, H. P. & Petruccione, F. *The Theory of Open Quantum Systems* (Oxford University Press, Oxford, UK, 2007).

100. Molmer, K., Castin, Y. & Dalibard, J. *J. Opt. Soc. Am. B* **10,** 524 (1993).

101. Hegerfeldt, G. C. *Phys. Rev. A* **47,** 1 (1993).

102. Plenio, M. & Knight, P. L. *Rev. Mod. Phys* **70,** 101 (1998).

103. Hegerfeldt, G. C. *Phys. Rev. Lett* **72,** 596 (1994).

104. J.Javanainen & S.Stenholm. *Appl.Phys.* **21,** 0035 (1980).

105. A.Perelmorov. *Generalised Coherent States and Their Applications* (Springer Verlag, Berlin, Heidelberg, 2006).

106. Feynman, R. P. *Rev. Mod. Phys.* **367,** 1948 (20).

107. Beige, A. & Hegerfeldt, G. C. *Phys. Rev. A* **53,** 53 (1996).

108. Isham, C. *Lectures on Quantum Theory: Mathematical and Structural Foundations* (Imperial College Press, London UK, 1995).

109. Schleich, W. P. *Quantum Optics in phase space* (Wiley, Verlag, Berlin, 2001).